Master's thesis

NTNU
Norwegian University of Science and Technology
Faculty of Engineering
Department of Geoscience and Petroleum

Silje Marie Tinderholt

Heat Transfer – Between Rock Mass and Tunnel Room

A study of in-situ measurements and numerical simulations of temperature profiles through concrete and rock mass

Master's thesis in Tekniske Geofag
Supervisor: Karl Gunnar Holter
June 2019

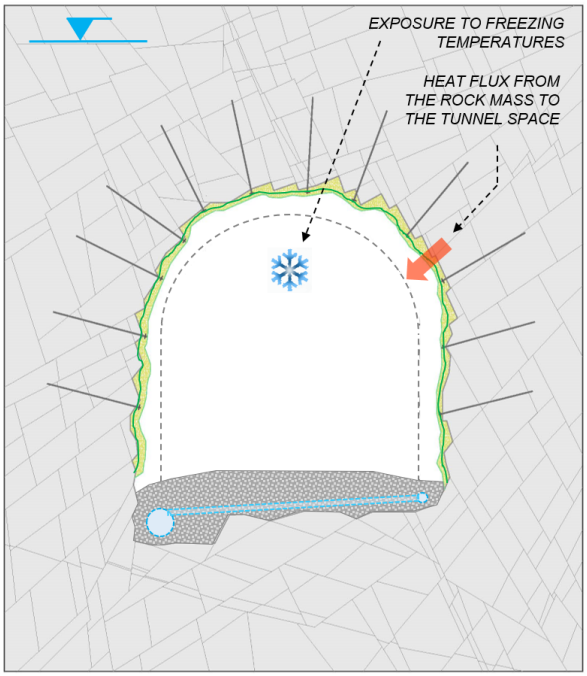

NTNU
Kunnskap for en bedre verden

Silje Marie Tinderholt

Heat Transfer – Between Rock Mass and Tunnel Room

A study of in-situ measurements and numerical simulations of temperature profiles through concrete and rock mass

Master's thesis in Tekniske Geofag
Supervisor: Karl Gunnar Holter
June 2019

Norwegian University of Science and Technology
Faculty of Engineering
Department of Geoscience and Petroleum

NTNU
Norwegian University of
Science and Technology

Abstract

Increasing utilization of bounded uninsulated lining systems in tunnels, and especially in rail tunnels, triggers the need for more information about how the bounded lining types functions during operation. Knowledge about how the air inside the tunnel influences the rock mass in an uninsulated tunnel is of great importance, especially when the temperature in the tunnel drops below zero degrees Celsius. Two tunnels are built with a bounded lining system and instrumented so that the temperature in the lining and adjacent rock mass can be logged. The Ulvin and the Gevingås Tunnel, constructed with respectfully a cast-in-place concrete lining, and a sprayed concrete and membrane structure.

The measurements from three succeeding winter seasons, from both tunnels, are presented. The data shows that at 1100m into the tunnel, the temperature in the rock mass does not drop below zero degree Celsius in any of the winter seasons.

The thermophysical properties of the Metasandstone which the Gevingås Tunnel is built through are tested, along with the mineral composition of the rock. The measurements showed that the thermal conductivity is the highest parallel to the foliation, the foliation is most likely composed of mica. The high content of quartz explains the high effective conductivity of the rock mass.

A COMSOL model is validated by utilizing both laboratory measurements and in-situ analysis. The laboratory for this project is a controlled environment, used to test the rock mass response to temperature loads. The in-situ analysis is based on the measurements from the Gevingås Tunnel. All the models used are primarily one-dimensional, built to illustrate the concrete and rock mass inward from the tunnel wall. A parameter estimation study is performed, to see which of the parameters the model is most sensitive towards, the study did not provide one unambiguous sensitive parameter but shows that control over the boundary conditions is the most important.

Two worst case scenarios are based on external temperature measurements from Værnes. The most extreme winter had 72 following days with temperatures below zero degrees Celsius. Using this as the external temperature in a numerical model, resulted in temperatures under zero degrees Celsius, up to 2.5m inward from the exposed surface.

Sammendrag

Bruk av tunnelkledning uten frostsikring er en økende trend, spesielt i jernbane tunneler. Dette er metoder som er lite brukt i Norge tidligere, og dermed er det også minimalt med kunnskap om hvordan kledningen faktisk fungerer over tid. Siden kledningen ikke er frostsikret, slik de tradisjonelle kledningene er, er det et spesielt behov for å øke kunnskapen om hvordan lufttemperaturen i tunnelen påvirker temperaturen i både kledningen og bergmassen når den faller under null grader celsius. Ulvintunnelen og Gevingåstunnelen er bygget med henholdsvis plass-støpt betonghvelv, og fiberarmert sprøytebetong med sprøytbar membran. Disse to tunnelene er begge instrumentert med måleutstyr, som måler blant annet luft-, betong og bergmasse temperaturen.

Temperaturmålinger fra tre sesonger for begge tunnelene er presentert. Temperaturen i bergmassen og betongen faller ikke under null grader på noe tidspunkt i disse sesongene, målingene er tatt 1100m fra portalen.

De termofysiske egenskapene til Metasandsteinen som Gevingåstunnelen er drevet igjennom er testet. Målingene viser at konduktiviteten er høyest parallelt med foliasjonen. Prøvestykkenes mineral sammensetning ble også testet, dette viste at foliasjonen mest sannsynlig består av glimmer. Det høye kvartsinnholdet i prøvestykkene, forklarer den relativt høye termiske ledningsevnen til bergarten.

En COMSOL modell er validert både ved å benytte et laboratorieforsøk og in-situ målinger. Forsøket i laboratoriet foregår under kontrollerte omgivelser, slik at sammenligningsgrunnlaget med en numerisk modell er optimalt. In-situ er den numeriske modellen sammenlignet med målingene fra Gevingåstunnelen. Alle de numeriske modellene er en-dimensjonale, geometrien er laget slik at den skal gjenspeile en linje gjennom betongkledningen og innover i fjellet. Et Parameter Estimering studie er gjennomført for å undersøke hvilke parameter den numeriske modellen er sensitiv ovenfor. Analysen kom ikke frem til en entydig sensitiv parameter, men viste viktigheten av å ha kontroll over grensebetingelsene i modellen.

To ekstreme temperaturbelastnings senarioer er simulert ved bruk av den validerte Gevingåsmodellen, dataen i senarioene er hentet fra en målestasjon ved Værnes. Simuleringen viste at en uisolert tunnel eksponert for en vinter med 72 påfølgende dager med temperaturer under null grader celsius, ga minusgrader inntil 2.5m fra tunneloverflaten.

Preface

This master thesis is the final part of my education in Engineering Geology and Rock mechanics at the Norwegian University of Science and Technology (NTNU). The work is carried out in the spring of 2019. I selected this topic to widen my theoretical perspective and because I was intrigued by the challenge of researching a topic that is relatively new in my field of study.

First of all, I would like to thank my supervisor Professor II Karl Gunnar Holter as well as co-supervisor Professor Erling Næss. Karl Gunnar's dedication, guidance, and motivation have helped me through this semester and driven me to perform my very best. Erling Næss's knowledge and guidance in a subject quite far from my own, has made this thesis possible.

Further, I would like to thank Torgeir Jensen at SINTEF for all the work he put into getting the laboratory working smoothly, and for taking me along on fieldwork in the Gevingås tunnel. I would also like to thank Gunnar Vistnes and Laurentius Tijhuis for the help and guidance in work relating to core extraction and XRD-analysis of the test specimen from the Gevingås Tunnel.

My greatest appreciation goes to Bane NOR for the financial support of this project. Without their support, the project would not have been feasible.

Last but not least, I would like to thank my classmates for five unforgettable years, and invaluable support and distraction through the writing prosses.

My dear Brage deserves my greatest appreciation for being my teacher on the topic of Parameter Estimation and simulation and, letting me borrow his personal computer when I needed more computation power, and most importantly for keeping my hopes up and always believing in me.

Trondheim, June 6, 2019
Silje Marie Tinderholt

Contents

List of Tables

List of Figures

Chapter 1

Introduction

1.1 Background - Modern rail-tunnels

In Norway Bane NOR has the responsibility of the national railway, which entails planning, developing, administrating, operating and maintaining the entire national railway system. Bane NOR has in recent years established that railway tunnels shall be constructed for 100 years of operation. This demand does not require large changes in current practice, as experience from several rail-tunnels, which have been in operation for over 100 years, support this requirement. However, modern and new solutions are important, when trying to ease inspection, and minimize the maintenance requirement of the tunnel, and by this also reducing the maintenance cost (Bane NOR, 2018*a*).

This master thesis focuses on rail tunnels, but since the Norwegian road authorities responsible for road tunnels go through some of the same modernization processes as Bane NOR, their finds and experiences are also of interest.

Water hitting the tunnel construction either as droplets or as running water, presents problems for the concrete and steel constructions and should be avoided in rail tunnels. Water that appears as moisture on walls or in the tunnel floor is generally not seen as an operational problem in rail tunnels. However, in combination with frost, free water represents a bigger challenge, because it can lead to build up of ice, which is not desirable neither in a rail or road tunnel. At the present, it is not realistic to make the rock mass watertight to the degree of eliminating the problem of leakage into the tunnel by means of injection (Bane NOR, 2018*a*). This means that the rock support system on its own is not sufficient as a tunnel lining.

The construction of a tunnel is based on the rock mass self-supporting capacity, this

primary construction is reinforced using rock bolts and reinforced sprayed concrete based on the Q-system (Bane NOR, 2018*a*).

Several types of water and frost protection methods have been tested. Today the most common structures can be divided into two main categories; the suspended and bounded systems. Of these categories, the suspended system can be seen as the traditional method. There are two lining types under this umbrella, namely suspended concrete arches and PE-foam arches. The bounded structures are cast-in-place concrete structures with sheet membrane, and sprayed concrete with a sprayed membrane, (Bane NOR, 2018*a*). The latter method is newer and not used to the same extent as the traditional methods. Under development is also a watertight sprayed concrete, which will function as a bounded structure.

Traditionally water and frost protection have been seen as one and the same structure. However, frost and water protection do not serve the same purpose, and one should consider using structures with only the protection that is needed in the given project. Experience in Norway shows that there are seldom problems related to mechanical fracturing/erosion in connection to water freezing in the rock mass or the rock reinforcement structure. Based on this, one can argue that there is no need for frost protection, i.e., insulation (Bane NOR, 2018*a*).

Given that there is no need for insulation to prevent water from freezing in the adjacent structure, one has for the suspended structures two choices. Either it is having frost protection which prevents the water from freezing in the air gap between rock support and lining structure, or using only water protection and dimensioning the structure so that it can carry the weight of the ice (Bane NOR, 2018*a*).

For the bounded lining constructions, there is limited knowledge on how cold temperatures influence the lining structure. Therefore when building the Ulvin Tunnel and the Gevingås Tunnel, sensors were installed to get a better picture of how the tunnel temperature influences the temperature inside the bounded structures (Bane NOR, 2018*a*).

1.1.1 Lining types

Lining structures, built with suspended concrete elements, uses sheet membrane installed behind the concrete element as water protection. If there is a need for frost protection, insulation is installed between the concrete element and the sheet membrane, Figure 1.1. Because the structure consists of several elements that might fail, there is a need for inspection of the structure and repairs through the structure's lifetime, never the less the structure is seen as a robust lining type. The suspended concrete lining is no longer used by Bane NOR, because they wish to eliminate the need for inspection behind the lining (Bane NOR, 2018*a*).

The other suspended structure uses PE-foam and sprayed concrete as a frost insulated water protection, without room for using only the water protecting abilities,

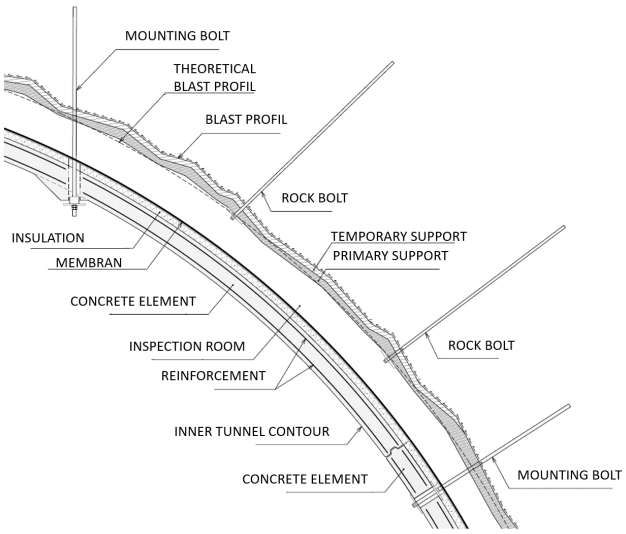

Figure 1.1: Traditional tunnel lining, suspended arch of concrete elements, reworked (Bane NOR, 2018*a*).

Figure 1.2. Bane NOR has decided to no longer use the PE-foam lining. There are several reasons why, one of which is that the PE-foam is highly flammable, and when using this construction type, one builds in large amounts of flammable material. Further, the construction is demanding to install, which results in uncertainty related to the quality of the finished structure. The lining also has an uncertain lifetime, and maintenance is challenging to perform. Because the structure is not dimensioned to carry a block of 60kN, which is the requirement after the accident in the Hanekleiv tunnel, one must perform inspections behind the lining. Inspection behind the lining does not only demand an increase of the tunnel contour but also presents a risk for the person performing the inspection (Bane NOR, 2018*a*).

Cast-in-place concrete with sheet membrane, is a continuous structure with no insulation, Figure 1.3. Fracturing due to frost is not seen as a problem, because the concrete is dry and protected from the water supply by the sheet membrane. Since this structure has fewer components that might fail, compared to the suspended linings, it is seen as a robust lining. Mistakes or flaws in the structure must be noticed under construction, because the maintenance of the membrane and structure is not possible afterward. However, if the structure is installed correctly, there will be no need for maintenance in the structure's lifetime (Bane NOR, 2018*a*).

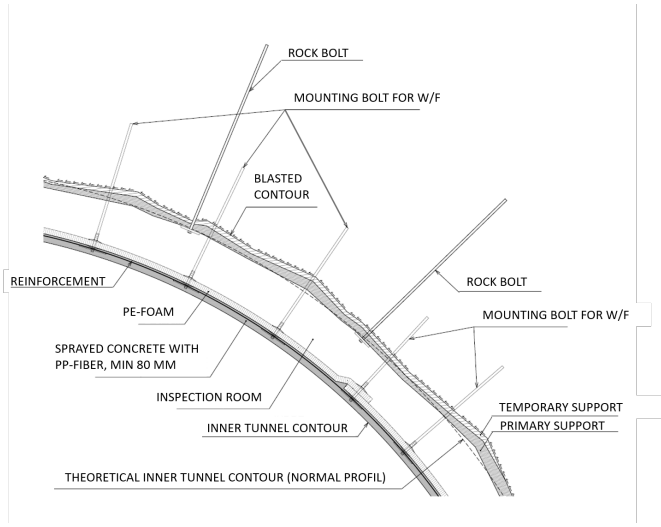

Figure 1.2: Traditional tunnel lining, suspended arch of PE-foam, reworked (Bane NOR, 2018*a*).

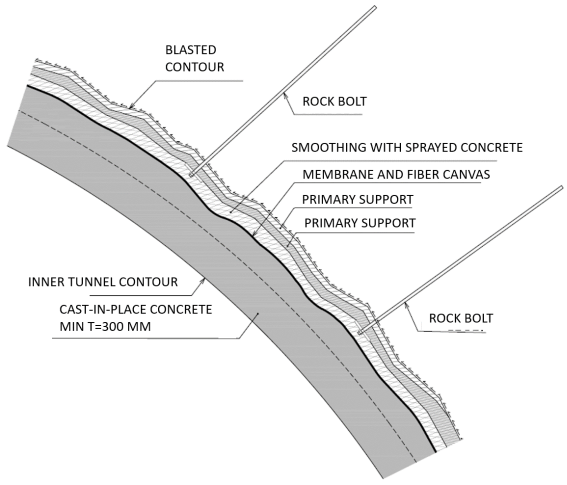

Figure 1.3: Bounded tunnel lining, cast-in-place concrete structure with sheet membrane, reworked (Bane NOR, 2018*a*).

The bounded system, using sprayed membrane in combination with fiber reinforced concrete, functions only as water protection and is therefore subjected to freezing. The membrane is sandwiched between two layers of concrete, Figure 1.4.

The structure is easy to install, but can't be installed on areas with leaking water. The method can work well in a hard rock environment, as in Norway, if the membrane material and the installation method is improved. There is expected some maintenance of this structure, in connection to point leakage (Bane NOR, 2018*a*).

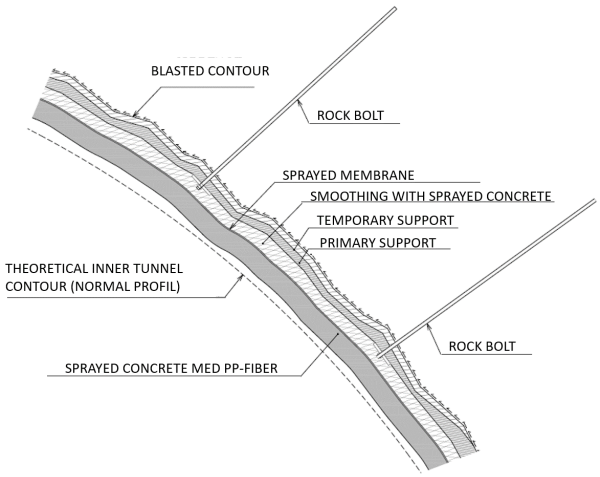

Figure 1.4: Tunnel lining, sprayed concrete structure with sprayed membrane, reworked (Bane NOR, 2018*a*).

The bounded structures have an advantage towards the suspended structures, because the bounded structures give a better overview of the condition and stability of the primary structure, without having to perform inspection behind the lining in a tight space. The bounded structures also have less mechanical components that can fail, compared to the suspended structures, which explains Bane NOR's decision only to use the bounded structures in the future (Bane NOR, 2018*a*).

The Norwegian road authorities still have the traditional lining methods in their building manuals, Håndbok, but the Norwegian road authority presents the cast in place concrete structure as a possible replacement for the traditional lining structure, because the cast in place concrete can be used for every degree of frost. The road authorities also emphasize the pros related to fewer construction elements. Fewer elements mean less building material which can be ruined by corrosion, therefore the lining is recommended especially for subsea tunnels where the environment is especially corrosive. The road authorities also highlight that the bounded system has no air gap behind the lining, which reduces the possibility of frost formation and hazardous fires (Statens vegvesen, 2016).

Experience from Norwegian road authorities shows that the reason for the largest amount of downtime is related to planned work. Planned work is categorized as maintenance of technical installation or building structures. The bounded structures have less downtime than the traditional structures. The main reason for a decrease in closed tunnel time, is related to the fact that the *new* methods require less rehabilitation than the traditional building techniques (Johansen, Johnny M. and Holen, Åsmund, 2012).

The *new* bounded systems will most likely reduce the need for tunnel downtime related to maintenance work and control of the lining, saving money both in the workforce and the need for traffic diversion. At the same time reducing the inconvenience, a closed tunnel has for the road and rail user. One can also save money on a smaller tunnel profile, because there is no need for an inspection room. However, the new methods demand a smoother blast contour, because a smoother contour uses less concrete and causes less damage to the adjacent rock mass, which gives fewer paths for the water to travel along. The demand for a smoother contour might cost more under construction, but saves money in the concrete costs.

1.1.2 Celsius hours - what now?

In Norway the climate changes through four seasons. In the winter time most places experience some degree of negative temperatures, which can result in ice formation. Therefor knowledge about how the outdoor temperature affects the temperature conditions inside the tunnel and inside the tunnel lining, is of great importance, especially when building infrastructures which are supposed to stand for 100 years.

The temperature on the earth surface is controlled by the amount of solar energy and the heat transfer to the atmosphere. Inside tunnels, the radiation from the sun can be neglected, but the convective heat transfer between the tunnel air and rock mass is of great importance (Pedersen, 2002).

Today the frost protection in a tunnel is based on the Celsius hour principle. The amount of frost is in this method defined as the time integral of negative temperatures through the winter. For the construction of road tunnels F_{10} is used as the dimensioning criteria. F_{10} is the amount of frost that is statistically exceeded one time every ten years. For rail tunnels F_{100} (h^oC) is used as dimensioning criteria (Pedersen, 2002). The amount of frost expected in an area is based on outdoor temperature measurements. This means that in this method, the amount of frost expected outdoors is also expected inside the tunnel.

Taking the outdoor temperature as the only dimensioning criteria, the solar radiation and the heat transfer to the atmosphere is the only mechanisms that effects temperature inside the tunnel. However, the need for frost protection depends on the surface temperature and the temperature inside the concrete lining and rock mass. As discussed, the main mechanisms controlling the temperature on the lining surface and inside the lining, is convection and conduction.

Based on this brief discussion, the Celsius hour method can be seen as too conservative, mostly because one does not take into consideration the heat transferred from the rock mass. The *new* lining methods have no insulation, meaning that the heat transfer from the rock will, to a larger extent, influence the tunnel air, than what is the case for the traditional methods. Therefore the Celsius hour method might fit the bounded linings less than the traditional lining types. The result of a conservative model, is an overuse of insulation in tunnels, and by this unnecessary financial expenses (Bane NOR, 2018*a*).

The concept of heat conduction and convection is the main focus of this thesis, and the goal is to obtain a better understanding of how the tunnel air temperature affects the lining temperature, by means of these heat transfer mechanisms.

1.2 Objective

This master thesis is a continuation of a project thesis written on the same topic in the autumn of 2018, (Tinderholt, 2018). This master thesis aims to build on the knowledge obtained through the work performed in the project thesis, so that one can estimate the temperature distribution in the tunnel contour, given the external temperature. Moreover, gain knowledge about the temperature conditions in a bounded lining, without insulation, which there is limited knowledge about, despite increasing use.

The main objectives of this Master's project are:

1. Field measurements of temperature from the Ulvin Tunnel and Gevingså Tunnel.
2. Validation of COMSOL - The existing numerical model from the project thesis is reworked and further evaluated based on laboratory tests. Recommended implementations presented in the project thesis are carried through.
3. In-situ validation of COMSOL - A numerical model of a real-life situation, the Gevingås Tunnel, is compared with the presented measurements from the tunnel.
4. Parameter Estimation study - To improve the numerical model of an in-situ case.
5. Scenario analysis - Evaluating the response of actual measured temperature loads on the tunnel lining, using the numerical model of the Gevingås Tunnel.
6. Evaluation of further work

The main objective is to find a method for predicting the temperature variation in the rock mass, due to varying surface conditions in the tunnel.

1.3 Limitations

The thesis has a main focus on rail tunnels, constructed with bounded lining, which are used to an increasing degree.

Data used in the thesis are mainly measurements from two tunnels, the Ulvin, and the Gevingås Tunnel, in the period from November 2015 to early April 2019. The data-set is not complete for all the measurement configurations, full insight to the data is presented in Chapter 3. The Ulvin Tunnel is constructed entirely with the bounded lining, but the Gevingås Tunnel is partly constructed with PE-foam. Visual inspection of the sensors is impossible, as they are mounted inside the tunnel wall, which limits the control over the state of the sensors.

The numerical program used is COMSOL, the author's knowledge of the program, can be seen as a limitation, but experience from the project thesis and help from the COMSOL support team should reduce the impact of this limitation.

The numerical simulations performed in COMSOL are mainly one-dimensional analysis, which alone is a clear limitation. Water is not taken into consideration in the numerical model, and the material properties are held constant, as is the heat transfer coefficient. In the numerical model, the sprayed membrane neglected.

The author's knowledge of the Principles of Heat Transfer must be considered in light of her educational background, which is a five-year education in Engineering Geology and Rock Mechanics.

1.4 Methodology

Figure 1.5 is a flow chart showing a course outline of the work performed throughout this master thesis.

Analysis

The initial literature study gave an overview of the Ulvin and Gevingås Tunnel. Information about the measuring configuration and material properties was appropriated.

Field and Laboratory testing

In total, three field inspections have been made, one in the Ulvin Tunnel, in connections with the project thesis in the autumn of 2018, and two in the Gevingås Tunnel in connection to this master thesis. The first inspection in the Gevingås Tunnel was performed night to the first of February, mainly in the escape tunnel, where a rock specimen was collected for testing of thermophysical properties. The second inspection in the Gevingås Tunnel, took place night to the ninth of April. The main focus under this inspection was to change batteries and collect data

from tunnel air sensors, and investigate the moisture conditions around the two measuring stations.

Laboratory tests were performed to acquire information about the thermophysical properties and the mineral composition of the rock mass in the Gevingås Tunnel.

Measurements in-situ

The measurements collected from the two tunnels, provided information about the tunnel air temperature, and temperature in the adjacent building material, throughout several winter seasons.

The data from the Gevingås and Ulvin Tunnel is presented in Chapter 3. Here the data is reworked and presented as illustratively as possible. The data is either presented as exact measures or as an average. The four-day average is obtained by first finding the daily average, and then the moving four-day average. The moving average calculates the average of four succeeding days, and then moves one day, finding the average of the next four, giving an overlap of three days with the previous result. This method is discussed in Chapter 7, evaluating it to a similar way of presenting data.

Numerical simulations

The numerical simulations are performed in COMSOL. Validation of the numerical model is performed using measurements from a controlled laboratory environment. The model is also validated using in-situ measurements from the Gevingås Tunnel. A Parameter Estimation study is performed using the Gevingås model to get insight into the sensitivity of the model.

Scenario analysis

The in-situ validated and improved model is used in a scenario analysis, looking at the impact of two cold winters, using measurements from the Norwegian Meteorological Institute station at Værnes.

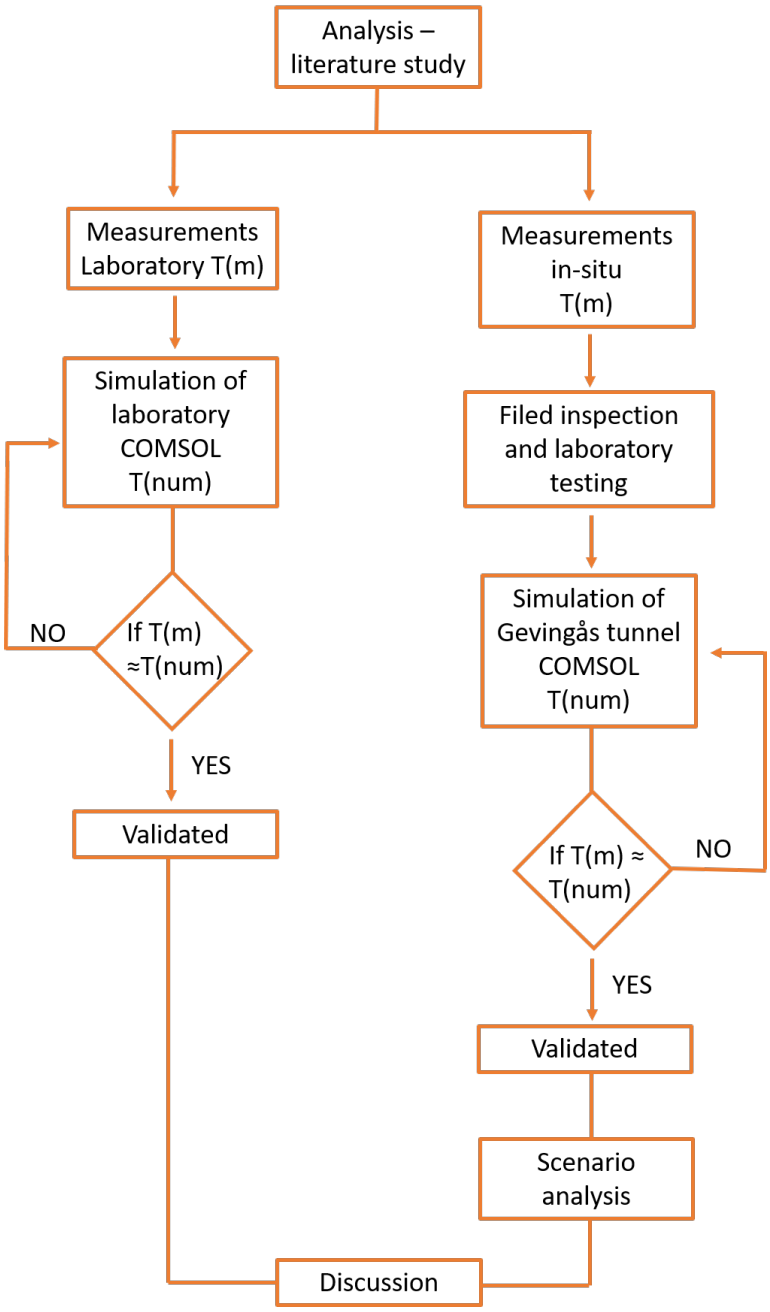

Figure 1.5: Flow chart indicating the main steps in the master thesis.

Chapter 2

Test sites

Two tunnels constructed with bounded lining, have been installed with measuring equipment, to get a better understanding of the temperature conditions inside the tunnel, and inside the lining and adjacent rock mass. The Ulvin Tunnel, located close to Oslo, is built with cast-in-place concrete. The second tunnel presented is the Gevingås Tunnel, located near Trondheim. In the Gevingås Tunnel, three sections of the lining are built with sprayed membrane and sprayed concrete.

This chapter presents the tunnels geometry, instrumentation, and the thermophysical properties of the building material. The measurement from both tunnels are presented and evaluated in Chapter 3.

2.1 Ulvin Tunnel

The Ulvin Tunnel is constructed with a bounded lining, using cast-in-place concrete, and is the first railway of its kind in Norway, Figure 2.1.

The Ulvin Tunnel is part of the Dovrebane, a railway line from Eidsvoll to Trondheim. The tunnel is constructed as a double-track, with a total length of 3985m, an average profile of 139.8m^2, and a span of 13.9m (Drevland et al., 2014).

2.1.1 Geometry and construction materials

When using the cast-in-place structure, this functions as water protection and has no load-bearing function. As a building principal, the primary rock support is based on the rock mass self-supporting capacity. The permanent rock support uses the self-supporting capacity along with the Q-system. The Q-system is a dimensioning

Figure 2.1: Ulvin Tunnel, (Ausland and Jonsson, 2014)

criterion, which recommends the amount of rock support that is required. The rock support is then a combination of rock bolts in a pattern, and sprayed fiber reinforced concrete (NGI, 2015).

The waterproof lining is constructed with smoothing concrete, sheet membrane, and unreinforced cast-in-place concrete, as shown in Figure 1.3. A fiber canvas is installed between the smoothing concrete and the sheet membrane. The membrane installed in the Ulvin Tunnel is 2mm thick thermoplastic polyolefin (TPO) sheets, which serve as the water protection. Figure 2.2, shows the installation of the membrane.

In the access tunnel, 60 linear meters of the lining is constructed with a sprayed membrane. This section is constructed as a full-scale test area. Lining thickness in the test section is 300mm, with the membrane located 150mm from the tunnel lining surface (Holter and Geving, 2016).

When considering the temperature distribution through the lining, the rock mass behind the structure is of interest. The Ulvin Tunnel is built in Gabbro and Granitic gneiss, Figure 2.3. The granitic gneiss has a texture of fine to average sized grains, with light veins in southeast, (NGU, 2019). The thermophysical properties of the bedrock and the sprayed concrete in the test site in the Ulvin Tunnel are listed in Table 2.1 and 2.2. The thermophysical properties of the bedrock in the access tunnel are representative for the rock around the main tunnel.

Figure 2.2: Installation of sheet membrane in the Ulvin Tunnel (Ausland and Jonsson, 2014).

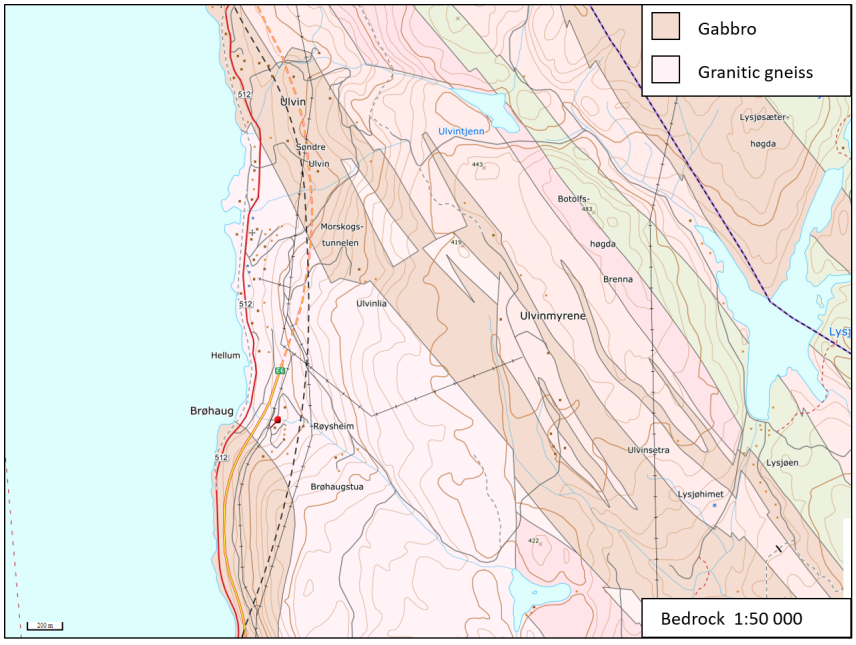

Figure 2.3: Bedrock map of the Ulvin site, (NGU, 2019).

Table 2.1: Thermophysical properties from the bedrock in the access tunnel at Ulvin, (Holter and Geving, 2016) and (Holter, 2016)

Rock type	Dark gneiss
UCS of intact rock	>140 MPa
Rock quality, Q	approx. 0.5
Density (kg/m^3)	2616
Thermal conductivity (W/m*K)	2.95

Table 2.2: Thermophysical properties of the sprayed concrete in the access tunnel at Ulvin, (Holter, 2016).

Sprayed concrete steel fiber	Density (kg/m^3)	Thermal conductivity (W/m*K)	Degree of Capillary saturation, DCS (%)
Dry	2138	1.64	70
Saturated	2214	1.85	100

2.1.2 Instrumentation

Cast-in-place tunnel lining is as mentioned a relatively new method in Norway. In order to collect knowledge about the lining, the tunnel is instrumented in four sections. Two different companies have installed sensors. SINTEF has measurements of different air parameters, one located inside the tunnel, the blue dot in Figure 2.4, and one outside each portal, yellow dots in Figure 2.4. In the measuring location inside the tunnel, the concrete is also installed with temperature sensors.

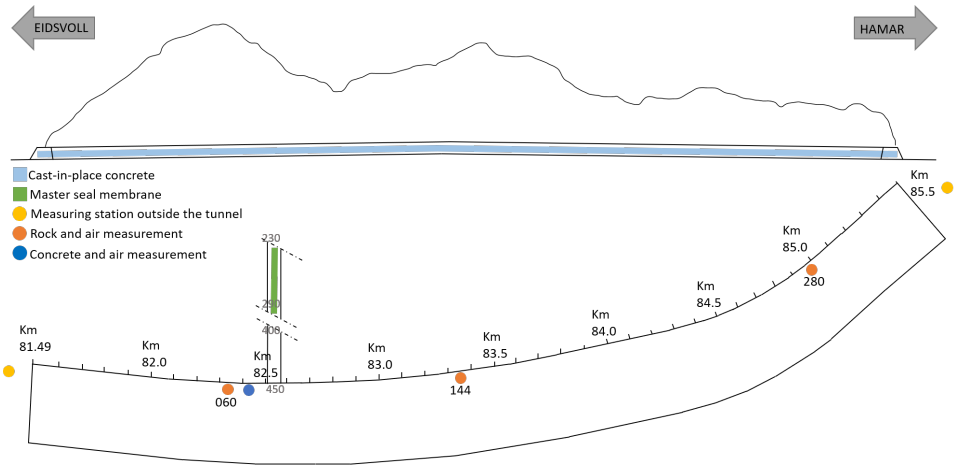

Figure 2.4: Horizontal and vertical cross section of the Ulvin tunnel, showing the rock mass cover, location of instrumentation and lining types, modified by author based on (Bane NOR, 2018*b*)

Cactus Geo AS has three measuring locations, indicated by orange dots in Figure 2.4. In every location, the strain on the concrete arch is measured. Pore pressure measurements are performed behind the arch inside the rock mass. Sensors measuring temperature are placed in the rock, concrete, and on the lining surface. Wind velocity inside the tunnel is also measured on the tunnel surface.

SINTEF loggers save the data locally in the loggers and transfer the data via a cellular network. The data from Cactus Geo is collected from a web page, where one also can confirm the correct operation of the sensors.

Temperature sensors in the concrete lining, SINTEF

The temperature sensors in the concrete structure were installed before the arch was cast, Figure 2.5. In total, nine temperature sensors, pt1000, are installed per location. The sensor rods were made adjustable by splitting the rod in two, to accommodate for varying arch thickness. The inner rod is welded to the tunnel membrane and has three sensors, and the outer rod consists of six sensors. In total the concrete is instrumented with three of these instrumentation configurations.

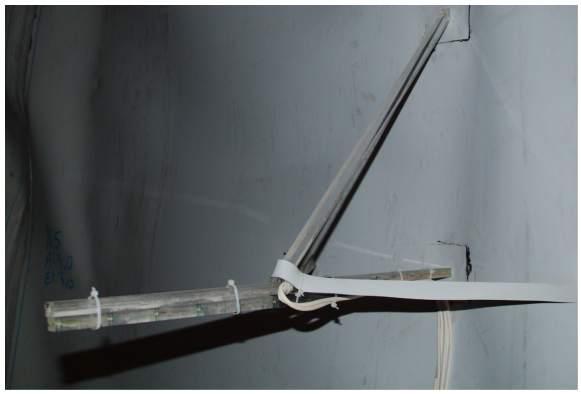

Figure 2.5: Setup of rods before the concrete arch is caste. Extra support was installed in the horizontal and vertical direction to prevent rotation or other movements of the rod under the construction of the arch (Torgeir Jensen, SINTEF).

Under construction, the outer most sensor in two of the measuring locations, as well as the second sensor in the third measuring location, stopped working. This means that the outermost measurement is only based on one sensor. The remaining eight sensors in all measuring locations are all operational.

The pt1000 sensors mounted on Plexiglas rods are located every sixth centimeter inward in the structure; this results in an overlap. The three sensors on the inner rod overlap the three last on the outer rod, shown in Figure 2.6.

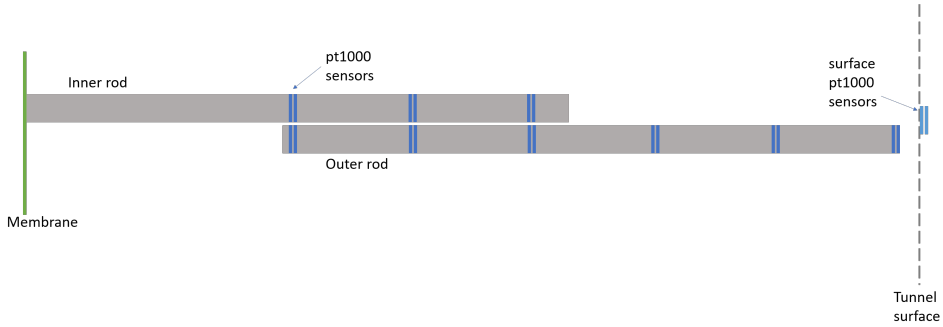

Figure 2.6: Principle sketch of sensor placement in the concrete arch. Distance between sensors are 6cm, first sensors in outer rod is located 1cm from the tunnel surface.

After the construction, the placement of the sensors where remeasured, and one of the rods had experienced some movement. Table 2.3 shows the measured location of the sensors.

Table 2.3: Placement of pt1000 sensors in the concrete arch in the Ulvin Tunnel, for each of the three measuring locations.

Pos	T1	T2	T3	T4	T5	T6	T7	T8	T9
K1 [m]	X	0.06	0.12	0.18	0.24	0.30	0.18	0.24	0.30
K2 [m]	X	0.06	0.12	0.18	0.24	0.30	0.18	0.24	0.30
L1 [m]	0.01	X	0.13	0.19	0.25	0.31	0.19	0.25	0.31

Three pt1000 surface temperature sensor was installed on the concrete surface in the rod positions after the concrete arch was finished, Figure 2.7.

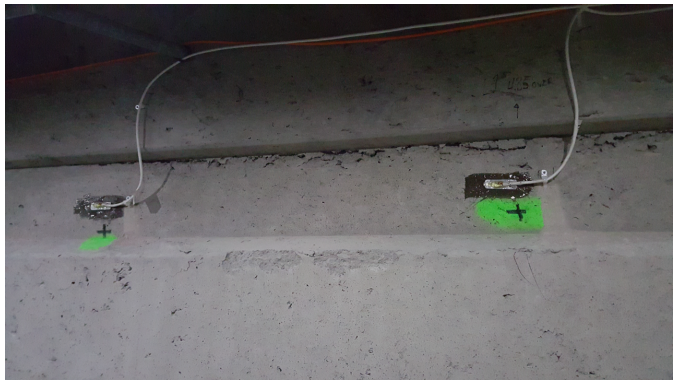

Figure 2.7: Surface measurements, sensor corresponding to K1 (right) and K2 (left), L1 is mounted 4.85m above (Torgeir Jensen, SINTEF).

Instrumentation in rock mass, Cactus GEO

The instrumentation operated by Cactus Geo is located in three different sections in the tunnel, each section consists of five measuring points along the contour, shown in Figure 2.8. The three sections are located 800m (060), 1865m (144) from the south portal, and 510m (280) from the north portal.

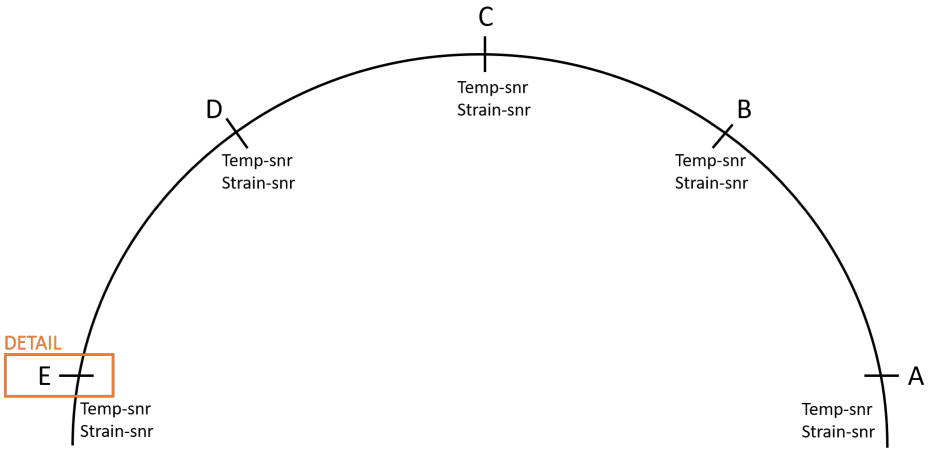

Figure 2.8: Measuring location, the configuration shown is equal in all three-cross section, 060, 144 and 280, as shown in Figure 2.4. The direction inward in figure is towards north, Hamar.

In each measuring point along the tunnel contour, there are sensors at 1, 3, 5, and 7 meters of rock mass depth, Figure 2.9. These sensors measure pore pressure and temperature. On the surface of the tunnel lining, at each measuring point, strain and temperature are measured. 25cm from the tunnel contour, the temperature is measured in the concrete, Figure 2.10.

The data presented from the instrumentation operated by Cactus Geo are all collected from the sensors in point A. The choice is based on the theory that the side wall is exposed to the coldest air, and the goal is to evaluate the effect of the absolute lowest temperatures in the tunnel.

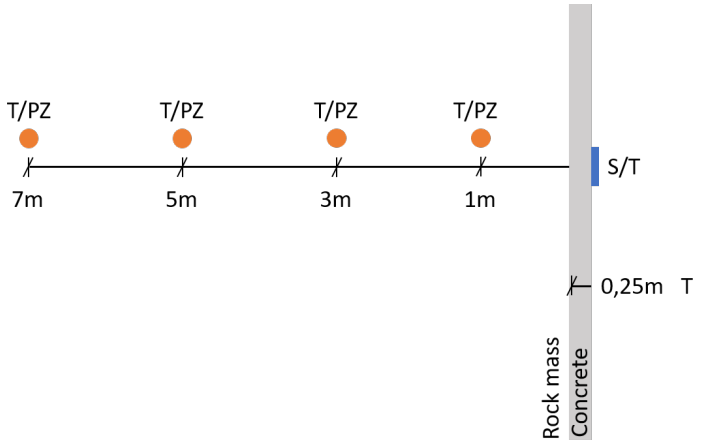

Figure 2.9: Placement of sensors, this configuration is an enhanced detail from measuring location E in Figure 2.8. The configuration is equal in all five locations along the tunnel contour. The abbreviations show which type of measurements the sensors take, T-temperature, PZ-pore pressure and S-strain.

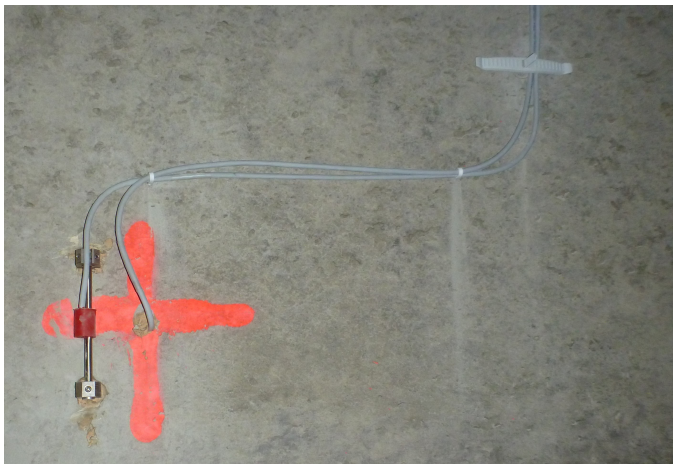

Figure 2.10: Picture of surface sensors in the Ulvin Tunnel, shows the hole leading to the concrete measurements and the surface sensor (Atle Gerhardsen, Cactus Geo).

Measures of tunnel air, SINTEF

Parameters connected to the tunnel air is also measured. Transport of air is measured continuously between two ultrasound sensors mounted on the tunnel wall, and a station measures the air temperature, barometric pressure, and humidity.

Table 2.4 shows the air parameters that are logged in the Ulvin Tunnel, with the most relevance to this thesis.

Table 2.4: Parameters of air being logged by the station positioned inside the Ulvin Tunnel. RH stands for relative humidity. The transport of air is more thoroughly logged than what is shown in this table.

Air measurements					
Parameter	Speed	Volume	Temperature	Barometer	RH
Unit	m/s	m^3	°C	kPa	%

Instrumentation on the outside of the tunnel, SINTEF

The measuring stations on the outside of the tunnel measure air temperature, barometric pressure, and humidity, Figure 2.11. For the stations to measure through the whole year, they are installed with solar cells and batteries. The stations are also installed with mechanical ventilation controlled by thermoelements, to prevent high temperatures in the summer months. Table 2.5 shows the parameters most relevant to this thesis that are logged by the stations positioned outside.

Table 2.5: Parameters of air being measures by the station positioned on the outside of the tunnel.

Air measurements outside			
Parameters	Temperature	Humidity	Barometer
Unit	°C	%	kPa

Figure 2.11: Measuring station on the outside of the tunnel, Ulvin (Torgeir Jensen, SINTEF).

2.2 Gevingås Tunnel

The Gevingås Tunnel is a 4500m long rail tunnel. The single-track tunnel is a part of the Norlandsbanen, which goes between Trondheim and Bodø. The tunnel was opened for traffic in August of 2011.

2.2.1 Geometry and construction materials

In 1.9km of the tunnel, the lining is constructed as a bounded system, with a sprayed membrane, Masterseal 345, and sprayed concrete. For the remaining parts of the tunnel, the traditional method with suspended waterproofing of polyethylene foam sheets is used (Holter and Geving, 2016). The building principle for these two lining types are shown in Figure 1.4 and 1.2.

The rock mass is the primary building material when constructing a tunnel. Therefore the local geology is of interest. Figure 2.12 shows the bedrock in the area where the Gevingås Tunnel goes through. The Moraine is a glacially formed assortment of glacial debris, composed of gravel, sand, and clay. The tunnel crosses for the most part Metasandstone, with thin veins and dark gray thinly foliated shale alternating with phyllite. The Conglomerate is mixed well, and partly Conglomerate Greywacke. Depending on how the rock layers are oriented, the tunnel might or might not cross the Tuffite composed of Rhyolite, (NGU, 2019).

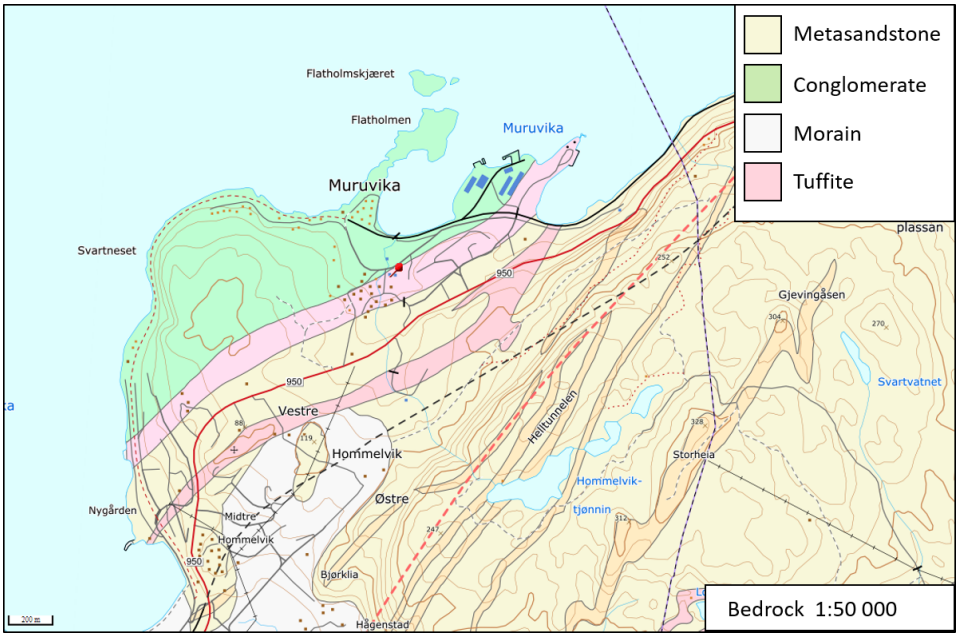

Figure 2.12: Bedrock map at the Gevingås site, (NGU, 2019)

The main material properties in the Gevingås Tunnel are listed in Table 2.6 and 2.7.

Table 2.6: Thermophysical properties from the bedrock in the Gevingås Tunnel, (Holter and Geving, 2016) and (Holter, 2016).

Rock type	Dark mica-schist, meta-sandstone, greywacke
UCS of intact rock	Not measured, >100 MPa
Rock quality, Q	3-4
Density (kg/m^3)	Table 2.8
Thermal conductivity (W/m*K)	Table 2.9

Table 2.7: Thermophysical properties from the concrete in the Gevingås Tunnel, DCS abbreviation for degree of capillary saturation and COV for coefficient of variance, (Holter, 2016).

Sprayed concrete PP fiber	Density [kg/m^3]	Thermal conductivity [W/(m K)]	COV %	DCS %
Dry	2211	1.65	70	0.5-1
Saturated	2281	1.85	100	2-3

Testing of thermophysical properties

The density, heat capacity, and thermal conductivity of the rock mass in the Gevingås Tunnel is not known. To be able to later perform a numerical simulation, which can be compared to the measured results from the tunnel, these thermophysical parameters should be known.

On the first of February in 2019, a survey in the Gevingås Tunnel was performed in the escape tunnel, parallel to the rail tunnel, and a rock specimen for testing was collected, Figure 2.13a. The specimen is from the Metasandstone area of the tunnel.

The rock has in this specimen a clear stratification, and the cores which are to be tested, are therefore extracted parallel and perpendicular to these structures. This allows evaluating if the structures affect the thermophysical properties, especially the conductivity, and at the same time, obtain more representative values for the parameters. Figure 2.13a shows the rock specimen ready for core drilling. Two discs in each direction, with a diameter of 60mm and a height of 30mm, are prepared for testing, Figure 2.13b. The specific properties of the core discs are tabulated in Table 2.8.

HotDisk TPS5500 transient plane-source apparatus, design according to the ISO-22001-7 standard, is used to test the thermophysical properties of the rock mass. The sensor used is a HotDisk 5501 with a radius of 6.401mm. The sensor is placed

between the two disks, with the same orientation to the lineament, in total, ten separate measurements are performed for each measuring set (Schlemminger and Ness, 2013).

(a)

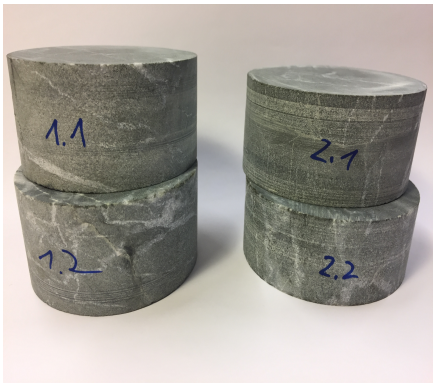

(b)

Figure 2.13: **(a)** Rock specimen from Gevingås Tunnel, ready for core drilling (Date: 05.02.19). **(b)** Core specimens used for testing of thermophysical properties. 1.1 and 1.2 are drilled parallel to the stratification, and 2.1 and 2.2 are collected perpendicular to the lineament (Date: 06.02.19).

The thermal conductivity is measured perpendicular to the sensor, k_{ax}, that is along the axis of the specimen, and parallel to the sensor, k_{rad}. The thermal diffusivity, α, is also measured and defined as:

$$\alpha = \frac{k}{\rho \cdot c} \, [\mathrm{m}^2/\mathrm{s}] \tag{2.1}$$

$$\text{where } k = \sqrt{k_{ax} \cdot k_{rad}} \, [\mathrm{W}/(\mathrm{m\ K})] \tag{2.2}$$

ρ [kg/m^3] the density of the specimen and c [J/(kg K)] the specific heat capacity. The average values of the 10 independent measures are presented in Table 2.9.

Ramstad et al. (2015) tested and mapped the thermal conductivity in the Oslo region. In total, 1,398 rock samples were used to calculate the thermal conductivity for the geological units in the area. Ramstad et al. (2015) found that the thermal conductivity in the data varied a great deal, with the most considerable variations found in the sedimentary and metamorphic rocks. Further, the study showed that

Table 2.8: Properties of core specimens used to test thermophysical properties.

	1.1	1.2	2.1	2.2
Diameter [mm]	59.2±0.05	59.01±0.1	59.3±0.05	59.2±0.05
Height [mm]	30.3±0.1	31.5±0.2	29.1±0.1	25.3±0.2
Mass [g]	226.128	235.673	220.21	186.21
Density [kg/m^3]	2711.6±13.5	2708.9±26.5	2740.0±14.0	2673.9±25.5

Table 2.9: Results from the test of the thermophysical properties, presented as the average of ten independent measures.

	Specimen 1	Specimen 2	
k_{ax}	4.03±0.03	3.60±0.07	[W/(m K)]
k_{rad}	4.00±0.13	4.46±0.05	[W/(m K)]
k_{eff}	4.0±0.2	4.2±0.1	[W/(m K)]
α	$2.144{\cdot}10^{-6}{\pm}22{\cdot}10^{-9}$	$1.568{\cdot}10^{-6}{\pm}33{\cdot}10^{-9}$	[m^2/s]
c	688±10%	979±10%	[J/(kg K)]

the thermal conductivity in foliated rocks is the highest parallel to the foliation. Because of the significant variations found within a rock that is seemingly the same type, Ramstad et al. (2015) expresses the need for a large number of samples to obtain a legitimate statistical value.

Based on this study, the four samples used in the analysis of the Gevingås bedrock is not statistically sufficient, but the data is still presented as representative values.

The results show that the thermal conductivity is the highest parallel to the foliation, that is $k1_{ax}$ is higher than $k1_{rad}$ and $k2_{ax}$ is lower than $k2_{rad}$, which corresponds well with the results from the study in Oslo, (Ramstad et al., 2015). The result might indicate that the lineament in the rock mass functions as insulation, for a more understandable image the lineament can be compared to a resistance element in an electrical circuit.

The thermal conductivity varies in regards to the measuring direction, but the effective thermal conductivity is close to equal for both test specimens. The calculated effective thermal conductivity is just outside the upper 3rd quartile of the thermal conductivity to Sandstone in the Oslo region, (Ramstad et al., 2015).

The deviation in the measured specific heat capacity between the two test specimens is relatively large, but the reason for this is unknown.

Analysis of mineral composition

The measured thermal conductivity is relatively large, compared to other common rock types in the Norwegian bedrock. A Greenstone which is an abundant rock

type in the Trondheim area has a thermal conductivity of 3.14 [W/m K], and a Gabbro or Syenite has a thermal conductivity of 2.62 [W/m K]. The thermal conductivity depends on the rock's mineral composition, as well as the lineament and abundance of each mineral. Of some of the most common minerals, Quartz has the highest thermal conductivity 7.68 [W/m K], whereas Feldspar and Mica are at the lower end, with respectively 1.98 and 2.09 [W/m K] (Nilsen, 2016). Because the mineral composition of the rock influences the thermal conductivity, it is of interest to measure the composition of the test specimens.

An XRD-analysis is performed at the NTNU laboratory. The result from the analysis is presented in Figure 2.14, the analysis graphs are found in Appendix A.1.

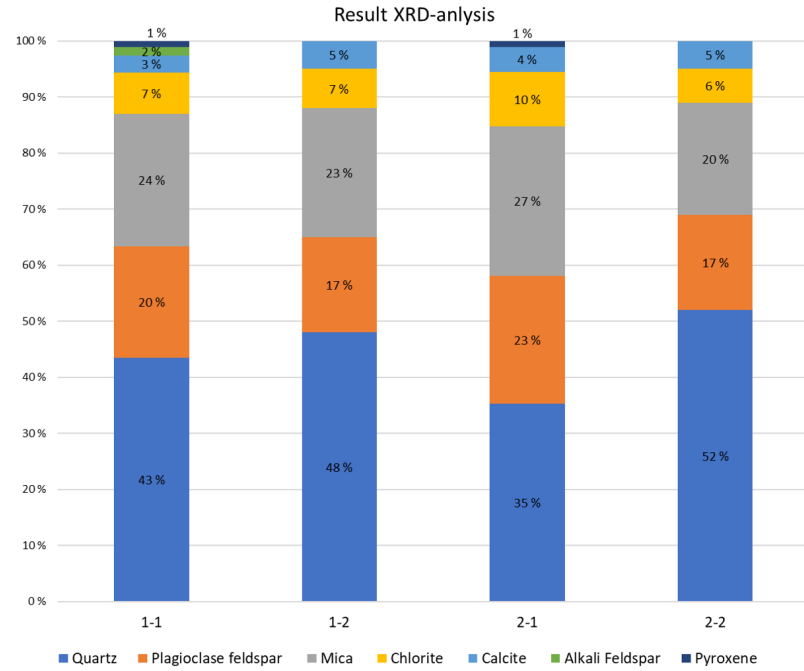

Figure 2.14: Result from XRD-analysis, the x-axis corresponds to the numbering of the core discs. The values are rounded up to nearest integer.

The results are rounded up to the nearest integer, and the components that are under 1% are excluded from the results. The compounds that are just above one percentage should be verified by analyzing a thin section in a microscope. This verification is not done for this test, because it is the compounds with the largest presence that affect the thermophysical properties the most.

The high thermal conductivity is most likely connected to the high amount of quartz in the rock. Specimen 2.1 has the highest content of mica, and it is also

specimen two that has the most significant difference between the axial and radial thermal conductivity - the orientations of the mica functions as an insulating material.

2.2.2 Instrumentation

Figure 2.15 shows the length profile of the Gevingås Tunnel, both as a vertical and horizontal cross section. The circles indicate the position of the measuring station inside the tunnel. In two of the locations, indicated by blue points, the measuring configuration is as shown in Figure 2.16 and 2.17. The remaining stations measures only the tunnel air, the exact location of these stations are shown in Table 2.10.

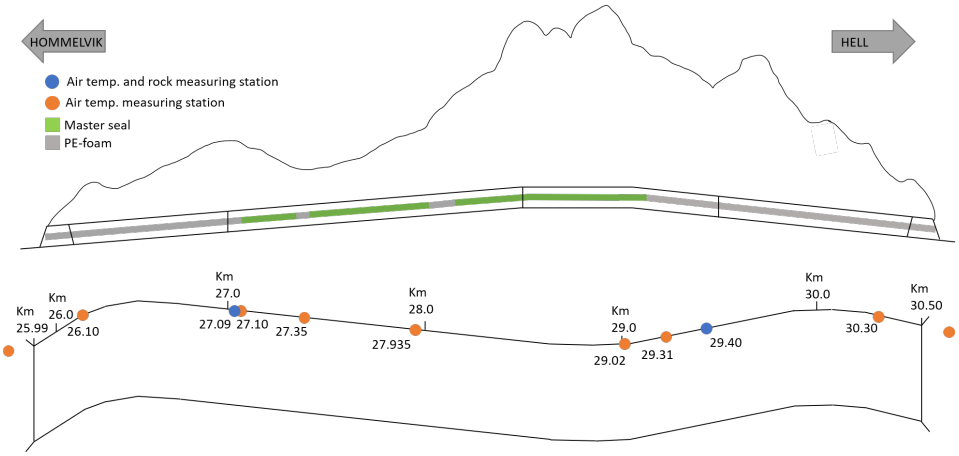

Figure 2.15: Horizontal and vertical cross section of the Gevingås Tunnel, showing the rock mass cover, location of the instrumentation and of the two lining types, modified by author based on (Bane NOR, 2018*c*).

Table 2.10: Measurement location in Gevingås.

Description	Chainage (m)	Location (km)
Hell protal	-	30.7
Hell 200 m	4400	30.3
Hell 1190 m, end PE	3410	29.31
Hommelvik 3120 m	3120	29.02
Hommelvik 2035 m	2035	27.935
Hommelvik 1450 m	1450	27.35
Hommelvik 1200, end PE m	1200	27.10
Hommelvik 200m	200	26.10
Hommelvik portal	-	23.9

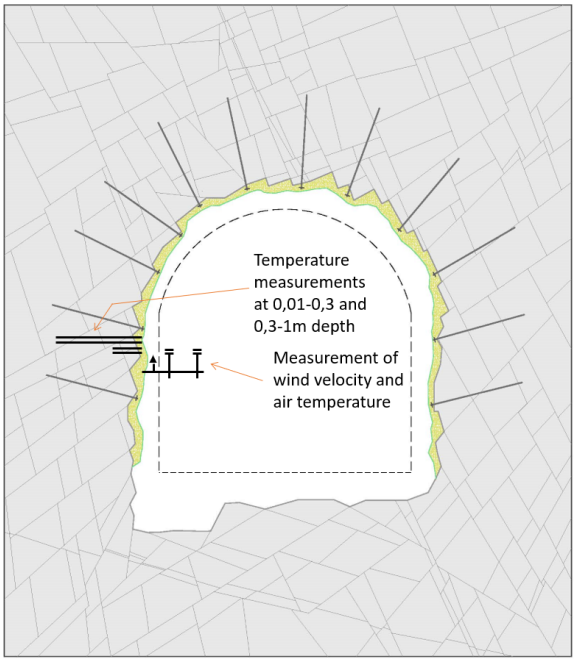

Figure 2.16: Principle sketch of the instrumentation in the rock mass and on the tunnel contour, reworked from (Holter and Geving, 2016).

Figure 2.17: Picture from the Gevingås Tunnel showing the measuring installation at the tunnel wall (Date: 01.02.19)

In the location measuring both air and rock mass temperature, the set-up is as follows; two sensors are logging tunnel air temperature and velocity at 50 and 10cm from the lining. The boreholes that contain heat sensors have a diameter of 20mm. There are two boreholes of each length, as indicated in Figure 2.16 and 2.17. Two rods of the same length, with temperature sensors in the same location, increases the possibility of obtaining a measured value, even if one of the sensors fails. It also provides a more reliable result, because one gets two measurements for each location. The shorter borehole, named K1 and K2, has sensors measuring from 0.01 to 0.30m, and the longest rods, named L1 and L2, have sensors measuring from 0.3 to 1m. In the north measuring station, the rock mass is also instrumented with sensors at two, three and four meters depth in one borehole, named D1. For both configurations, the length is measured from the tunnel wall, and with positive values inward through the concrete, and further into the rock mass (Holter and Geving, 2016).

The sensors for measuring temperature in the lining and rock mass, are PT1000 resistance element thermal sensors. Their small size gives an accurate point measure. To be able to place the sensors in the borehole, they are placed on a Plexiglas rod (Holter and Geving, 2016).

In the seven points inside the tunnel, without the rock instrumentation, air temperature, humidity, and dewpoint are logged every other hour - the two measuring points outside the portal measures only the air temperature. Tinytag produces the sensors used, and these are small sensors positioned approximately 50cm from the tunnel lining, Figure 2.18.

Figure 2.18: Tinytag senor installed in the Gevingås Tunnel (Karl Gunnar Holter).

Chapter 3

Field measurements

This chapter presents the data from the Ulvin Tunnel and the Gevingås Tunnel. The data history stretches from November 2015 to 2019. As described in Chapter 2, the data contains both measurements of the tunnel air temperature and the temperature in the concrete lining and adjacent rock mass.

3.1 Ulvin Tunnel

Since different operators log the data from the Ulvin Tunnel, the availability of data varies. The consistency of the data is also of varying quality. To be able to evaluate the data, the period which is used in this presentation is narrowed down. The period of the available data is presented in Table 3.1.

Table 3.1: Overview of the measuring period in the Ulvin Tunnel.

Operator	Location	Available	Break in continuity
SINTEF	Outdoor North	29.11.15 - 06.05.18	18.05.16 - 10.07.16
	Outdoor South	30.11.15 - 20.04.18	18.05.16 - 06.10.16
	Interior	26.11.15 - 12.05.18	05.02.16 - 10.07.16
	Tunnel temp.	26.11.15 - 12.05.18	06.02.16 - 09.07.16
			27.11.16 - 30.04.17
Cactus geo	All	04.11.15 - 05.02.19	

3.1.1 Tunnel air measurements

To get a better perspective of how the tunnel air temperature is distributed along the tunnel axes, the lowest temperature is plotted against the position of the measuring stations, Figure 3.1. The lowest temperature at each station is obtained from a four-day average. The temperatures inside the tunnel are measured on the tunnel lining surface, and the portal measurements are collected from the outside stations. Note that the data do not represent the same date in time, never the less Figure 3.1 gives an illustration of the worst case in each season.

For the purpose of this data presentation, the south portal towards Eidsvoll is set as a length reference point. The temperature at each portal is assumed to be equal to the temperature measured by the stations placed outside. Winter season is chosen to be from November to April, and the summer season from May to October.

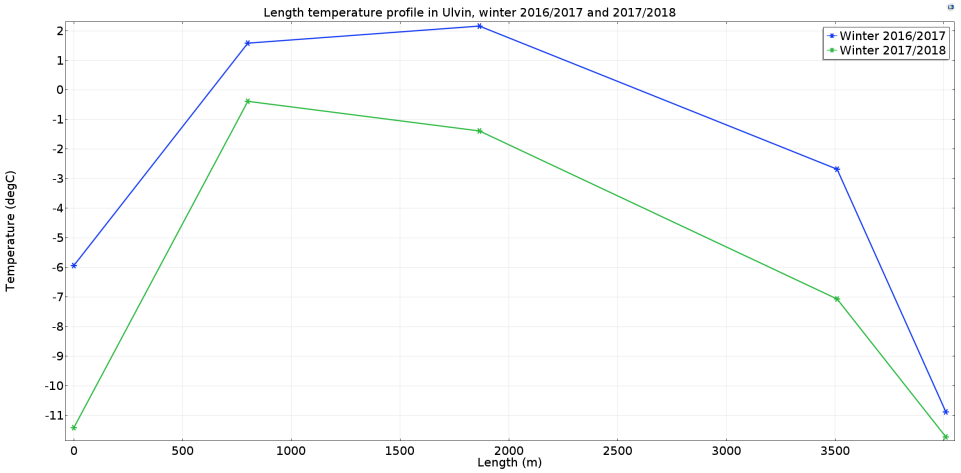

Figure 3.1: Temperature distribution through the length of the tunnel. Length = 0m represents the temperature at the south portal towards Eidsvoll. The asterisks indicate the measuring locations in the tunnel. The temperature profile represents the coldest day in the measuring point, as a four-day average.

In Figure 3.2 the outside temperature at each portal is plotted together with the measured temperature inside the tunnel, 1km from the south portal.

The tunnel air temperature measured some distance from the tunnel surface, and the temperature on the concrete surface is shown in Figure 3.3. The surface temperature is measured on the surface by two different configurations, both by SINTEF and Cactus Geo. Figure 3.3 shows the temperature as a daily average over one year, May 2017 to mid-April 2018.

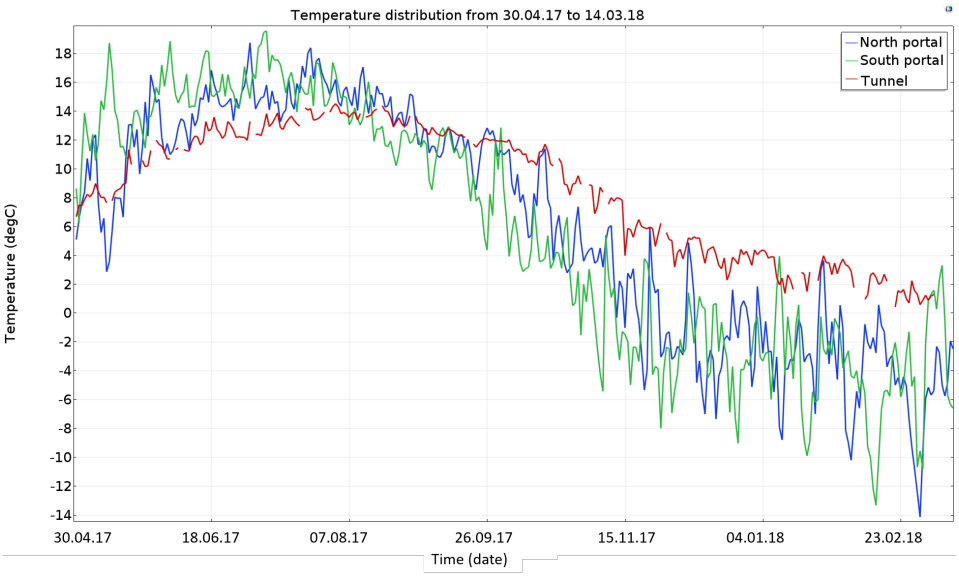

Figure 3.2: Daily average temperature measured outside of the north and south portal, plotted with the daily average of the tunnel air temperature 1km from the south portal.

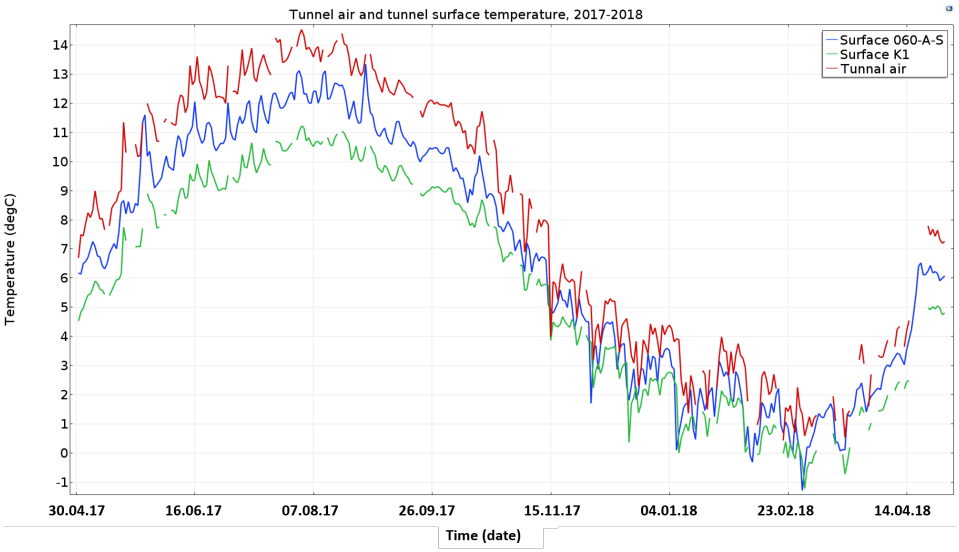

Figure 3.3: The tunnel air temperature measured ten centimetres from the surface. The surface temperature is measured both by SINTEF, presented by sensor K1, and Cactus Geo using the sensor positioned closest to the tunnel air measurement, at 060.

3.1.2 Concrete measurements

Measurements of temperature in the concrete structure at Ulvin, are shown from winter 2016/2017 and the winter season of 2017/2018, in Figures 3.4, 3.5, 3.6 and 3.7, 3.8. The data is based on the instrumentation operated by SINTEF.

Figure 3.4 and 3.5 shows the temperature distribution as time vs. temperature; the measurements are plotted as a daily average. In Figure 3.4 three different positions in the concrete arch is plotted for two winters and one summer season. In Figure 3.5 only the winter season of 2017/2018 is plotted since this is the season with the longest consecutive period of measured outside temperatures below zero degrees Celsius.

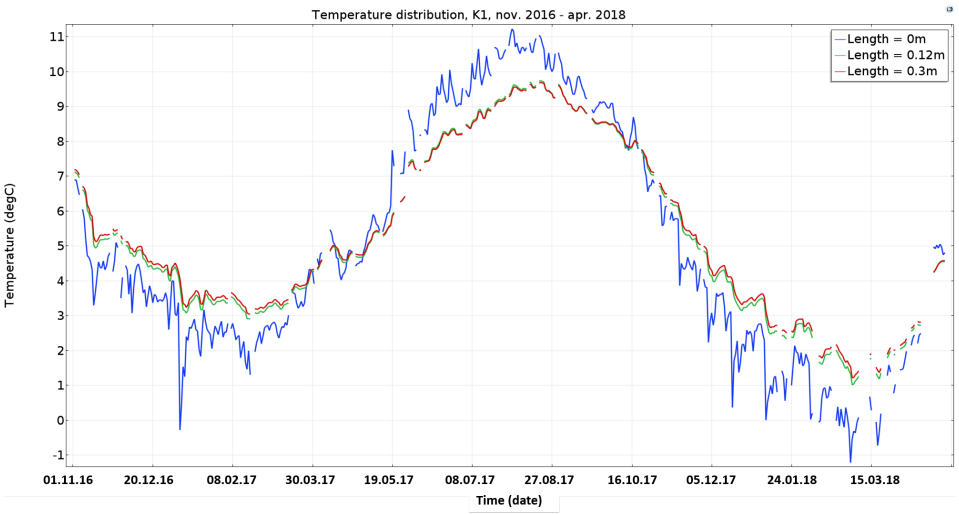

Figure 3.4: Temperature distribution, plotted as time vs. temperature, length measured inward from the tunnel surface. From sensor K1. The distribution shows two winters, winter 2016-2017 and winter 2017-2018, and the summer season of 2017 as a daily average.

Figures 3.6, 3.7 and 3.8 are plotted as temperature vs. distance from tunnel surface, and the measured temperature is presented as a monthly average. Notice that these figures are plotted for different sensors sets. Sensors set K1 and K2 are missing the measuring point closest to the tunnel surface, and L1 misses the point located 0.06m from the surface. The overlapping sensors in each set are presented as an average value of the double measurement. The graphs are plotted separately instead of presenting an average value of the three sets because the measurements deviate from each other. All the sensor sets are plotted in the same way, and the ones not presented in the running text are found in Appendix A.2.1.

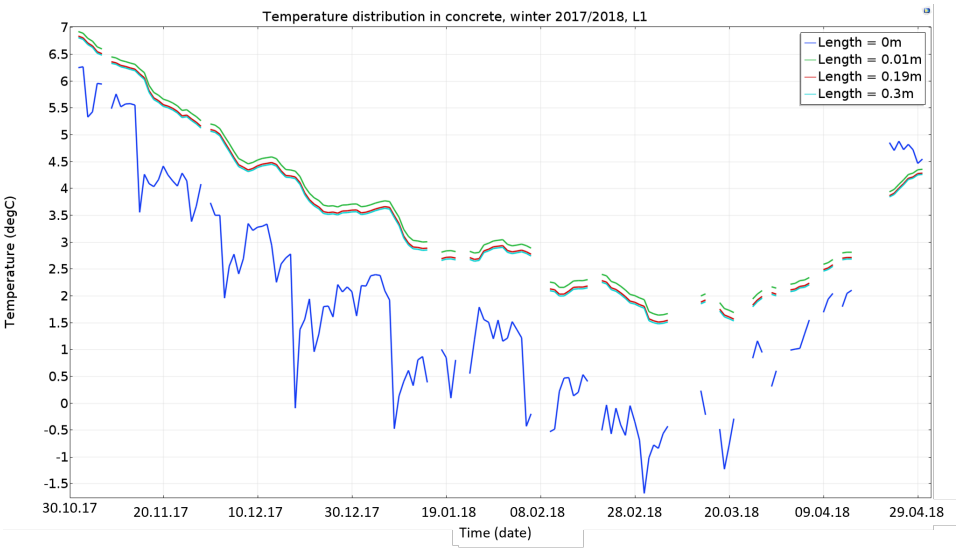

Figure 3.5: Temperature distribution, plotted as time vs. temperature, length measured inward from the tunnel surface. From sensor L1. Distribution shows the winter of 2017/2018 as a daily average.

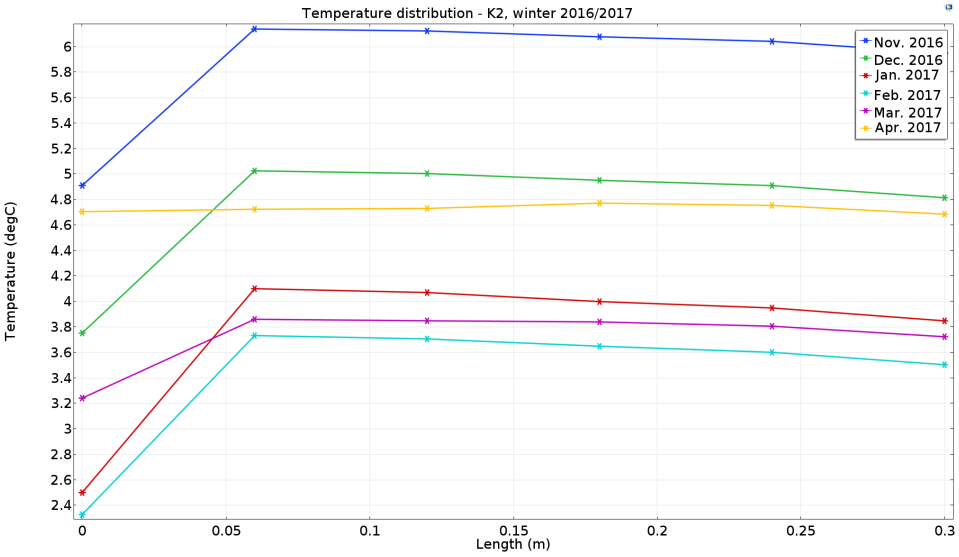

Figure 3.6: Temperature distribution in the concrete lining in the Ulvin Tunnel, in measuring location K2, plotted as length vs. temperature, showing the winter season of 2016-2017, as a monthly average.

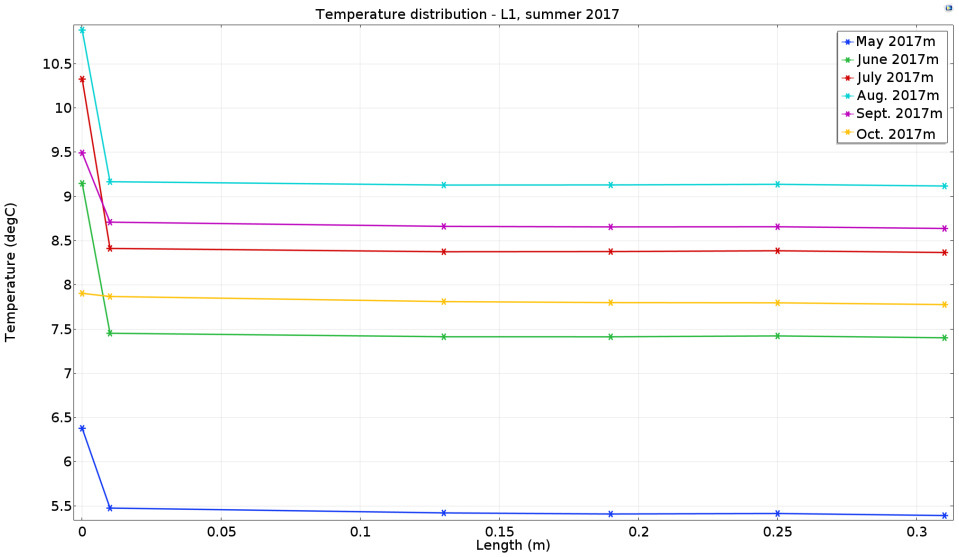

Figure 3.7: Temperature distribution in the concrete lining in Ulvin Tunnel, in measuring location L1, plotted as length vs. temperature, showing the summer season of 2017 as a monthly average.

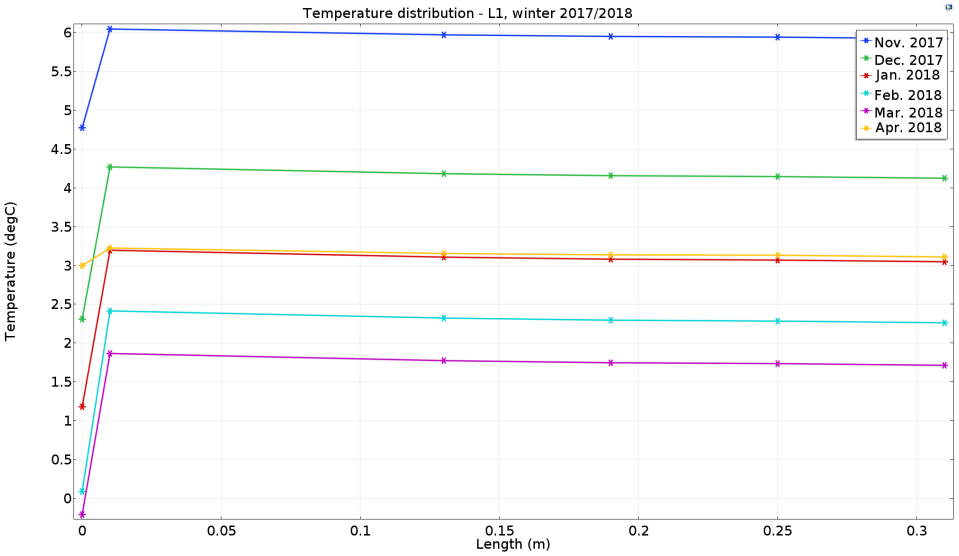

Figure 3.8: Temperature distribution in the concrete lining in Ulvin Tunnel, in measuring location L1, plotted as length vs. temperature, showing the winter season of 2017-2018 as a monthly average.

Figure 3.9 shows the highest and lowest single measurement, from the winter 2015/2016 through winter the 2018/2019, in the concrete lining in the Ulvin Tunnel. The measurements are located one kilometer from the south portal. As described, this location contains three similar measuring setups spaced relatively close together. Therefore all three measuring points are included in Figure 3.9. The inner rod is not included in this presentation because there is uncertainty related to the sensors exact location.

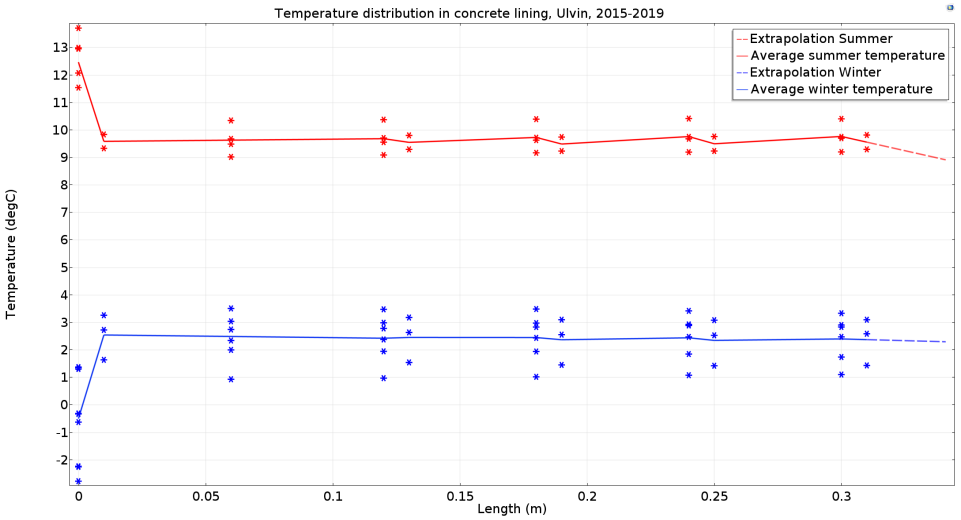

Figure 3.9: Lowest and highest single temperature measurements from the winter of 2015 through the winter of 2018 in the concrete arch.

3.1.3 Rock mass measurements

The temperature variations inside the rock mass behind the concrete arch are presented in Figures 3.10, 3.11 and 3.12. The data is based on the instrumentation operated by Cactus Geo. In these figures, the length is the measure of rock mass depth, and the surface temperature is measured on the concrete surface. Presented are the season of 2017/2018 for all the three instrumented cross sections, the plots for the season of 2016/2017 and 2018/2019 are found in Appendix A.2.2.

Figure 3.13, shows the lowest and highest temperature in each measuring position inside the rock mass from 2015 to 2019. The temperatures do not represent the same time stamp but give an illustration of the worst case scenario over an extended period. The solid line shows the average temperature in each point with linear interpolation and a linear extrapolation into the rock mass.

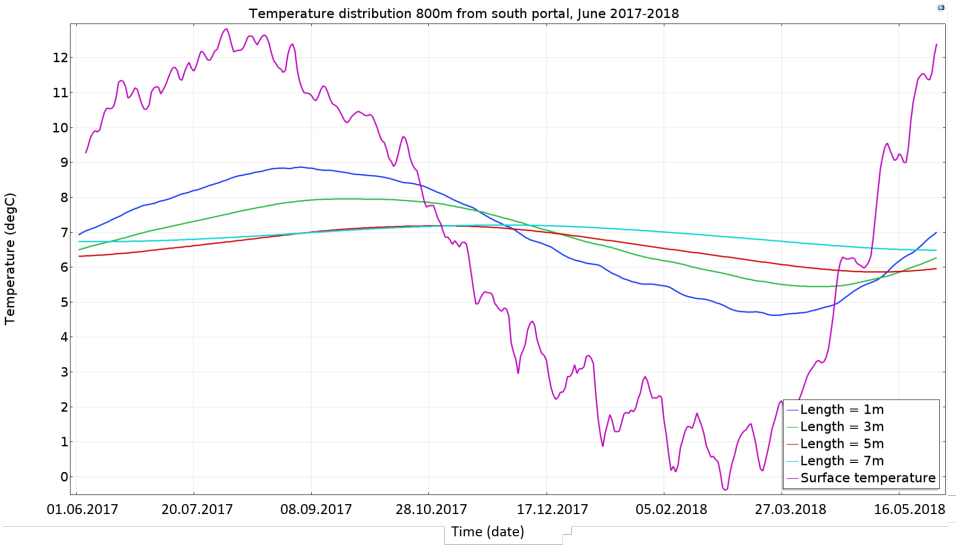

Figure 3.10: Measuring block 060. Tunnel surface temperature is presented as a four-day average. The temperature inside the rock mass is plotted as a daily average. The length is a measure of rock mass depth.

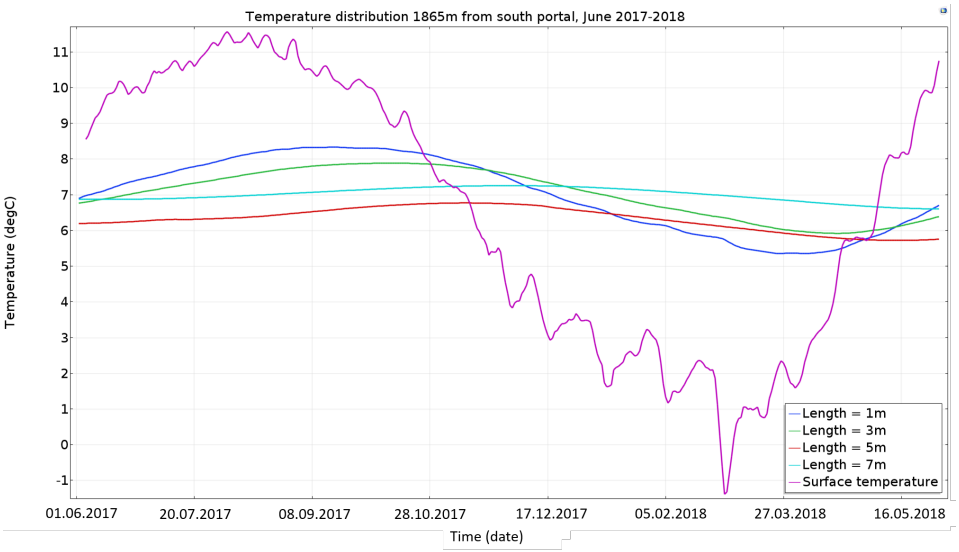

Figure 3.11: Measuring block 144. Tunnel surface temperature is presented as a four-day average. The temperature inside the rock mass is plotted as a daily average. The length is a measure of rock mass depth.

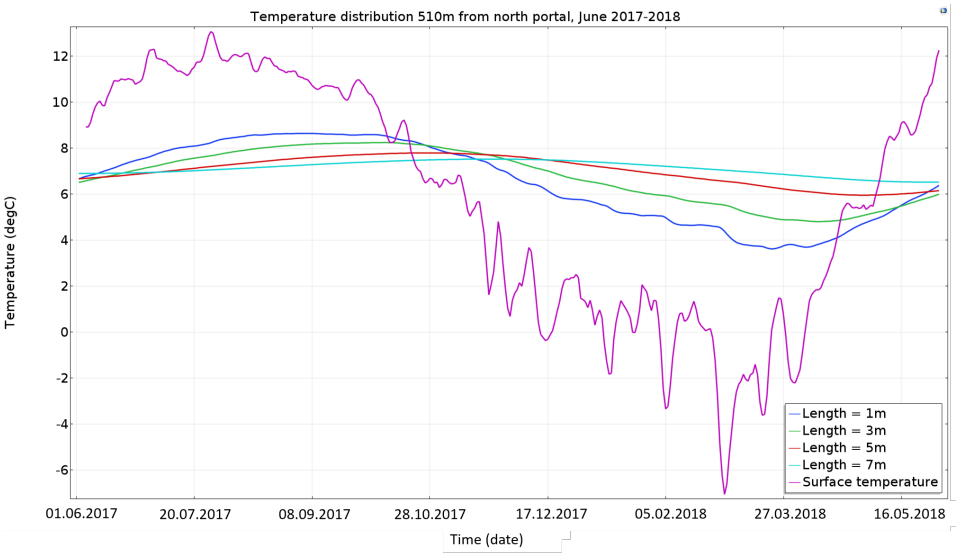

Figure 3.12: Measuring block 280. Tunnel surface temperature is presented as a four-day average. The temperature inside the rock mass is plotted as a daily average. The length is a measure of rock mass depth.

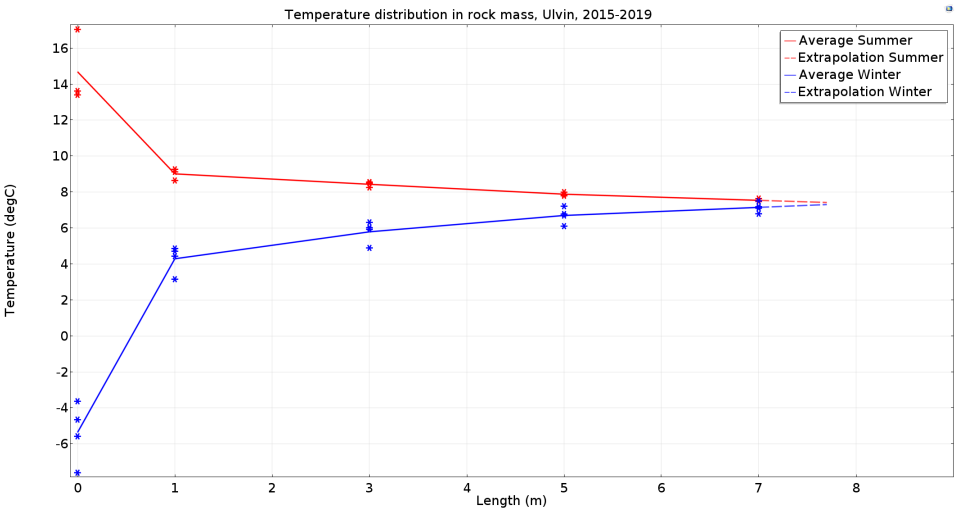

Figure 3.13: The lowest and highest temperature in each measuring point through the summer and winter season of 2015-2019 plotted against length. Length zero is located on the tunnel surface, and the onward length represents rock mass cover. The concrete layer is not taken into account. Data from Cactus Geo in measuring block 280.

3.2 Gevingås Tunnel

The data available and used in the presentation of the Gevingås Tunnel is mainly from the winter season, November through April, an overview of the exact periods is presented in Table 3.2.

Table 3.2: Overview of the measuring period in the Gevinås tunnel.

Measuring station	Data period
North	29.12.16 - 04.04.17
	18.10.17 - 05.03.18
	26.10.18 - 01.02.19
South	29.12.16 - 01.03.17
	29.09.17 - 06.03.18
	26.10.18 - 01.02.19
Tiny tag	20.10.16 - 04.04.17
	27.10.17 - 18.04.18
	26.10.18 - 09.04.19

3.2.1 Quality of data

Data from the Gevingås Tunnel contains measurements from sensores that seem to be out of order. Some sensors are taken out completely since they show deviation in several seasons. Other types of deviations are hard to explain, and if the deviation from the expected value is so large that it must be due to some mishap, the measures connected to that specific sensor is removed for that season. If there is doubt connected to whether the measure is wrong or not, the measured result is presented. An overview of the available data, and whether the data is valid, is presented in Table 3.3 and 3.4. The plausible reasons for the corrupted data is discussed in Section 3.3.

3.2.2 Tunnel air measurments

The coldest temperature in the measuring location is plotted against the tunnel length, for the winter season of 2016/2017, 2017/2018, and 2018/2019 in Figure 3.14, to get a better image of how the outside temperature affects the air temperature inside the tunnel. The temperatures presented is a moving average over four days, and the data is not collected form the same time stamp.

In Figure 3.15 the tunnel air temperature in five locations toward the middle of the tunnel, is plotted as a four-day moving average, for the winter season of 2017/2018, for the winter season of 2016/2017 and 2018/2019 see Appendix A.3.1. Length is measured from the portal at Hommelvik and inward in the tunnel towards the Portal near Hell.

Table 3.3: Overview of the available data at the South station, near Hommelvik. RR stands for removed from raw data, and I for data evaluated as invalid. X indicates the data which is presented, in the running text or found in the appendix.

	Position	Discarded			Plotted		
Sensor rod	[m]	16/17	17/18	18/19	16/17	17/18	18/19
K1	0.01			I	X	X	
	0.03				X	X	X
	0.05	RR	RR	RR			
	0.08				X	X	X
	0.1		I	RR	X		
	0.15				X	X	X
	0.3				X	X	X
L1	0.3				X	X	X
	0.5				X	X	X
	0.75				X	X	X
	1	RR	RR	RR			
K2	0.01				X	X	X
	0.03		RR	RR		X	
	0.05			I	X	X	
	0.08				X	X	X
	0.1		I	I	X		
	0.15				X	X	X
	0.3				X	X	X
L2	0.3				X	X	X
	0.5				X	X	X
	0.75				X	X	X
	1		RR	RR	X		

Table 3.4: Overview of the available data at the North station, near Hell. RR stands for removed from raw data, and I for data evaluated as invalid. X indicates the data which is presented, in the running text or found in the appendix.

	Position	Discarded			Plotted		
Sensor rod	[m]	16/17	17/18	18/19	16/17	17/18	18/19
K1	0.01	RR		RR		X	
	0.03				X	X	X
	0.05		I		X		X
	0.08				X	X	X
	0.1				X	X	X
	0.15				X	X	X
	0.3				X	X	X
L1	0.3		I		X		X
	0.5		I		X		X
	0.75		I		X		X
	1		I		X		X
K2	0.01				X	X	X
	0.03				X	X	X
	0.05				X	X	X
	0.08				X	X	X
	0.1				X	X	X
	0.15	I	I	I			
	0.3	I	I				X
L2	0.3		I		X		X
	0.5	I	I				X
	0.75		RR		X		X
	1		I		x		X
D1	2				X	X	X
	2				X	X	X
	3	I	I				X
	3	I	I				X
	4				X	X	X
	4				X	X	X

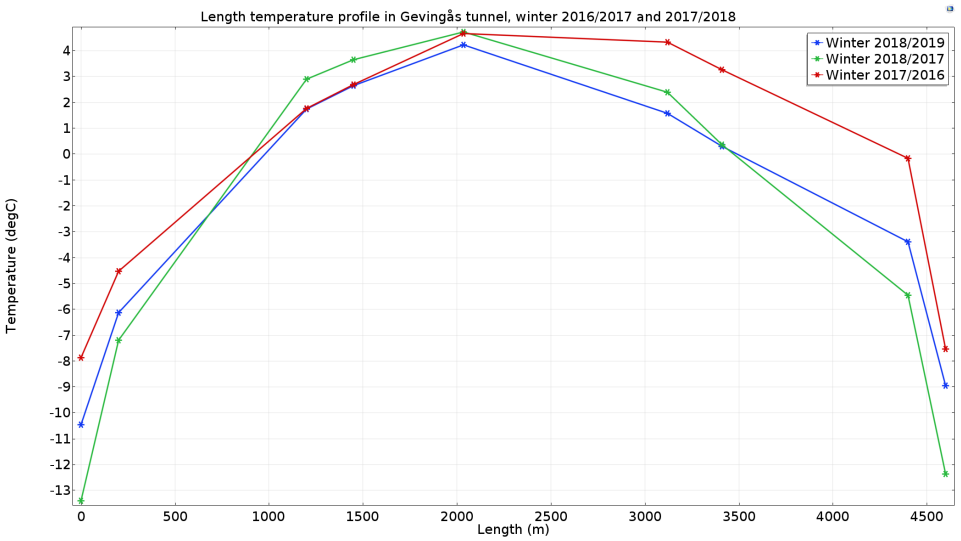

Figure 3.14: The x-axis represents the tunnel length, length=0m is equal to portal at Hommelvik. The asterisk indicate the measuring location in the tunnel. The temperature profile represents the coldest days in the measuring point, as a four day average.

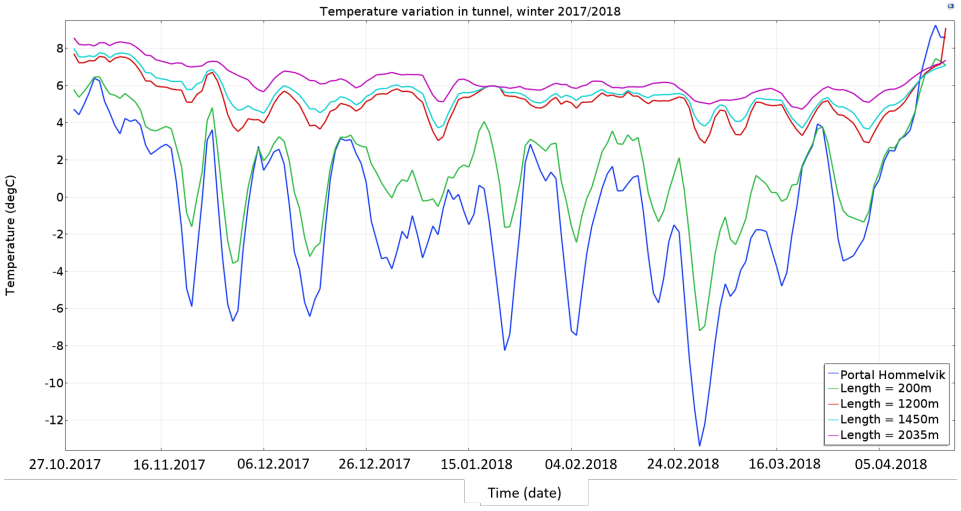

Figure 3.15: Temperature variations in tunnel air, over a winter season in different locations inside the tunnel. The temperature is plotted as a four-day average.

3.2.3 Concrete and Rock mass measurements

Figures 3.16 and 3.17, shows the lowest measured temperature inside the rock mass at the North and South measuring station. The temperatures do not represent the same timestamp but give an illustration of the worst case scenario over a longer period. The dashed line shows the average temperature at each point.

The temperature distribution inward in the rock mass, for the winter season of 2016/2017, at both the South and North portal, are plotted in Figure 3.18 and 3.19. The figures give an image of how the temperature variations in the tunnel affect the adjacent rock mass. The temperatures are all presented as a four-day average. The temperature distribution for the remaining two winter seasons, 2017/2018 and 2018/2019, are presented in Appendix A.3.2.

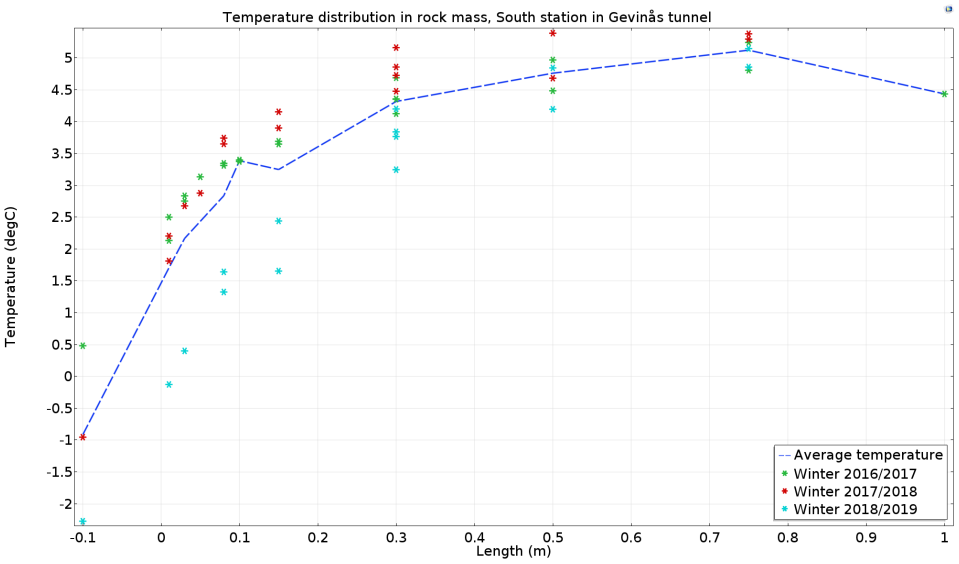

Figure 3.16: The lowest temperature measured in the particular location over three winter seasons, presented as exact measures. The asterisks indicate the exact measuring location. The solid line represents the average temperature distribution. The data I collected from all measuring roads, K1, K2, L1 and L2 by the South station.

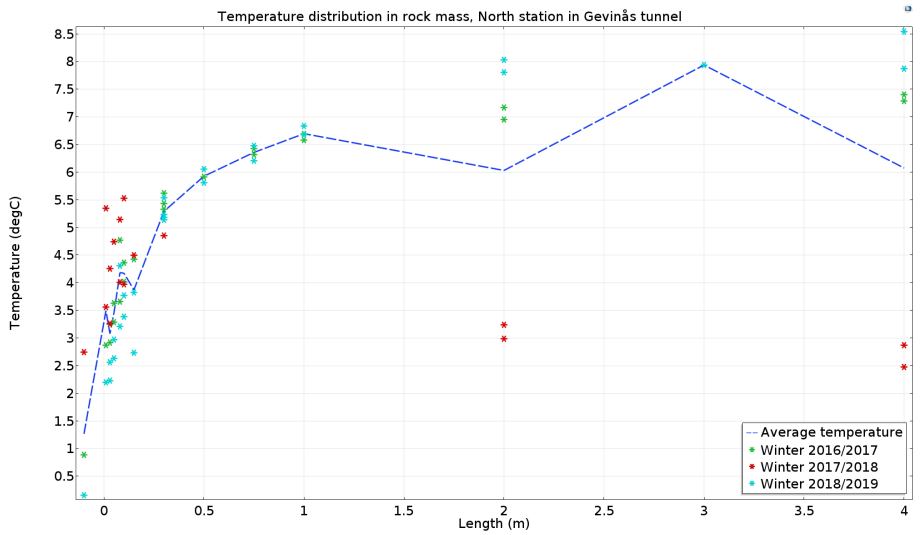

Figure 3.17: The lowest temperature measured in the particular location over three winter seasons, presented as an exact measure. The asterisks indicate the measuring location. The solid line represents the average temperature distribution. The data I collected from all measuring roads, K1, K2, L1, L2 and D1 by the North station.

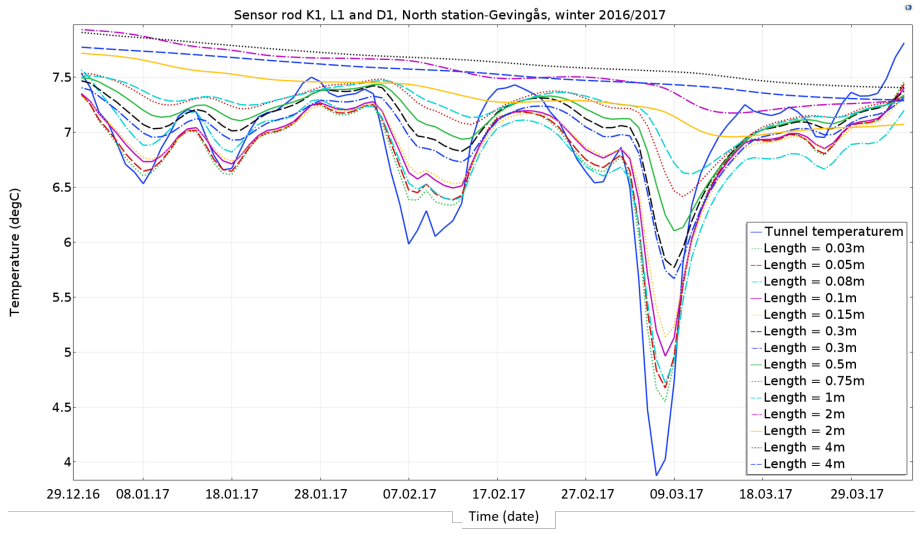

Figure 3.18: Temperature distribution inward in rock mass plotted against time. The temperature is presented as a four-day average for sensors set K1, L1, and D1 at the North station, through the winter season of 2016/2017.

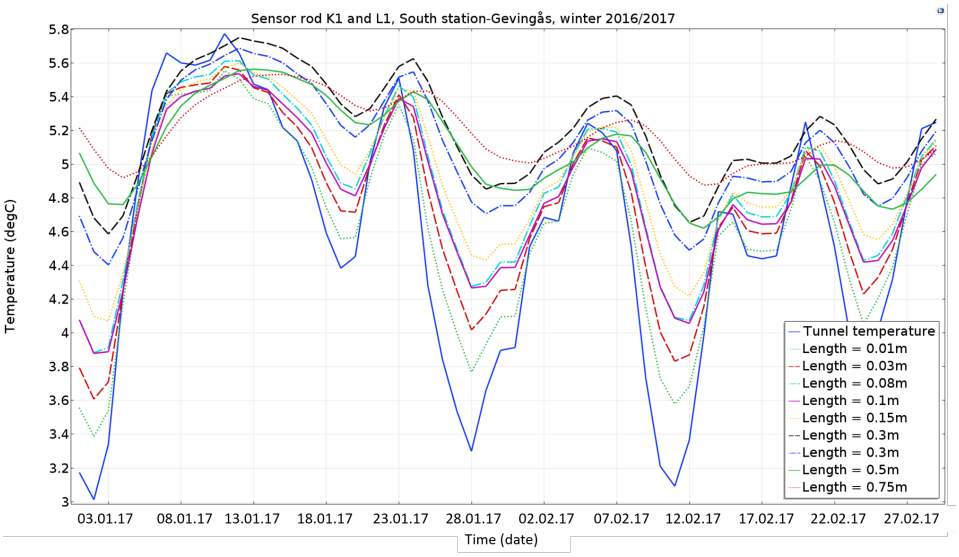

Figure 3.19: Temperature distribution inward in rock mass plotted against time. The temperature is presented as a four-day average for sensors set K1 and L1 at the South station, through the winter season of 2016/2017

3.3 Discussion

The uncertainty connected to the measurements obtained for the two tunnels can be related to several aspects as the logger, the sensors exact position, mounting of sensors in the boreholes, water in boreholes and the handling of data from the raw format.

If the assumed position of the sensor does not correspond to the actual position, errors in the presentation of the data can occur. In the Ulvin Tunnel, uncertainty is mainly connected to the position of the sensors in the concrete, because they have been subjected to the concrete arch building prosses. This entails pouring of concrete over the sensor along, with several rounds of vibration. Little information about the uncertainties connected to the sensors operated by Cactus Geo is obtained. However, the aspects of mounting of the sensor, and passing water are also relevant aspects that can inflict on these sensor results as well.

If the boreholes were not sufficiently filled with mortar when the plexiglass rod, with the sensors, was installed, air gaps might occur. These air gaps might influence the measurements. Cracks or poorly filled boreholes might also result in water leaking past the sensors, and this might affect measurements in periods and give deviations in the measured results.

Night to the ninth of April, an inspection of the Gevingås Tunnel took place to

collect data from the Tinytag sensors, and at the same time change the sensor's battery. An inspection of the two logger location logging the rock mass temperature was performed to investigate if there is water flowing past the sensors. No sign of water seepage at present or signs of earlier seepage were evident at any of the measuring locations. This does not entirely rule out water in the vicinity of the heat sensors as a source of error, but the errors seen in the measured data is most likely connected to more than just water.

3.3.1 Ulvin

Tunnel air measurements

Figure 3.20 shows the surface temperature in the middle of the wall, in the transition between roof and wall, and roof. The largest difference between wall and roof temperature is seen when the tunnel is subjected to negative temperatures. The roof temperature is also more stable, and not as easily affected by the temperature variation. The reason for the temperature difference is mainly that cold air is heavier than warm air. The warmest air travels up to the arched roof and settles. Since the tunnel has a large span, the effect on the roof air temperature imposed by a passing train, is not extensive. This means that the temperature distribution above the tunnel roof inward in the rock mass has an average higher temperature, which varies less than the temperature inwards from the side walls. Since the wall experiences the lowest temperatures, it is a legitimate decision to only look at the middle wall measurement.

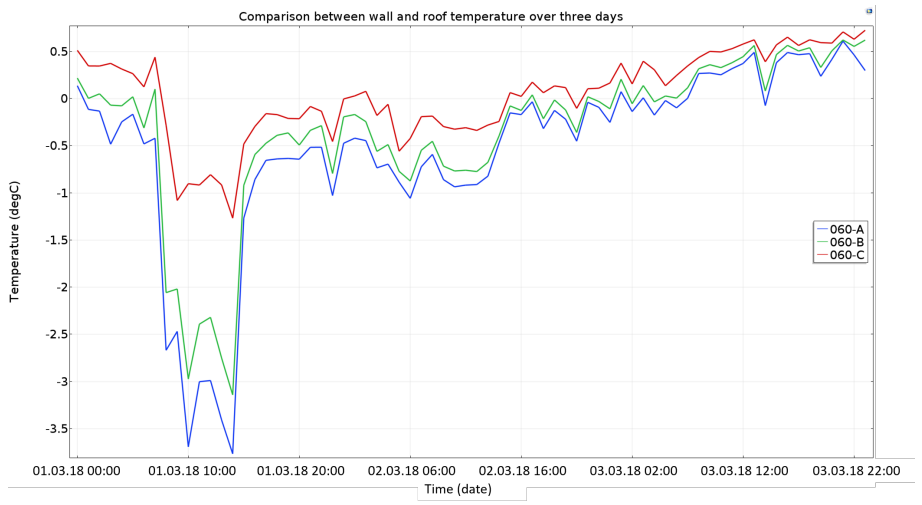

Figure 3.20: Comparison between the temperature in the middle of the wall (060-A), transition wall and roof (060-B) and roof (060-C). The temperature is a surface measure shown over three days.

Figure 3.1 shows the temperature distribution through the tunnel length and gives a depiction of how the outside temperature affects the temperature inside the tunnel. The length profile shows the coldest temperature, at each measuring station through two winter seasons. This indicates that the lowest temperature measured outside is not equal to the lowest measured temperature inside the tunnel. Figure 3.1 shows that through the entire tunnel length, the surface temperature might drop below zero degrees Celsius. The slight shift in symmetry seen in the distribution of the temperature profile might be related to the wind blowing in from the south portal, and therefore transporting cold air further into the tunnel. The few measuring points through the tunnel length gives uncertainty in the graphical presentation, one does not know how the distribution is between the measuring point, but most certainly the distributions is not linear as presented in Figure 3.1.

When a body of air passes through a tube, like a tunnel, the air temperature is expected to be influenced by the tube's temperature. The rock mass holds a constant temperature some distance from the tunnel contour, which means that the rock mass temperature six meters from the tunnel contour, is not the same as the one on the tunnel surface. This is due to heat transfer between the rock and tunnel air. This transfer of heat is expected to influence the measured tunnel temperature, especially in an uninsulated tunnel as Ulvin, but as Figure 3.2 shows the tunnel air is to a limited extent different from the temperature measured outside the portal. One aspect that might explain this phenomenon is the wind direction in the area. Wind blowing into the tunnel might transport cold air further into the tunnel than what one would initially expect, which is the same trend as seen in Figure 3.1. The only difference one can see between the tunnel air, one kilometer inside the tunnel, and the portal temperature is slight a subdued amplitude. The tunnel temperature is lower than the outside temperature in the summer and higher in the wintertime, as a result of the lower amplitude. The tunnel temperature experiences a phase shift, though small. The phase shift is to be expected since the outside air must have some time to influence the tunnel air.

Figure 3.3 shows the difference between the tunnel air and surface temperature. The largest difference measured in the summertime is around 3°C. Figure 3.3 shows that the tunnel air is above the surface temperature, through the entire year. That the surface temperature is lower than the tunnel air, also in the winter time, is not as expected, because one would think that in the winter months the tunnel air is lower than the rock mass temperature, and therefore the rock mass would keep the surface temperature above the tunnel air temperature. Two surface sensors are shown, and both have measured a surface temperature that is continually lower than the tunnel air-temperature. The difference between the two surface measurements shows how difficult measuring the surface temperature is and that these data should be handled with caution. To have an exact surface temperature measurement, one must know that the measured result is not affected by any other temperatures, as the tunnel air.

Concrete measurements

Figure 3.4 shows that the temperature on the tunnel lining oscillates around a mean temperature of 6°C. The same trend can be seen inside the concrete lining. However, in the lining, the amplitude of the oscillating trend has been subdued, and the phase has been shifted slightly. The phase shifts show that it takes some time for the temperature inside the concrete to react to the changes happening on the surface. The concretes thermophysical properties govern the concretes reaction to the changing boundary conditions.

Looking at the measurement inside the concrete, on an hourly basis over a month shows that the internal temperature is less affected by the daily temperature variations compared to the large scale variations. Regardless, Figure 3.4 shows that the internal temperature is affected by the seasonal variations, and that tunnel air and concrete lining temperature distributions, mirror each other.

The concrete measurements stretch over three winter seasons, the season with the most prolonged period with portal temperature under zero degrees Celsius is the season of 2017/2018 with 32 days. Figure 3.3 shows that the tunnel air in this winter does not drop below zero degrees, but the surface temperature on the tunnel lining drops below zero for some periods at the end of February and through March. The winter season of 2017/2018 is plotted in Figure 3.5, which shows that one centimeter inside the concrete structure the temperature does not drop below zero at any point. The measurements further into the concrete lining show a slightly lower temperature than the measured temperature ten centimeters from the tunnel surface. One would expect the temperatures inward in the lining to steadily increase, and a reason why this is not the case here might be connected to the sensors positioning. There might be a mismatch between where the sensor is believed to be positioned and where it is.

The drop below zero degrees in March, also show up in Figure 3.8. From Figure 3.8 one can also see that the temperature quickly increases well above zero degrees inward in the concrete structure. The surface temperature does not drop far below zero, and the cold period lasts a limited amount of time, this is possibly why the concrete inwards in the lining are not affected to a larger degree.

The temperature distribution in Figure 3.6, 3.7 and 3.8, shows how the surface temperature is lower than the concrete temperature in the winter, and higher in the summer. This is because the concrete functions as an insulating material. In the summer periods, the surface temperature is higher than the concrete temperature, and this results in inward heat flux. However, in the wintertime, the direction of the heat flux is reversed and is in the direction out towards the tunnel air. April is clearly a transition month where the heat flux is zero and changing. The quick increase in temperature only a couple of centimeters into the concrete shows how deep the daily or high-frequency temperature variations affect the concrete temperature. The horizontal shift in temperature inside the concrete profile shows the effect of the long-term variations. Quick temperature variations, with high

frequency, effects shallow because the variations knock each other out. However, the more seasonal long-term variations have low frequency and effects, therefore, deeper into the rock mass.

Figure 3.9 illustrates the worst case temperatures distribute in the tunnel lining. The temperatures do not correspond to the same time stamp but show the minimum temperature measured in the lining, based on three winter seasons. Even though the tunnel surface experiences temperatures below zero, there is not a single measured temperature below zero in this period at any depth of the lining. To ensure that the data presented is as reliable as possible, the inner rod is not part of the figure, there is uncertainty connected to the location of the sensors and the positioning of the rod. There is also some uncertainty connected to the outer rod, especially because the sensors were installed before the concrete arch, there is no easy way to control if the rod has turned or misplaced in any way.

Rock mass measurements

The measurements from the rock mass behind the concrete lining show the same trends as the concrete measurements, Figures 3.10, 3.11 and 3.12. The rock mass temperature oscillates with the surface temperature, but the amplitude is noticeably smaller then what was the case for the concrete temperature, which is as expected since the temperature variations travel a more substantial length. The phase shift is also more predominant in the rock than in the concrete. The figures illustrate that the measurements furthest away from the tunnel lining is affected the least by the temperature variations on the surface.

At 800 meters from the tunnel south portal, Figure 3.10, the temperature seven meters inside the rock mass varies with only one degree Celsius, which is also the case for the measurements taken in the middle of the tunnel. However, seven meters into the rock mass, 510 m from the north portal, the temperature varies with two degrees Celsius over a year, and this is because the surface temperature variation is more substantial in this location.

Figure 3.11 shows the measurements which are positioned furthest from the tunnel portals. Looking at the temperature distribution three meters inside the rock mass, the temperature variation over one year is approximately two degrees Celsius, compared to the point closest to the portal, where the temperature varies with three point five degrees Celsius. This is a substantial difference.

Even though the surface temperature experiences negative degrees, the rock mass temperature oscillates around seven degrees Celsius, which is the case in all the measuring sections throughout the tunnel.

The temperature profile showing the lowest measured temperatures in the rock mass, Figure 3.13, indicates that in the winter season there is an increase in temperature as one progresses inwards in the rock mass. The extrapolation done both

for the winter and summer season shows that the surface temperature variations influence the rock mass temperature to approximately eight meters depth.

Combining the temperature profile in the concrete, and rock mass plotted against length, Figure 3.9 and 3.13, gives Figure 3.21. The figure shows that the trend of the temperature distributions matches quite well, especially for the summer season. Note that the data for the two plots are collected from either side of the tunnel, the rock measures from 510 meters from the north portal, and the concrete one kilometer from the south portal. Never the less the brake in the temperature distribution might be connected to the material transition. As described earlier, the cast-in-place lining has a membrane installed between the lining and rock support, to transport water down to the invert. The gap that is created because of the membrane and drainage is about 3-4mm wide and filled with air and moisture. Air has low thermal conductivity, 0.024-0.025 [W/(m K)] for temperatures between 0 and 12°C (Incropera et al., 2017), and the jump in Figure 3.21 is, therefore, most likely connected to the heat transfer being delayed by the air.

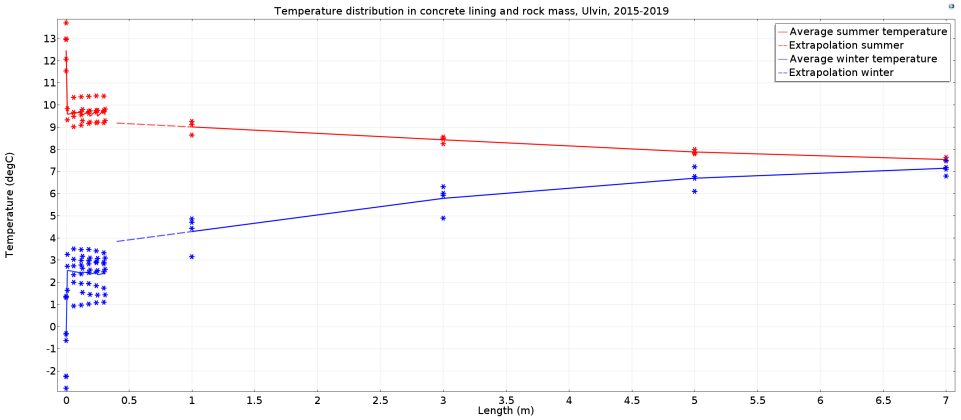

Figure 3.21: Combination of Figure 3.9 and 3.13

3.3.2 Gevingås

Tunnel air measurements

The temperature distribution through the length of the Gevingås Tunnel, shown in Figure 3.14, is close to symmetrical in all three winter seasons. One reason for the symmetry is connected to the location of the tunnel portals. If the tunnel portals were placed at different heights in the terrain, the tunnel air would be transported through the tunnel simulating a chimney effect. The chimney effect would make the temperature distribution lopsided, with cold air traveling further into the tunnel from the lower portal. Cold air is heavier than the warm air, and as the tunnel

air is heated due to the surrounding rock mass, the hot air raises to the higher portal.

The winter of 2017/2018 and 2018/2019 have approximately the same distribution. The tendency to shift in the winter of 2016/2017 is most likely related to the wind blowing cold air into the south portal. In the Gevingås Tunnel, the dominant wind direction is from South to North, and in the winter of 2016/2017, the transportation of air was most likely relatively high.

One would expect that the insulation by the portals on both sides would delay heating of the tunnel air. PE-foam is an insulating and water protecting material, which is built to prevent the formation of ice. The structure insulates so that the cold tunnel air is kept away from the water behind the PE-foam, and this also results in keeping the rock mass from heating the tunnel air. As a result, the cold air travels further into the tunnel, than if the rock mass temperature could heat the air. This effect might explain why the tunnel air is not heated more the first kilometer of the tunnel.

The cold air, temperatures below zero degrees, is transported 1km into the tunnel from the south portal, and from a couple of meters to 1km on the north side in the worst case. Figure 3.14 shows that approximately 50% of the tunnel always has a air temperature above zero degrees Celsius. Figure 3.15 shows that the temperature 200m inside the tunnel varies as the portal temperature. Whereas 1200m from the portal, the temperature is more stable varying around five degrees.

Rock mass measurements

The temperature profiles showing the lowest exact measure inwards in the rock mass at both the south and north stations show the worst-case scenario possible in the respective locations, Figure 3.16 and 3.17.

At the south station the lowest tunnel air temperature, measured ten centimeters from the lining, is below zero degrees Celsius, in two of the three logged seasons. However, as one progresses, only five centimeters into the lining, the temperature is continuously above zero. The lowest measured temperatures near the surface inside the lining/rock mass varies around 1.75 to 2.75°C. The winter of 2018/2019 shows temperatures below zero, the first centimeter, and a generally lower temperature profile compared to the two other seasons. As one progresses further into the lining and rock mass, the temperature increases. The measured temperatures from 2018/2019 is on the same level as the other two seasons at 30cm into the concrete. Overall the lowest measured temperatures line up well through the three seasons, showing the same trend and to a large extent the same temperatures.

At the northern station, Figure 3.17, the rock mass is also instrumented with sensors at two, three and four meters into the rock mass. The northern station shows the same trend as the south station, with increasing temperatures from the surface. Close to the surface, the temperature always measures above zero. At this

station, the temperature close to the surface varies between 2.75 to 3.75°, which is some degrees higher than at the south station. This corresponds to a general higher tunnel air temperature, compared to the south station. This again matches with the tunnel air temperature profile, where the trend is, colder tunnel air in the southern part of the tunnel. The measured temperatures by the deeply positioned sensors, in the winter of 2017/2018, deviate with three degrees Celsius, from the other two seasons. The deviation is not registered in the earlier evaluation of the data set and therefore plotted. The trend of the average curve seems to indicate a continuous increase in temperature onwards from four meters, meaning that the surface temperature influence further into the rock mass than four meters.

The assumption that the rock mass temperature is affected, even after four meters, is verified by Figure 3.18, showing the temperature distribution at various lengths in regards to time. This shows that the temperature at four meters is decreasing with time as the tunnel temperature is low in the winter months. The four meters curve has most likely a quite flat curve, oscillating slightly between seven and eight degrees Celsius, which also corresponds well with the measurements from Ulvin. In Ulvin the temperature at five meters rock cover oscillated between six and eight degrees Celsius over a year. The temperature further towards the tunnel surface, closer than two meters varies the most, it is evident that depth reduces the temperature variation range and provides a phase shift.

At the south station, the temperature also varies above zero degrees through the whole winter, both for the season of 2016/2017, 2017/2018 and 2018/2019. For the winter season of 2017/2018, Appendix A.3.2, parts of October are included, this shows the transition from summer with high temperatures. Inside the lining and rock mass the temperature peak, connected to the summer temperatures, appears after the summer temperature peak outside. Figure 3.19, shows a shorter period, with focus on January and February, which gives a better image of the short term temperature changes. The quicker temperature changes affect the first parts of the tunnel lining/rock mass the most. The graphs from the south stations show the same trend as seen through all the previous figures, decreasing temperature variations and a slight phase shift as one advance inward, measuring at increasing depth.

Chapter 4

Validation of COMSOL

In the project thesis (Tinderholt, 2018), a numerical model was established to validate the numerical modeling program COMSOL. The validation was based on the comparison with an experiment in a controlled environment.

By validating COMSOL, one can use the program in more complex situations. The goal is to establish a method that can be used to get knowledge about how the temperature in the tunnel affects the temperature distribution inward in the rock mass through the concrete lining.

The validation of COMSOL is done by changing the uncertain components of the numerical model so that the result matches the measured results from the laboratory. The laboratory is presented in detail by Tinderholt (2018). A quick presentation of the laboratory is presented in the following, to ease the readers understanding of the following chapter.

4.1 Short introduction of the laboratory

The laboratory consists of an insulated box divided into three parts, in total 62 cubic meters, (320 cm $\times$ 240 cm $\times$ 802 cm). The middle section of the box is a construction of rock (Tonalite), the side sections are cooling rooms, one representing the tunnel room temperature, and one the rock mass temperature, as shown in Figure 4.1.

The rock used in the laboratory is a Trondhjemite from Støren, approximately 50km south of Trondheim, geologically the rock classifies as a Tonalite, a plutonic rock. The lining is constructed as a bounded lining, with sprayed membrane and concrete.

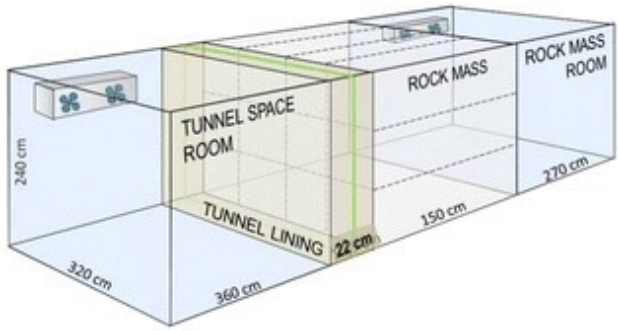

Figure 4.1: Principal illustration of the laboratory set up, (Holter, 2015).

The longitudinal positioning of the sensors in the rock is shown in Figure 4.2. The sensor location in the lining is shown in Figure 4.3. Table 4.1 shows the exact position of temperature sensors in the rock mass and concrete.

The termophysiacal material parameters from the laboratory are presented in Table 4.2, along with the values of uncertainty represented by the standard deviation.

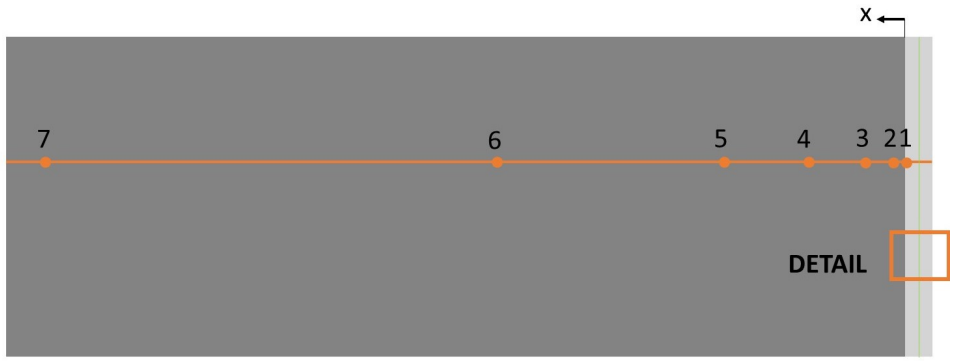

Figure 4.2: Placement of measuring points in the rock, x in the direction towards the rock mass room, modified by author based on (Vassenden, 2010).

Table 4.1: Position of temperature sensors in the rock mass and concrete, corresponding to Figure 4.2 and 4.3.

x	1	2	3	4	5	6	7	8	9
Sensor in rock mass [mm]	20	40	80	160	320	640	1280		
Sensor in concrete [mm]	6	36	63	89	115	126	155	185	215

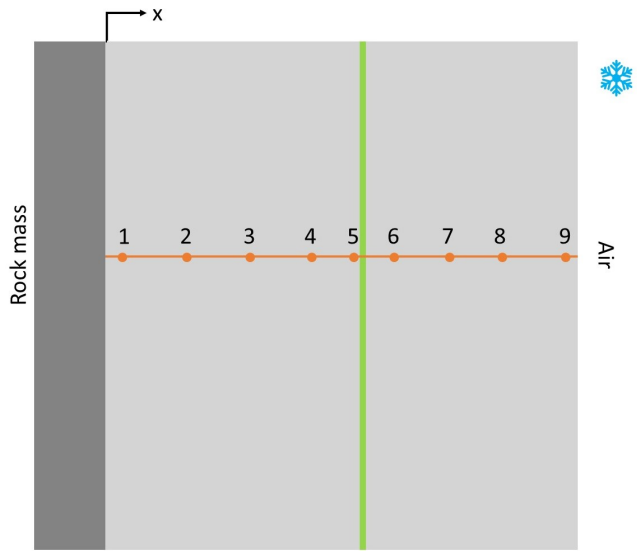

Figure 4.3: Detail enhanced from Figure 4.2. Measuring points in concrete, x in the direction towards the tunnel room.

Table 4.2: Thermophysical properties of Tonalite, rock mass, from double side measurement. Thermophysical properties of spry concrete with polymer. Both measurements are average of 5 single measurements, without resampling (Schlemminger and Ness, 2013).

Parameter		Rock mass	Concrete
Density	ρ [kg/m^3]	2659 ± 7	2211 ± 6
Thermal conductivity	k [W/(m*K)]	2.7562 ± 0.002	1.653 ± 0.155
Specific heat capasity	cp [kJ/(kg*K)]	0.840 ± 0.0047	0.939 ± 0.2

4.2 Sensitivity analysis

A sensitivity analysis is performed using COMSOL, to get a better understanding of how the material properties influence the temperature distribution. The numerical model used is the same, as that which is used for the validation of COMSOL.

The result of the analysis is presented in Figure 4.4 and 4.5. The solid blue line shows the reference temperature based on the mean material properties, as presented in Table 4.2. The asterisks symbolize the variation in temperature distribution when varying one parameter within two standard deviations.

In Figure 4.4 and Figure 4.5 the parameters of the concrete and rock mass are in turn held constant at the mean value, varying only one parameter at the time.

The presentation of the sensitivity analysis shows that the material parameters of the concrete have a more significant impact on the temperature distribution, then what the material properties of the rock mass have. The heat capacity and thermal conductivity are the parameters that have the largest impact - reducing the heat capacity results in a temperature distribution, which lays half a degree under the reference temperature.

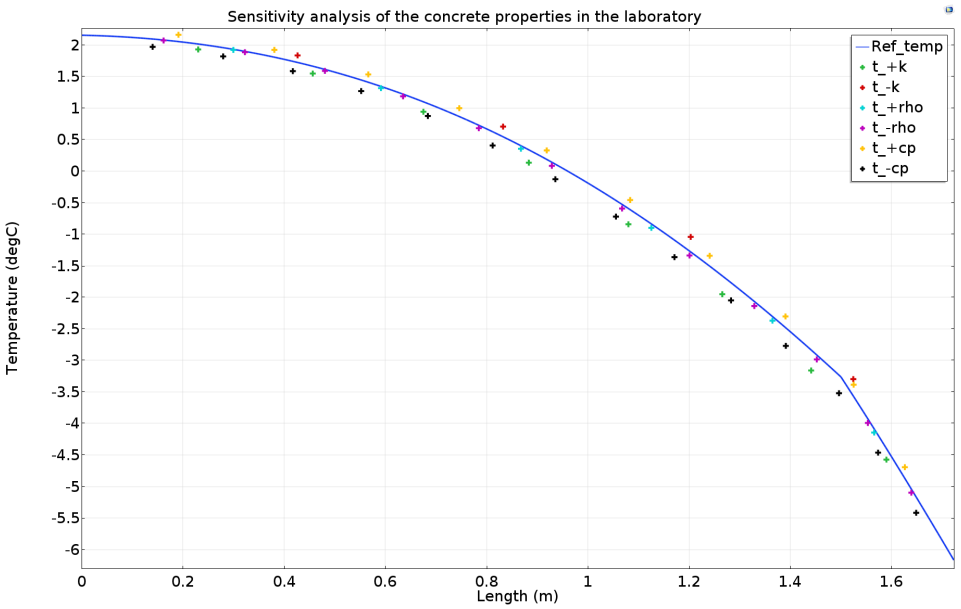

Figure 4.4: Sensitivity analysis of the concrete material properties in the laboratory. The solid line represents the reference temperature distribution, after six days, using mean values. The asterisks indicate how the temperature distribution would take place, given the change indicated in the legend, where t_+k showd the temperature distribution when the mean thermal conductivity is increased with two times the STD, and t_-k means that two times the STD is subtracted from the mean thermal conductivity.

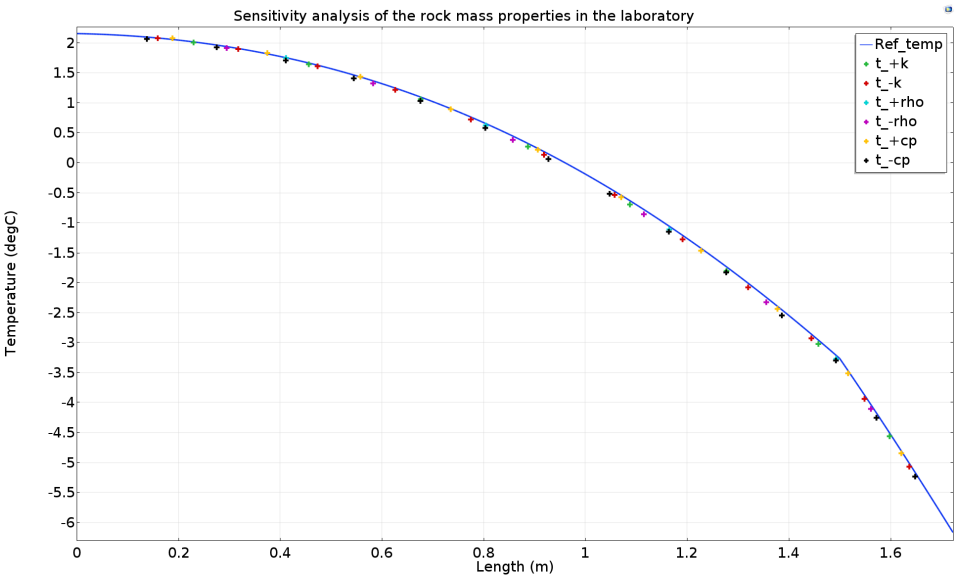

Figure 4.5: Sensitivity analysis of the rock mass properties in the laboratory. The solid line represents the reference temperature distribution, after six days, using mean values. The asterisks indicate how the temperature distribution would take place, given the change indicated in the legend, where t_+k shows the temperature distribution when the mean thermal conductivity is increased with two times the STD, and t_-k means that two times the STD is subtracted from the mean thermal conductivity.

Figure 4.6 and 4.7 shows the variation range where the laboratory results will place by a 95% certainty. These graphs are based on two times the standard deviation, Table 4.2. The numerical simulation is done by varying one parameter at the time. By evaluating the temperature, in certain points for each parameter, and finding the maximum and minimum deviation from the reference temperature, the basis for the range plot is made. Equation 4.1 is used to evaluate all the parameters at the same time, evaluating the max and min values separately. Extracting/adding ΔT to the reference values gives the graphs in Figure 4.6 and 4.7.

$$\frac{\Delta T}{T} = \sqrt{\left(\frac{\partial T}{\partial c_p} \times \Delta c_p\right)^2 + \left(\frac{\partial T}{\partial \rho} \times \Delta \rho\right)^2 + \left(\frac{\partial T}{\partial k} \times \Delta k\right)^2} \tag{4.1}$$

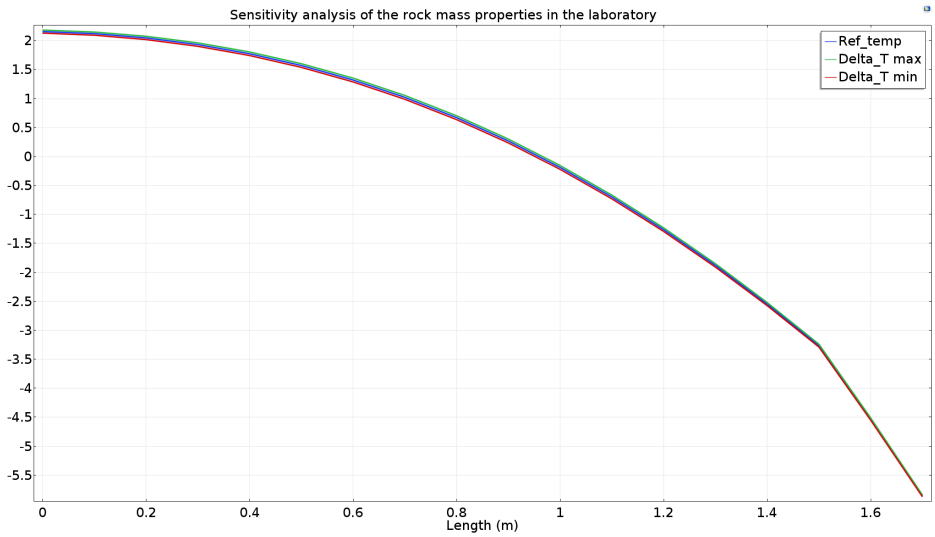

Figure 4.6: Confidence interval, with a 95% certainty the temperature distribution lies inside this interval, based on the uncertainty related to the rock mass material properties.

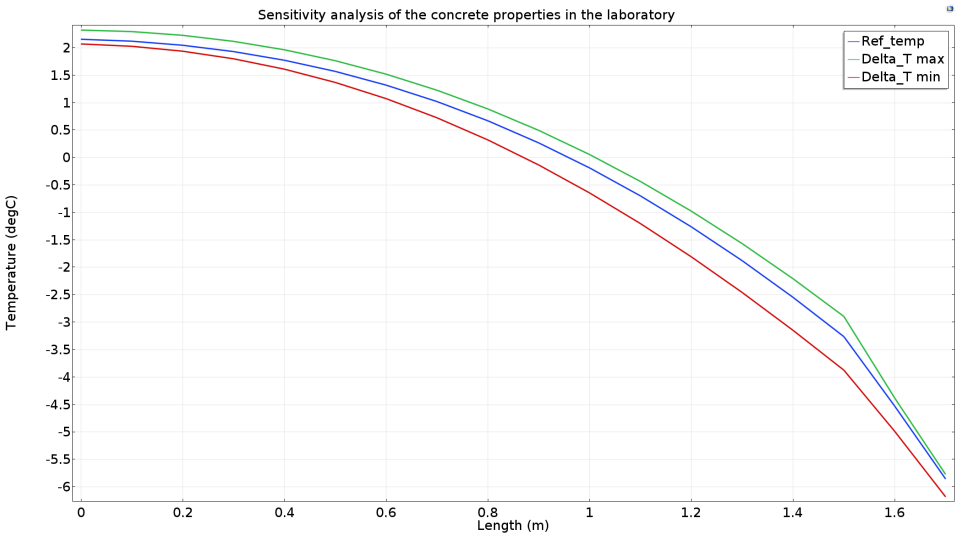

Figure 4.7: Confidence interval, with a 95% certainty the temperature distribution lies inside this interval, based on the uncertainty related to the concete material properties.

Figure 4.6 and 4.7 shows that the uncertainty connected to the concrete properties

gives a wider confidence interval than the rock mass, which in turn means that there is more uncertainty connected to the concrete properties. Looking at Figure 4.6 the variation of the rock mass properties has little effect on the temperature distribution. The overlapping graphs indicate that the values of the rock mass properties, within the standard deviation, give the same temperature distribution.

In total, the sensitivity analysis shows that the material properties have a limited effect on the temperature distribution. When it comes to validating COMSOL, the goal is to fit the numerical simulation to the measured results. In the case of validating, changing the material properties of the rock mass away from the mean values would give minimal effect. For the concrete, on the other hand, one should evaluate changing the properties from the mean values.

4.3 Validation

In order to have the best possible basis of comparison between the numerical model and the measured results from the lab, the geometry in COMSOL is built to match that of the laboratory, Figure 4.8. In the numerical model, the membrane is neglected, because of the membrane thickness, the effect of this simplification is insignificant. The model is constructed in two dimensions, but the analysis in COMSOL and the data extraction is done in the middle of the geometry, giving a 1D analysis. A one-dimensional analysis is possible because the concrete and rock material in the laboratory is assumed to be isotropic and homogeneous, and the laboratory fully insulated.

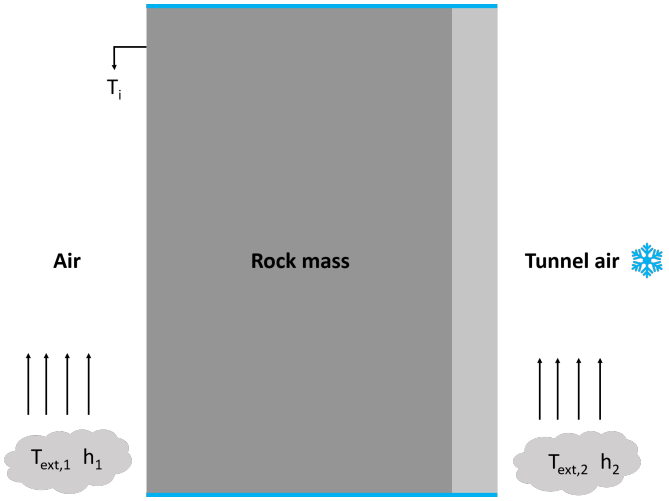

Figure 4.8: Geometry of the numerical simulation, nearly identical to the laboratory. The blue line indicates thermal insulation, T_i is the initial temperature and T_{ext} is the air temperature in the respective rooms.

The experiment in the laboratory consists of two phases. The first phase entails evening out the temperature so that the whole test site has the same temperature. Then the temperature in the tunnel room is turned down to minus ten degrees Celsius. This last phase is the case that is attempted to simulate in COMSOL.

The first step to match the numerical simulation to the laboratory measurements is for the two to have the same initial condition. Since the first phase in the laboratory had limited time, the temperature in the rock mass is not constant. Therefore the rock mass has a temperature distribution which in COMSOL is presented as a piecewise function.

The heat transfer coefficient is the parameter with the most considerable uncertainty when considering this type of heat transfer problem. In the project thesis (Tinderholt, 2018), the heat transfer coefficient was calculated by COMSOL. In this simulation the heat transfer coefficient is set constant, to have better control over the parameter, instead of letting COMSOL calculate the value. Considerable uncertainty connected to the value of the heat transfer coefficient gives room for changing its value, to a larger degree compared to the measured values. The natural range of the heat transfer coefficient is estimated by using mathematical principles presented in the project thesis (Tinderholt, 2018). The heat transfer coefficient should have a value around three [W/(m*K)] on the tunnel side, and around one [W/(m*K)] at the rock mass side.

4.3.1 Results

Changing the heat transfer in order of the estimated value, along with varying the material parameters inside the standard deviation, using the sensitivity analysis as a tool, gave the best fit when the values are as presented in Table 4.3 and 4.4. The external temperature T_{ext}, is set equal to the temperature measured in the laboratory.

Table 4.3: Values of material properties used in the best fit numerical simulation.

Parameter	Rock mass	Concrete
ρ [kg/m^3]	2659	2211-2×6
k [W/(m*K)]	2.7562	1.653-2×0.155
cp [kJ/(kg*K)]	0.840	0.939-2×0.2

Table 4.4: Input values in the numerical model. The temperature is based on temperature measurements in the laboratory and the heat transfer coefficient on trial and error.

Parameter	Rock mass room	Tunnel room
h [W/m^2*K]	1.1	5.7
T_{ext} [C^o]	2.5	-10.5

The best fit of the numerical simulation is presented in Figure 4.9. To get a better image of which measuring points that deviate from the numerically obtained results, the graph is plotted as position versus time in Figure 4.10. In Figure 4.10 the asterisks indicate the measuring points from the laboratory and the solid lines show the numerical calculation. Length equal to zero is located at the surface of the rock mass side. Figure 4.11 is presented to get a better image of the quantitative difference between the numerical simulation and the laboratory results.

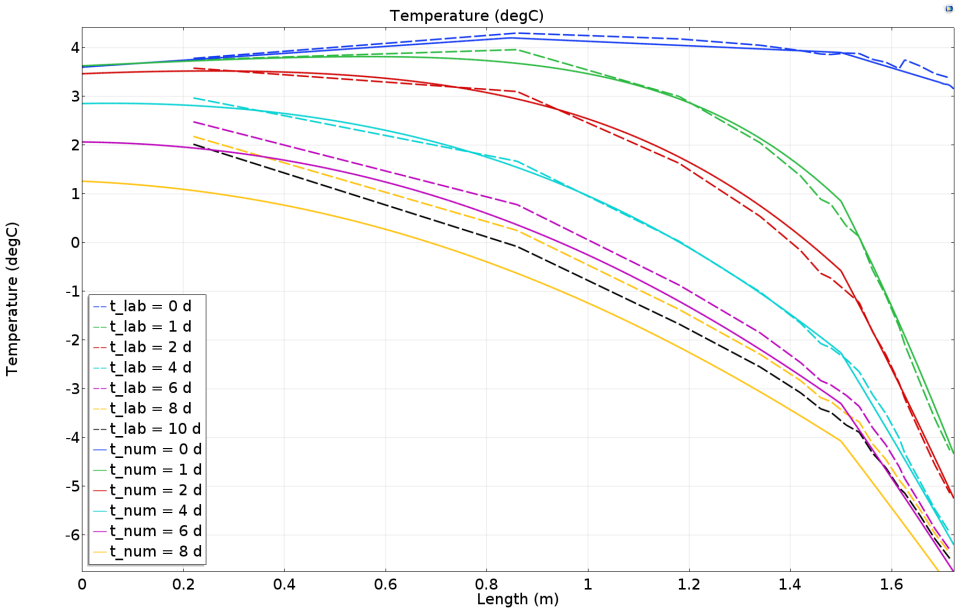

Figure 4.9: Validation of COMSOL, best fit numerical simulation indicated by solid lines. The measured results are plotted as dashed lines.

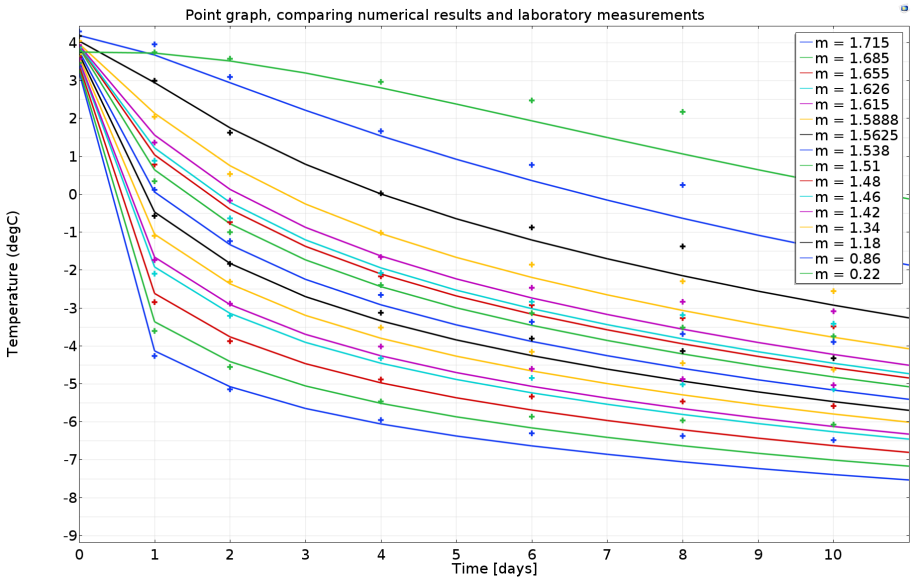

Figure 4.10: Validation of COMSOL, best fit numerical simulation plotted as time (days) vs. temperature. Each solid line indicates the numerical simulation in one measuring point. The asterisks show the measured temperatures from the lab, the colors between the numerical and measured values corresponds.

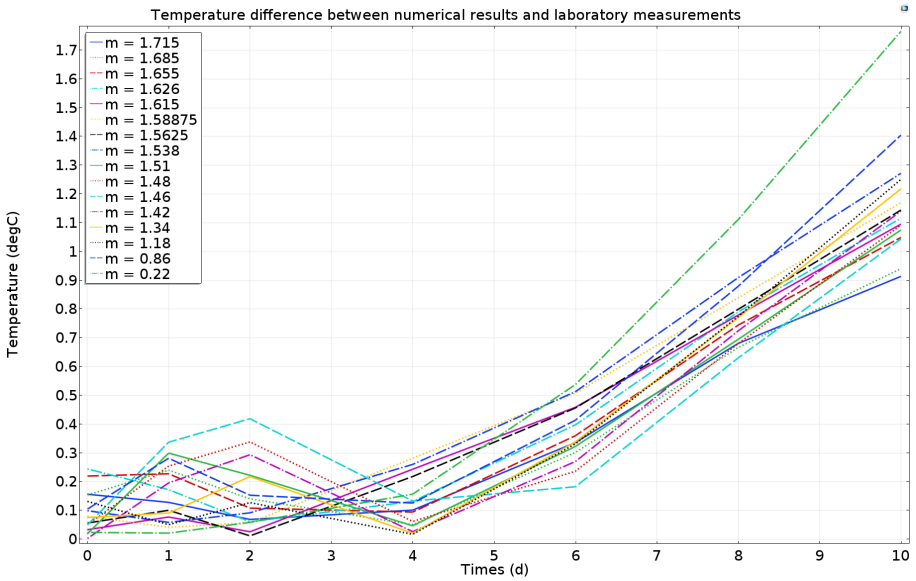

Figure 4.11: Difference between the numerical and measured temperature in each measuring point is plotted as time vs. temperature.

4.4 Discussion

The heat transfer coefficient on the tunnel side is above the expected value, but it is not unnaturally large. Therefore, the value is seen as acceptable. The heat transfer on the tunnel side gives a good correlation on the surface, and further into the rock mass, though there is some deviation in the intersection between the rock mass and concrete. The heat transfer coefficient on the rock mass side is within a reasonable range of the estimated value. Regardless, a good match between the measured and calculated results has been hard to obtain in the vicinity of the rock mass room. One reason for the deviation might be the uncertainty related to the heat flux. There is a trend in the numerical values that the temperature is underestimated, but the correlation between the two does not increase, even if the heat transfer coefficient is lowered further. The nearest measuring point to the rock mass room is located 0.22m into the rock mass, and this means that the boundary temperature is not measured. Without a measured boundary temperature, the correlation at the boundary between the numerical and measured results is not legitimate.

Figures 4.10 and 4.9 shows a good correlation between the measured and calculated results. The trend of the curves matches well, and the deviation between the two is reasonable in the first four to six days. Every measuring point has an uncertainty in its location and its measured value. A good fit of the numerical simulation should lay inside this range of uncertainty, which could be represented as a cross in each measuring point in Figure 4.10. The uncertainty related to the sensors and placement is not found for the laboratory, but the numerical simulation is most likely inside this interval in all points the first four days and within a reasonable range up to six days.

Figure 4.11 shows quantitative difference between the numerical simulation and the laboratory. The graphs follow the same trend for the most part. Six-days after the temperature change, the average temperature difference is around 0.35°C, which must be viewed as a good correlation. Figure 4.11 indicates that the accuracy of the numerical simulation decreases with time, shown by the uniform increase of difference between the numerical and measured results. The reason for this increase in deviation is probably related to aspects in the laboratory, which is not accounted for in the numerical simulation.

The loss of correlation after some time can be connected to the material properties, the laboratory layout, sensor accuracy, and the heat transfer coefficient.

From the validation process, Figure 4.11, one can see that after eight days, the numerical and measured results do no longer match. One possible reason for this deviation might be due to heat that is being transferred from the surroundings into the assumed insulated test area. When setting the temperature in the tunnel room to a temperature lower than the rock mass, heat flux from the rock mass to the tunnel room is activated. If the insulation is not sufficient, there is also a heat flux inward through the insulated sides from the surroundings into the rock mass. The numerical simulation is based on a fully insulated rock mass, which means that

there is no influence from the surrounding area. Total insulation is one of the main reasons why the laboratory can be simulated as a one-dimensional problem. If the effects of the surrounding areas should be considered, the problem would no longer be one-dimensional, and therefore, much more complex to evaluate.

When considering the measuring point in the middle of the geometry, it takes some time before the heat flux through the insulated sides starts to inflict on the measured results. The fact that the deviation is visible after some time fits well with the assumption that there might be leakage of heat into the test area. As discussed, if leakage of heat into the laboratory is a reality, the numerical prognosis should deviate from the measured results since this effect is not taken into account in the model. Figure 4.9 show that the numerical results overestimate the cooling effect in the laboratory. This also supports the assumption that there is heat being transferred to the rock mass.

How long time it takes for the inward heat flux from the surrounding area, to affect the interior of the rock mass, can be estimated using theoretical concepts from Incropera et al. (2017). In this approximation, it is assumed that the air temperature outside the laboratory is constant and that the measuring points are located in the middle of the geometry. A cross section of the rock mass can be seen as a plane wall of thickness 2L = 3.2m. Splitting the length in two gives each side a thickness L. Assuming constant temperature, gives a symmetrical temperature profile along the midline. This approximate solution has a maximum error of 1.7% and the Fourier number, Fo, is assumed to be larger or equal to 0.2. Incropera et al. (2017) presents the following equations to estimate the temperature distribution for transient heat transfer with constant surface temperature, for an interior case of a plane wall of thickness 2L:

$$\theta = 2\exp(-\zeta^2\, Fo) \tag{4.2a}$$

$$\zeta = \pi/2 \tag{4.2b}$$

$$Fo = \frac{\alpha\,\mathrm{t}}{\mathrm{L}^2} \tag{4.2c}$$

Using the rock mass properties from the laboratory. Equation 4.2 gives:

$$\theta = \frac{\mathrm{T}-\mathrm{T}_\infty}{\mathrm{T}_i-\mathrm{T}_\infty} = 2\exp\left[-\left(\frac{\pi}{4}\times\frac{\alpha}{\mathrm{L}^2}\right)t\right]$$

$$\alpha = \frac{\mathrm{k}}{\rho \mathrm{c_p}} = \frac{2.7562}{2659\times 840} = 1.23\times 10^{-6}$$

$$\frac{\mathrm{T}-\mathrm{T}_\infty}{\mathrm{T}_i-\mathrm{T}_\infty} = 2\exp[(-\mathrm{x})\mathrm{t}]$$

$$\mathrm{x} = 1.19\times 10^{-6}$$

Further, it is assumed that the temperature on the outside is around 15°C, T_∞, and the temperature in the rock mass is zero degrees Celsius. If one wishes to find out how long time it takes for the inward heat flux to influence the rock mass with one degree Celsius, T must be equal to one. The above assumptions give the following solution:

$$0.93 = 2\exp[-1.19 \times 10^{-6}\mathrm{t}]$$
$$t = 643460\,\mathrm{sek} \approx 7\,\mathrm{days}$$

This approximation is based on several simplifications of the situation, but after seven days one must expect a deviation between the measured and numerical results of approximately one degree Celsius, which correspond well with the situation seen in the laboratory, Figure 4.11. One degree after seven days also means that one should see some influence before seven days, which again corresponds well with the laboratory case, where one can observe deviation between the measured and numerical results after four days. This quick estimate supports the assumption that there is an inward heat flux through the walls surrounding the rock mass.

Another aspect of the laboratory set-up is that the heaters do not provide a steady temperature, but oscillates around the mean value with ± one degree. This effect is not accounted for in the numerical simulation, where the temperature is set constant at the mean value in the laboratory. The effect of this oscillating temperature could cause the numerical and laboratory measurements to deviate because the two do not have the same boundary condition throughout time.

The instrumentation in the laboratory is beginning to age, and there is also uncertainty in the exact location of the sensors. These two aspects might result in a deviation between the numerical and measured results. Comparing a point value from the numerical simulation to a sensor that might be positioned in a slightly different position, gives a result with a more significant error than the reality.

As a test, a simulation considering the temperature distribution after one month and forward was performed. This showed that fitting the numerical simulation to the measured results, the same way which was performed for the first eight days, was not possible. The lack of concurrence between the numerical and laboratory results in a study, which has run for some length of time, confirms that there is an effect that is not taken into consideration in the numerical model.

4.4.1 Measured heat flux

One measure has been taken to monitor the heat transfer coefficient in the laboratory, namely the installation of heat flux sensors. Along with the thermoelements measuring the temperature inside the rock mass and lining, there are installed instruments on the concrete surface of the tunnel side measuring the heat flux

through the rock mass. Since the rock mass has the highest temperature, the heat is transferred through the rock mass, towards the cold tunnel air. In total there are installed 3 heat flux sensors. The median of the measured heat flux, from the three sensors, are used to create a trendline, Equation 4.5. The best curve fit was obtained by having a logarithmic trendline. Flux measurements from day one and to the fourth of December, make up the basis for the trendline. The trendline is then used in the numerical simulation as a constant inward heat flux. In this case, the heat flux is outward from the rock, and therefore, the expression is set as negative. The argument in the expression is time, t, in seconds.

$$q = -14.98 \times ln(t[s]) + 195.34 \tag{4.5}$$

Having control over one of the most uncertain parameters in the laboratory, namely the heat transfer coefficient, by measuring the heat flux, should give a better match between the numerical and measured results. However, setting the heat flux equal to Equation 4.5 gives a temperature distribution which does not give a plausible result. Using a constant heat flux in COMSOL neglects the temperature difference between the surface and air, and the effect is that the heat flux becomes overpowering in the simulation. The measured heat flux is therefore of little use in the validation prosses other than that it shows that the heat flux decreases over time, as expected.

4.5 Measures for a better validation process

In order to have a perfect validation without any uncertainties, there are some measures which could have been taken in the laboratory.

Some insulation has been installed in the laboratory. Between the floor and rock, a matt of insulating material is placed, between the rock and walls silicon is used, and against the roof insulating foam, (Vassenden, 2010). These measures work as insulation to some degree, but from the laboratory results, it seems that the insulation is too spars and not sufficient to say that the rock mass is fully insulated.

The cooler/heater installed in the tunnel and rock room oscillates, turning on and off to keep the temperature in a range of ± one degree of the set temperature. For an optimum comparison basis, the oscillations should have been kept to a minimum or non-existing, keeping a steady temperature, for the laboratory and numerical model to have the same conditions.

Better control over the boundary effects, which includes the heater/cooler, as discussed, and the heat transfer coefficient, would increase the reliability of the numerical simulation.

The material properties in the laboratory are tested, but the number of test specimens is few, and therefore, the reliability of the parameters is weakened. The

accuracy of the thermophysical properties of the conductive material affects the results.

The instruments in the rock mass are beginning to age, and the reliability is unknown. At the same time, the accuracy of the measuring location is also uncertain. Knowing measuring and location accuracy would have increased the quality of the validation.

A measuring point in the Tonalite closer to the rock mass room would have improved the basis of comparison between the numerical and measured results.

Heat flux sensors and air shields have been installed on the tunnel side, but on the rock mass side, there has been taken no measures to control the air flow or measure the heat flux and air temperature. Implementing this would not have had a direct difference for the validation processes, but it would have provided more control over the parameters that go into the numerical calculation.

4.6 Final remarks

The numerical program COMSOL is validated by using the laboratory as a basis of comparison. The COMSOL model provides a prediction with an accuracy of 0.35°C.

The validation shows that there is a good correlation between the theory, COMSOL, and the measured results in the laboratory. The well-founded validation of the theoretical program means that COMSOL can be used to estimate the temperature distribution in rock mass and concrete subjected to an external temperature. The rock mass in the laboratory is homogeneous, which is not usually the case for bedrock. An inhomogeneous rock mass has thermophysical properties that vary in a large or small scale. This means that the numerical program can only provide an estimate because the variations of the rock are impossible to foresee.

The validation also shows that for a more complex heat transfer situation, there might be a need for a two-dimensional analysis.

Chapter 5

Numerical presentation of Gevingås Tunnel

The validation preformed in Chapter 4 confirms that COMSOL can be used to estimate the temperature in a controlled environment. But how does the program work when looking at a real-life tunnel, in an uncontrollable environment? To examine this, the measuring results for the Gevingås Tunnel and the measured thermophysical properties of materials are used to build a numerical model of the tunnel.

5.1 Two-dimensional simulation

A two-dimensional model is built in COMSOL, to show the larger perspective of the temperature distribution around the tunnel opening. The simulation geometry is shown in Figure 5.1, the dimensions are approximately equal to those of the Gevingås Tunnel. The dimensions of the tunnel room are shown in Table 5.1, along with the material properties. The rock mass has a scale, so the effect of the tunnel temperature does not reach the boundary of the geometry.

The mesh is built to obtain reliable results, and at the same time having the computation time in mind. Because of the models relatively large size, it would be unnecessary to build the model with the same extremely fine mesh. Therefore the model is meshed so that the areas closest to the tunnel opening has a finer mesh, with an increasing mesh size as one progresses away from the opening, Figure 5.1.

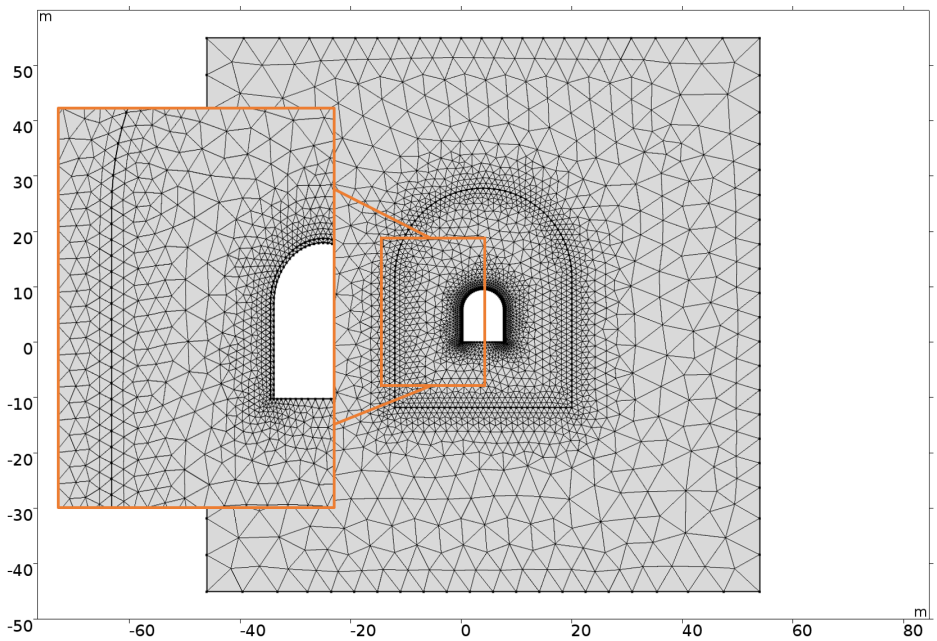

Figure 5.1: Meshed geometry of the two-dimensional numerical simulation built to match the Gevingås Tunnel.

Table 5.1: Overview of the tunnel room dimensions and material properties, used in the two-dimensional analysis of the Gevingås Tunnel.

Property	Value
Height side wall	5.9 m
Width floor	7.5 m
Height of arch	3.75m
Concrete thickens	26 cm
Mestasandstone	
Density, ρ	2708 kg/m^3
Thermal conductivity, k	4.2 W/(m K)
Heat capacity, Cp	688+10% J/(kg K)
Concrete	
Density, ρ	221 kg/m^3
Thermal conductivity, k	1.65 W/(m K)
Heat capacity, Cp	800 J/(kg K)

When simulating in 2D, with a curved surface, the initial values and heat flux configurations, changes and becomes more complex compared to a one-dimensional analysis. In this model, the heat flux is mainly based on COMSOLs calculations. The geometry of the half circle, making up one side of the roof, is simplified to

an inclined wall, to be able to estimate the heat transfer coefficient. COMSOL calculates the heat transfer coefficient based on this inclined wall and external natural convection. The inclined wall is five-point tree meters long, with a tilt angle of 0.75 radians. On the floor, COMSOL is used to define the heat transfer coefficient. The convection is set to be external and natural, and the floor is seen as a horizontal plate, with air exposure on the upside. COMSOL also calculates the heat transfer coefficient on the side walls.

A four-day moving average of the temperature measured ten centimeters from the tunnel surface in the Gevingås Tunnel, in the winter season of 2016/2017, is used as the external temperature, Figure 5.2.

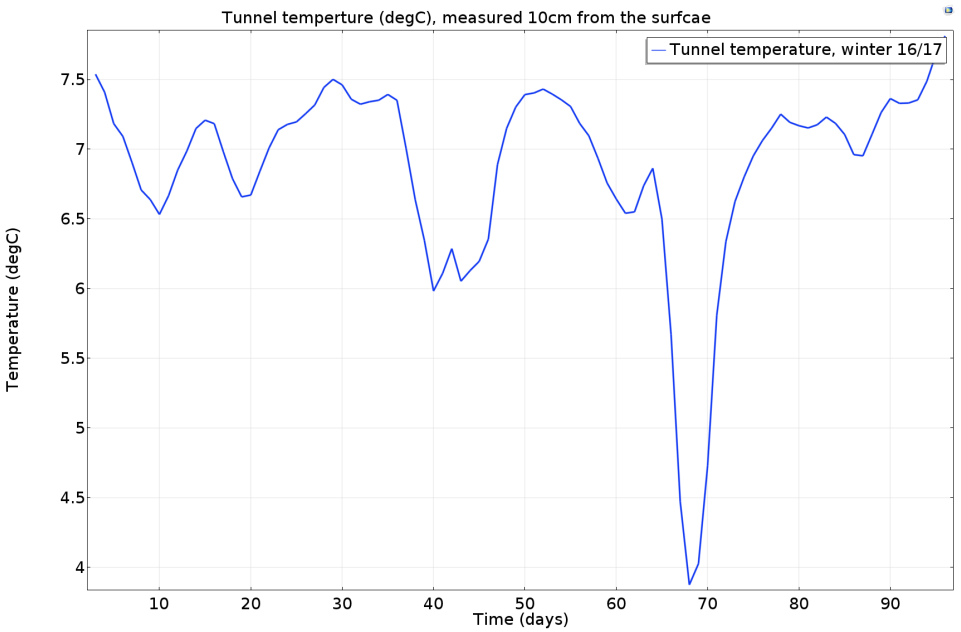

Figure 5.2: Four-day gliding average of the measured tunnel temperature in the Gevingås Tunnel. The measuring period shown, stretches from 29.12.16 to 04.04.17, winter of 2016/2017.

The simulation is a time-dependent study, plotted with a one-day time step, over 96 days. To obtain an initial condition that would match that of a real situation, the initial temperature in the solid could not be a constant value. To solve this, the simulation consists of two studies, where the second study uses a time interval from the first study as an initial condition. Figure 5.3 shows the initial condition in the second study used in the presiding analysis. The temperature distribution after 70 and 96 days of winter are shown in Figure 5.4 and 5.5 as contour plots.

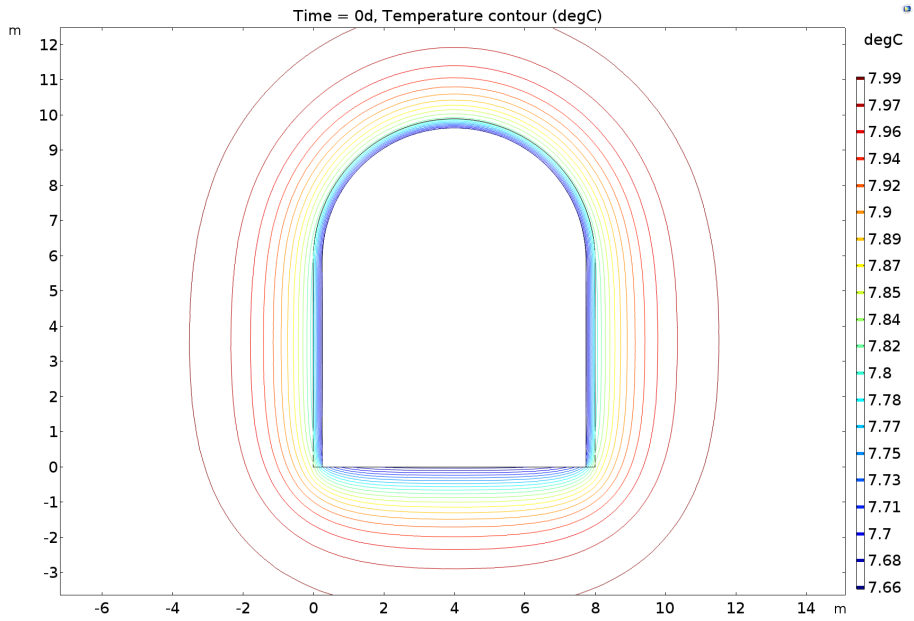

Figure 5.3: Initial temperature in study two, using day ten from study one as the initial temperature, shown as a temperature contour.

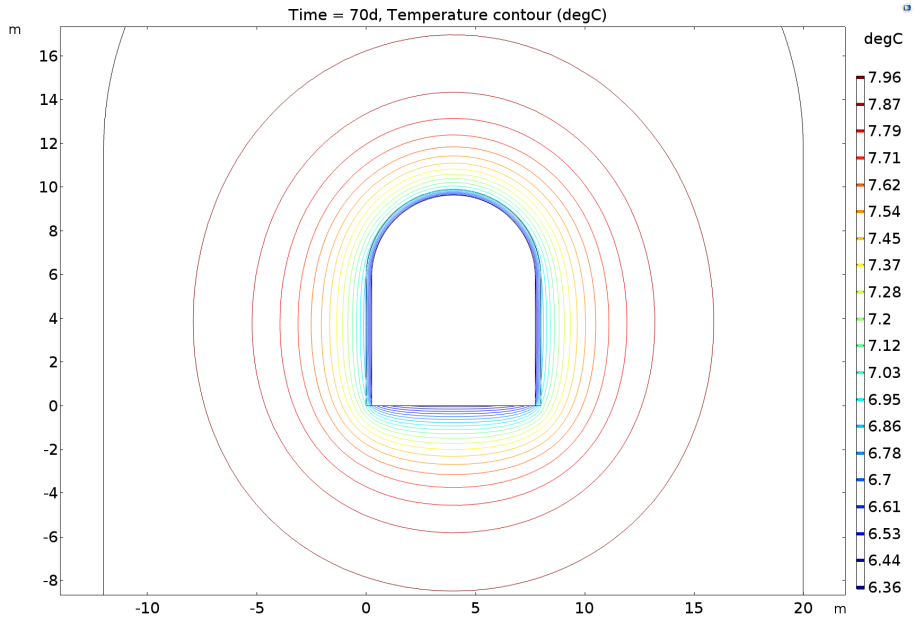

Figure 5.4: Temperature contour after 70-days.

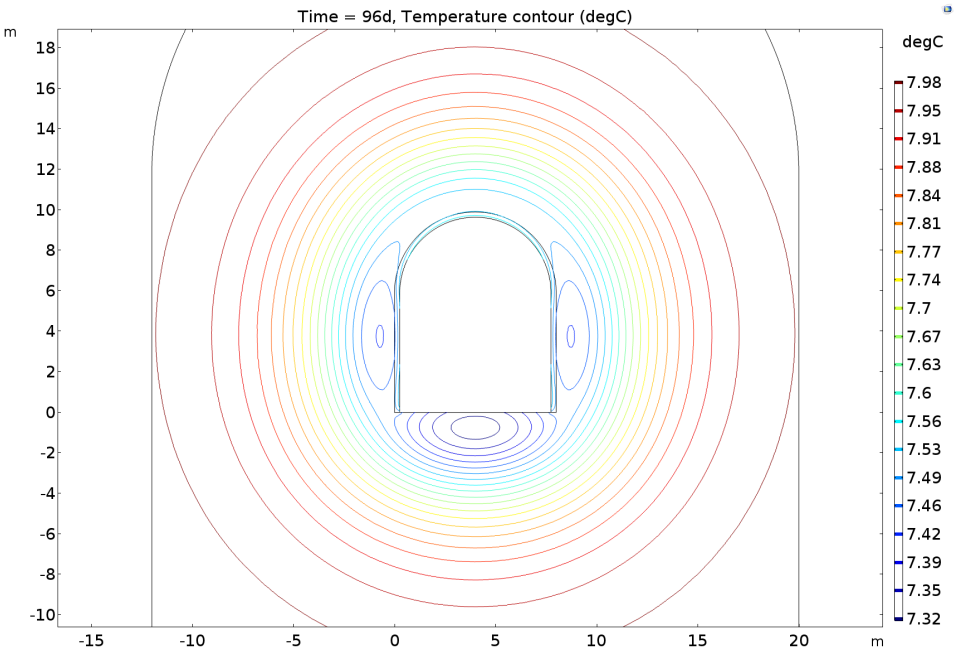

Figure 5.5: Temperature contour after 96-days, beginning of April.

5.1.1 Remarks

The two-dimensional simulation shows an approximation of the temperature distribution around the tunnel opening. The coldest period in the simulation is just before the 70-day profile, and the distribution shows that the side walls and floor have the lowest temperatures. At this instant, the temperature distribution inside the rock mass is affected by the tunnel temperature up to approximately eight meters. After 96-days the winter is nearing an end, and the rock mass temperature is affected to approximately 12 meters. However, the variation range, as shown by the legend, is minimal; the largest variation is seen in the first five meters, which corresponds with the measurements from the tunnel. The roof shows a higher temperature compared to the side walls and floor.

The floor in the model is highly simplified. In the simulation, the tunnel temperature is in direct contact with the rock in the invert. This would not be the case in a real tunnel, where the floor is composed of several layers of aggregate, creating a layer between bedrock and tunnel air. Based on this, the temperature in the vicinity of the invert is probably higher than what the simulation shows.

5.2 One-dimensional

A one-dimensional simulation should be sufficient when analyzing the temperature distribution inwards in the wall. Because the rock mass can be seen as an infinitely large slab. Keep in mind that the bedrock is not homogeneous, so the simulation can only provide an estimation, as mentioned in the laboratory validation. As shown from the measurements at the Ulvin Tunnel and the 2D simulation the temperatures in the roof are higher than in the wall, and to evaluate the temperature distribution concerning negative temperatures, the wall temperature is, therefore, the focus point.

The one-dimensional numerical analysis of the Geinvgås tunnel is performed in COMSOL. All the measuring stations are placed in areas where the tunnel lining is constructed as a bounded system using a sprayed membrane, for the geometry of the simulation, the membrane is neglected because compared to the other components the effect of the membrane is insignificant. The concrete thickness is set to 30cm, this thickness varies inside the tunnel but only by a couple of centimeters. The rock mass length is set long enough so that the temperature variations do not reach the back end of the geometry. The material parameters used in the model are shown in Table 5.2, based on the measured material properties as presented in Chapter 2. For the concrete properties, the dry parameters are used, since the concrete has had substantial time to dry to DCS of approximately 70%.

Table 5.2: Material parameter used in the numerical simulation of the Gevingås Tunnel.

	Density [kg/m^3]	Thermal conductivity [W/(m K)]	Heat capacity [J/(kg K)]
Meta sandstone	2708	4.2	688+10%
Concrete	2211	1.65	800

The data from the winter of 2016/2017 at the north measuring station seems to be the most reliable. Therefore, this season is used as the basis for the simulation. The initial temperature in the concrete and rock is set equal to the average temperature of the first measuring day. The external temperature in the numerical model is set equal to the four-day moving average of the measured tunnel temperature, as for the 2D simulation, Figure 5.2. In total the winter of 2016/2017 was logged for 96 days, and so the numerical model is run for 96 days, as a time-dependent analysis.

5.2.1 Results

Figure 5.6 shows the absolute difference between the measured daily average and the simulated numerical values. In Figure 5.7, the tunnel air temperature is included, to show in which situations the numerical and measured results deviate the most.

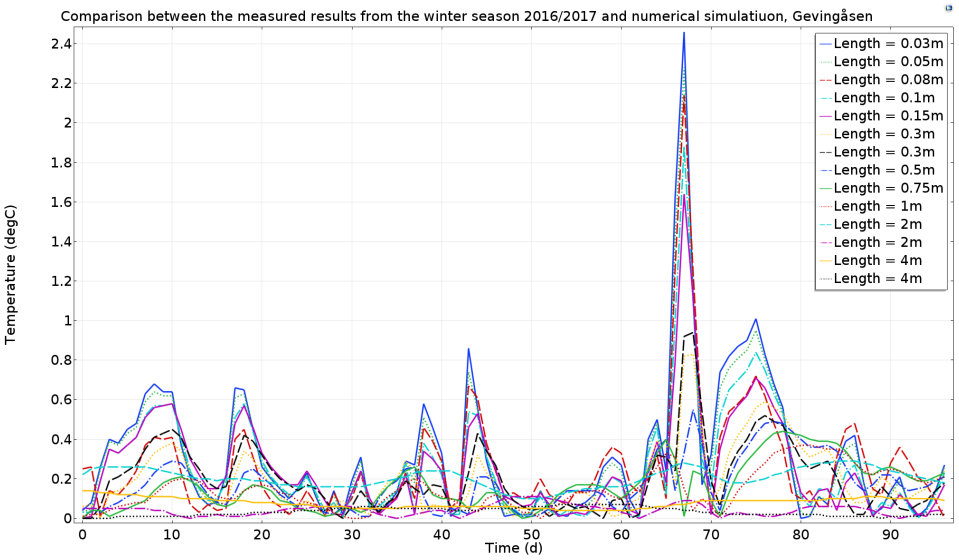

Figure 5.6: Deviation between the measured and numerical simulated temperature distribution in the concrete and rock mass at the north measuring station in the Gevingås Tunnel, based on the winter season of 2016/2017.

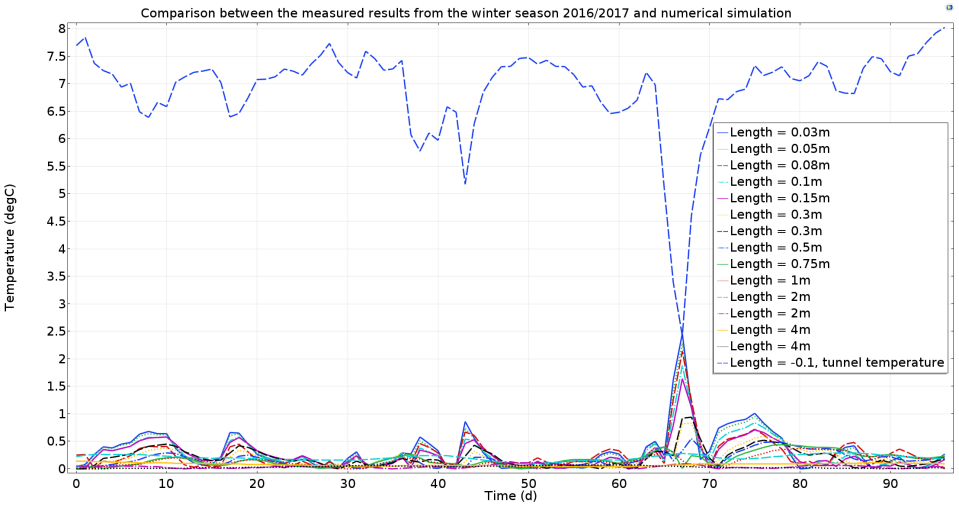

Figure 5.7: Deviation between the measured and numerical simulated temperature distribution in the concrete and rock mass at the north measuring station in the Gevingås Tunnel, based on the winter season of 2016/2017. Including the tunnel air temperature, measured ten centimeters from the surface.

5.3 Discussion

Overall the one-dimensional simulation obtains a good representation of the temperature variations. The average deviation is less than 0.5°C. However, from Figure 5.7 it is also notable that the numerical simulation works best for the temperature changes with lower frequency, the relatively quick drops in temperature are inaccurately simulated in COMSOL. This is also confirmed by observing that the measuring points in the outer layers of the structure, the concrete and first parts of rock, are the measuring points with the largest deviations. As mentioned earlier, the temperature variations with high frequency penetrate shallow compared to the seasonal variation. Therefore, the area closest to the surface is most affected by the quicker temperature variations, meaning that COMSOL simulates the temperature variations with the lowest frequency the best.

The reason that the measured results show a quicker and more pronounced response, compared to the numerical simulation is hard to pinpoint at one specific source. The parameters that might influence this deviation is the thermal diffusivity, the heat transfer coefficient, and the temperature difference. The thermal diffusivity, Equation 2.1, is probably lower than calculated/assumed, or/and the heat transfer coefficient is larger than assumed, at the same time the temperature difference might be larger than assumed.

One reason why the numerical model simulates the deeper parts of the rock mass better might be connected to the use of the four-day average of the external temperature. The four-day average based on the daily variation smoothens out the quick variation, and to some degree also the larger variations. However, as there is more concern connected to the temperature situation in the rock mass this inaccuracy in the first 30cm has little consequences for the applicability of the numerical model, as the rock mass is well simulated. However, if the goal of the numerical analysis is to simulate the concrete this might be a source of error to investigate further.

Figure 5.6 shows the difference between the measured and numerical temperatures. The deviation between the two might also be connected to the measured values. The measured values have, as discussed in the previous chapter, uncertainty connected to the accuracy in both measured values, and location. Uncertainty related to the measurements means that the direct comparison, between the simulated numerical values and the measured temperatures, might be erroneous.

Chapter 6

In-situ validation

COMSOL has a built-in functionality, which makes it possible to perform parameter estimation, using the study step called Parameter Estimation. The study step works by letting COMSOL know that one or more of the parameter values used in the simulation are unknown or uncertain, and asking the program to vary these, so the simulation fits some reference data. This study might contribute in making the numerical model, presented in the previous chapter, an even better representation of the Gevingås Tunnel, and providing a sensitive parameter, which might result in a more reliable simulation result.

6.1 Benchmark analysis

Before the Parameter Estimation study is used on the Gevingås model, a benchmark analysis is carried out to get a better understanding of how Parameter Estimation works. The Gevingås model is quite complex, composed of several materials. Therefore a simpler model is used in this initial analysis.

The benchmark model is one-dimensional, consisting of only one homogeneous material. In this case, the external temperature is constant at two different levels; the temperature changes instantaneously to -10^{o}C, as a switch.

First, the model is run with known material parameters, tabulated in Table 6.1. From this simulation, data is extracted, which is then used as the reference data in the Parameter Estimation study.

The SNOPT algorithm is used as the optimization method. COMSOL also provides two other optimization algorithms, the BOBYQA, and the Levenberg-Marquardt methods. The BOBYQA method should be used, when the parameters that are to

be estimated control the geometry or mesh, which is not the case in this optimization problem. The Levenberg-Marquardt method does not support constraints. Later, when evaluating the Gevingås Tunnel model, one wishes to constrain the parameters within a plausible range, securing that the result is within what is naturally acceptable values. Therefore, the Levenberg-Marquardt method is not suitable for the Gevingås Tunnel, and therefore not used in the benchmark study leading up to this more complicated case.

Table 6.1: Properties of the benchmark analysis.

Parameters	Values
k [W/(m K)]	2.9
ρ [kg/m^3]	2600
Cp [W/(m^{2}4 K)]	850
h [W/(m^2 K)]	5
$T_{external}$ [^{o}C]	-10

The set-up of the Parameter Estimation study is presented in Table 6.2. Since all the material parameters have an interconnected effect, all of the model parameters are estimated at the same time.

Table 6.2: Set-up of the benchmark Parameter Estimation study, showing the parameters initial values, scale and value constraints.

Parameter	Initial value	Scale	Lower b.	Upper b.
k	2	1	2	4
ρ	3000	1	1000	4000
Cp	750	1	450	1200
htc	4	1	4	8

Table 6.3 shows the numerical estimated parameters, along with the deviation from the correct value. The Parameter Estimation is performed using one reference point, two meters from the surface. The estimated parameters give the numerical solution shown in Figure 6.1, which also shows the reference data, used to obtain the estimated values.

Table 6.3: Result from benchmark Parameter Estimation study, showing the estimated value along with the deviation from the known correct value.

Parameter	Estimated value	Deviation
k [W/(m K)]	2.95	2%
ρ [kg/m^3]	3000	13%
Cp [W/(m^{2}4 K)]	750	12%
h [W/(m^2 K)]	5 .1	2%

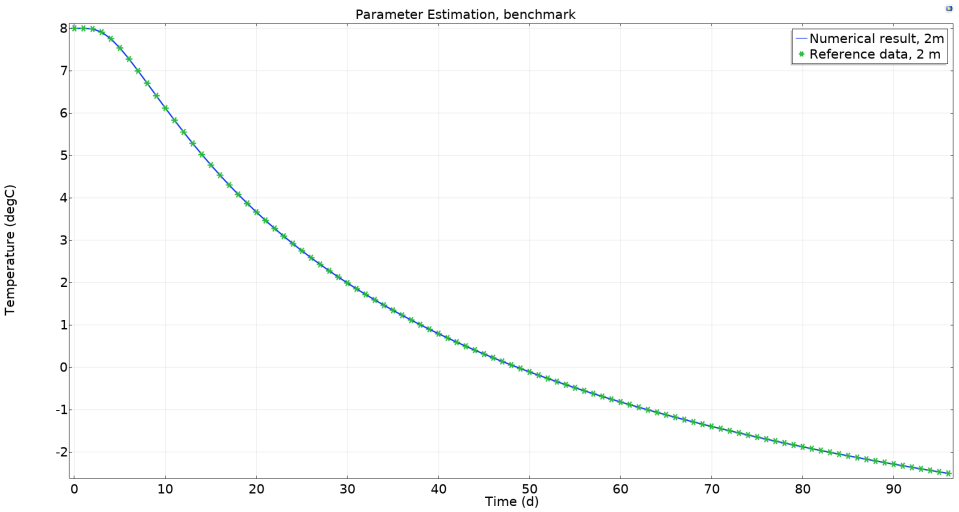

Figure 6.1: Result from the benchmark analysis, showing both the Parameter Estimated result and the reference data.

6.1.1 Remarks

The benchmark analysis shows that the Parameter Estimation study can obtain a perfect curve fit. However, the study provides parameters that do not match those of the reference data. This again means that there are several parameter values, several solutions to the parameterization problem, that gives a good curve fit.

The benchmark study is a relatively simple model, and therefore, an average deviation of 7% from the parameter's value must also be expected in a more complex model, as for that of the Gevingås Tunnel.

6.2 Parameter Estimation

The one-dimensional numerical model of the Gevingås Tunnel deviates from the measured results, as discussed in the previous chapter. Two of the possible reasons for the deviations that were highlighted in Chapter 5, was the material parameters as well as the heat transfer coefficient. A Parameter Estimation study can hopefully minimize the error connected to these parameters. The Parameter Estimation study is a type of back calculation, which is performed by evaluating each parameter, and choosing the value for this parameter, inside a range, so that the simulation is as equal as possible to a reference value.

The reference data is measured results from the north station in the Gevingås

Tunnel in the winter of 2016/2017. The data used both as the external temperature and as reference data are smoothed using the four-day moving average, over the daily average. The numerical model is used to estimate the parameters in eighth of the measuring location, Table 6.5. Since the Parameter Estimation study node only handles reference data presented in seconds, the argument in the measured results is transferred from days to seconds. The SNOPT algorithm is used as the optimization method in all the studies. The optimality tolerance is set to 1e-9, and the maximum number of model evaluations is 4000.

In total, six different Parameter Estimation studies are performed to find the study set-up that provides the best representation of the Gevingås Tunnel.

6.2.1 Initial Parameter Estimation study

Table 6.4, shows an overview of the parameters that are back calculated. The parameters upper and lower bound in the two initial studies are calculated using two times the parameters standard deviation. For parameters where several measurements are available, as the rock mass conductivity, the highest and lowest mean value is used as the reference to which the uncertainty of the parameters is added or subtracted.

Study no.1

The scale factor in the first initial study, no.1, is equal to the difference between the upper and lower bound, Table 6.4. The initial value is equal to the parameters mean value.

Table 6.4: Overview of the parameters that are estimated using back-calculation, in study no.1. The initial value is the mean value of the parameters from the Gevingås materials, found in Section 2.2, and the bounds are two times the parameters standard deviation (STD).

no.1	Parameter	Initial value	Scale	Lower b.	Upper b.
	htc [W/(m^2 K)]	5	10	0	10
Rock	k [W/(m K)]	4.1	1.1	3.32	4.56
	rho [kg/m^3]	2708.6	145.1	2622.9	2768
	Cp [J/(kg K)]	688	624.4	550	1175
Concrete	k [W/(m K)]	1.65	0.4	1.58	1.96
	rho [kg/m^3]	2211	251	2167	2418
	Cp [J/(kg K)]	800	250	750	1000

Table 6.5 shows the results from Parameter Estimation study no.1, along with the average value for each parameter and the standard deviation. Figure 6.2 shows the numerical result based on the Parameter Estimation study step and the reference data which the numerical model has tried to match.

Table 6.5: Overview of the result from the Parameter Estimation study no.1, along with the average value and standard deviation (STD).

no.1	Rock			Concrete			
Location	k	rho	Cp	k	rho	Cp	htc
0.03m	3.46	2622.9	550.4	1.9412	2166.8	750	10
0.08m	3.46	2622.8	550.4	1.9610	2417.9	1000	10
0.1m	3.46	2622.9	550.4	1.961	2282.9	991.41	10
0.3m	3.46	2709.1	1008.9	1.961	2205.6	786.09	10
0.5m	3.46	2720.9	1075.9	1.961	2166.8	750	10
0.75m	4.56	2713.3	949.07	1.617	2166.8	750	10
1m	4.56	2712.6	1012.3	1.961	2166.87	750	10
2m	3.46	2694.7	566.83	1.961	2417.9	1000	10
Average	3.7	2677.4	783	1.92	2248.9	847.6	10
STD	0.5	42.8	230.8	0.11	104.4	116.5	0
STD [%]	12.8	1.6	29.5	5.9	4.6	13.8	0

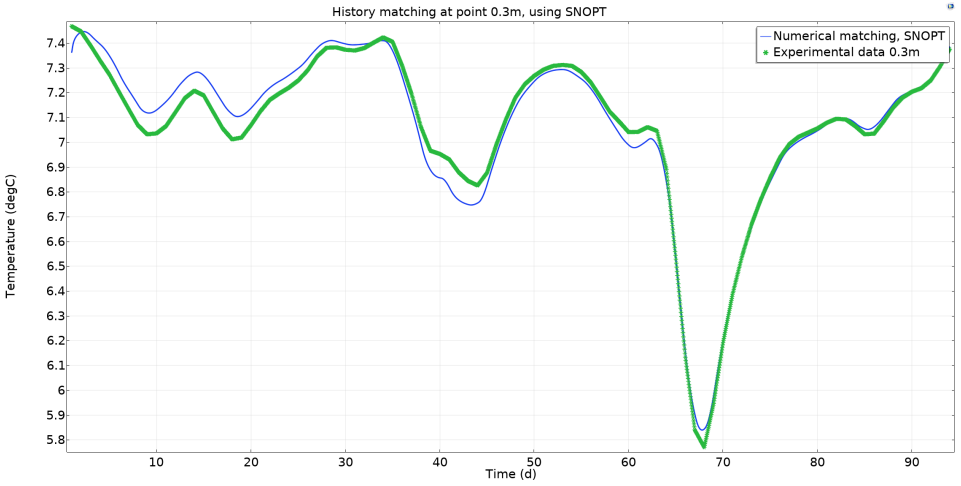

Figure 6.2: Result of the Parameter Estimation in measuring point 0.3m, study no.1, showing the reference data i.e. the measured temperature and the result from the numerical Parameter Estimation study.

For the previous model of the Gevingås Tunnel, the deviation between the measured and numerical estimated value where presented, by finding the absolute difference between the two in each point of measurement. The same comparison is made for this model to get a better intuition of how well the Parameter Estimation study works. The average value from the Parameter Estimation study is used as the basis for comparison. The deviation between the numerical and measured results are shown in Figure 6.3. The largest deviation is 1.36°C, seen in the outermost

measuring point, at 0.03m from the tunnel surface. This is an improvement from the previous model.

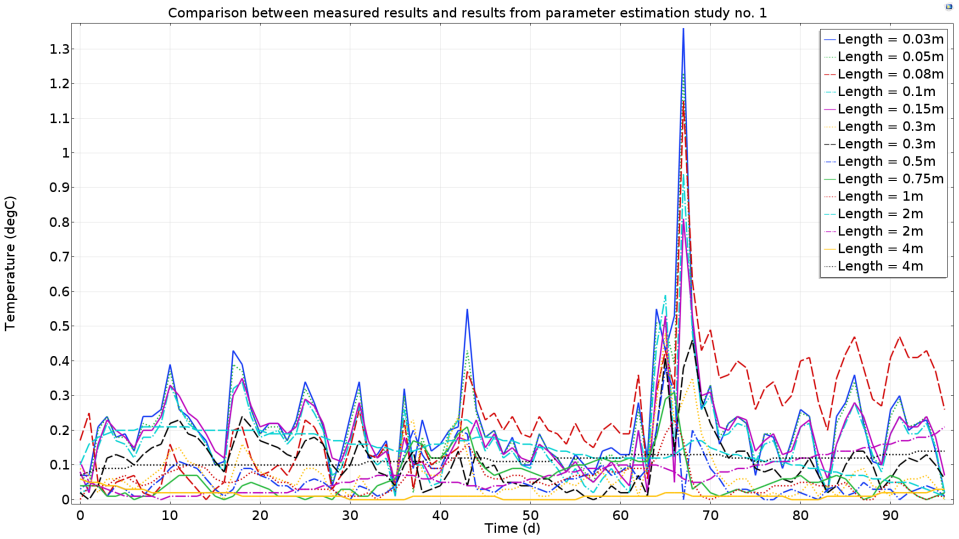

Figure 6.3: Showing the absolute difference between the measured temperature, and the numerical estimated values based on Parameter Estimation study no.1, in all measuring points.

Study no.2

The second study of the Initial Parameter Estimation studies, study no.2, is calculated using a scale factor of one for all the parameters. Table 6.6 shows the average result along with the standard deviation from study no.2. The difference between the average values from study no.1 and no.2 is small; the most significant difference is seen for the heat transfer coefficient, which varies more in study no.2. Comparing study no.2 to the measured result as done for study no.1, study no.2 has a large deviation in measuring point 0.03m, of 1.41°C. Between these two studies, the set-up of study no.1 provides the best fit to the Gevingås Tunnel.

6.2.2 Parameter Estimation study continued

Because the numerical simulation in study no.1 and 2, tended to give results equal or close to the boundary conditions, the boundaries in study no.3 and 4 are expanded. The boundaries are expanded beyond the standard deviations of the material parameters, but at the same time held relatively tight so that the values obtained by the Parameter Estimation are plausible, Table 6.7.

Table 6.6: Result from Parameters Estimation study no.2, showing the scale factor used in the study, average estimated value and the standard deviation of the results.

no.2	Parameter	Initial value	Scale	Average	STD[%]
	htc [W/(m^2 K)]	5	1	9.3	13.39
Rock	k [W/(m K)]	4.1	1	3.59	12
	ρ [kg/m^3]	2708.6	1	2700.4	2.11
	Cp [J/(kg K)]	688	1	730.8	23.88
Concrete	k [W/(m K)]	1.65	1	1.8	9.26
	ρ [kg/m^3]	2211	1	2241.44	4.21
	Cp [J/(kg K)]	800	1	830	13.52

Study no.3

The set up of study no.3, is presented in Table 6.7. The results from study no.3 are presented in Table 6.8. Of the average value obtained through study no.3, four out of seven values lay within two times the standard deviation of the parameter, even though the bounds are expanded.

Table 6.7: Overview of the parameters that are estimated using back calculation, in study no.3. The initial value is the mean value of the parameter for the Gevingåsen tunnel, found in Section 2.2, the upper and lower bound is expanded beyond the parameteres standard deviation (STD).

no.3	Parameter	Initial value	Scale	Lower b.	Upper b.
	htc [W/(m^2 K)]	5	1	0	10
Rock	k [W/(m K)]	4.1	1	2	6
	rho [kg/m^3]	2708.6	1	2200	3200
	Cp [J/(kg K)]	688	1	500	1200
Concrete	k [W/(m K)]	1.65	1	1	2.2
	rho [kg/m^3]	2211	1	2000	3000
	Cp [J/(kg K)]	800	1	600	1200

Comparing the results from a numerical simulation of the Gevingås Tunnel using the average value from study no.3, with the measured results, gave an even better match than for the first study, Figure 6.5 and 6.4. The largest difference detected is 1.27°C, again seen in measuring point 0.03m, the mean difference over all the measuring point is 0.11°C, with a standard deviation of 0.12°C.

Table 6.8: Overview of the result from the Parameter Estimation study no.3, along with the average value and STD. (*) means that the value lay within two times the parameters standard deviation.

no.3	Rock			Concrete			
Location	k	rho	Cp	k	rho	Cp	htc
0.03m	2	2200	500	1.2	2225	911.83	10
0.08m	2	2200	500	1.2	3000	1024	10
0.1m	2	2200	500	1.2	2319.2	1081.4	10
0.3m	2.23	2708.6	687.98	1.15	2211	799.96	10
0.5m	2.16	2747.1	837.56	1.2	2000	600	10
0.75m	4.69	2708.6	687.93	1.2	2211	799.96	10
1m	3.78	2714.1	709.8	1.2	2202.8	777.44	10
2m	2.58	2200	500	1.2	3000	1200	10
Average	2.68	2459.8	615.41*	1.19	2396.13*	899.32*	10*
STD	0.94	260	123.5	0.01	358.36	181.47	0
STD [%]	35.16	10.57	20.07	1.43	14.96	20.18	0

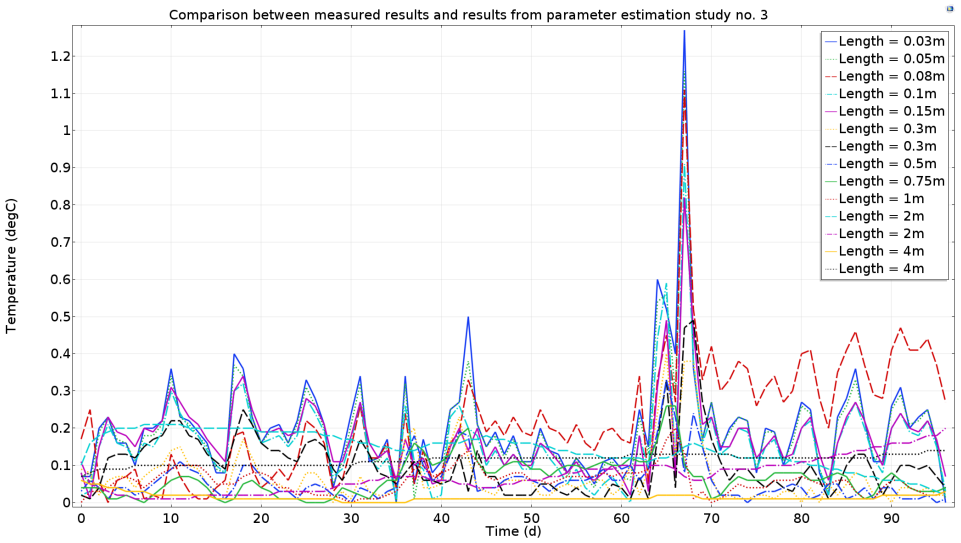

Figure 6.4: Showing the absolute difference between the measured temperature, and the numerical estimated values based on Parameter Estimation study no.3, in all measuring points.

Study no.4

In the initial studies, the study with the scale equal to the difference between the upper and lower bound gave a better match to the measured results. Therefore

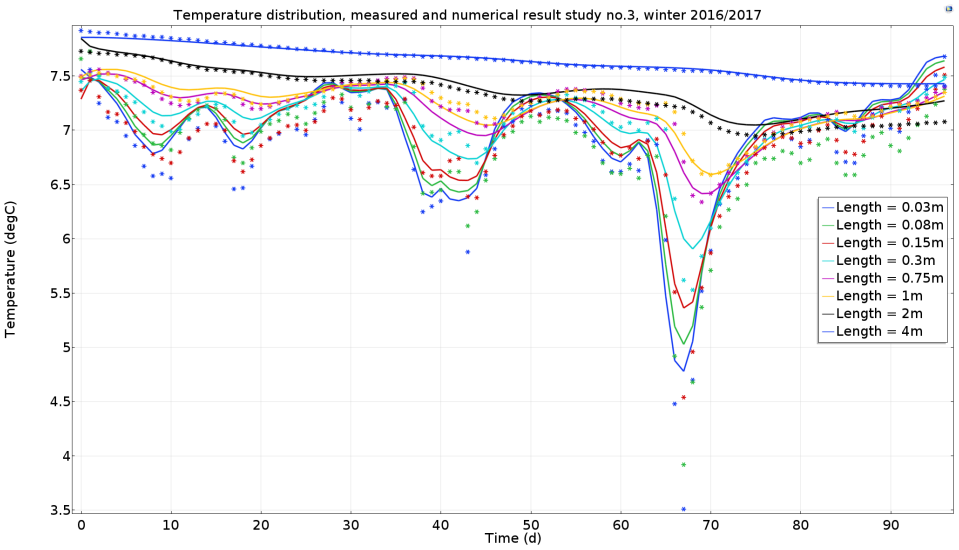

Figure 6.5: Numerical simulation based on the average values from study no.3, plotted as time (days) vs. temperature. Each solid line indicates the numerical simulation in one measuring point. The asterisks show the measured temperatures, the colors between the numerical and measured values corresponds.

study no.4, is run with this type of scale, along with the expanded bounds as study no.3. Table 6.9 shows the set-up of study no.4. The parameters are estimated in eight points as in the previous studies, the average values of the eight evaluations are shown in Table 6.9, with the standard deviation. Comparing the numerical model of the Gevingås Tunnel using the mean values obtained in study no.4, to the measured temperatures, did not give a better match than study no.3. The maximum difference was again seen in point 0.03m and is the highest of all the studies, of 1.42°C.

Table 6.9: Result from Parameters Estimation study no.4, showing the scale factor used in the study, average estimated value and the standard deviation of the results.

no.4	Parameter	Initial value	Scale	Average	STD[%]
	htc [W/(m^2 K)]	5	10	9.65	11.1
Rock	k [W/(m K)]	4.1	4	3.3	42
	ρ [kg/m^3]	2708.6	1000	2721.7	13.7
	Cp [J/(kg K)]	688	700	881.8	32.9
Concrete	k [W/(m K)]	1.65	1.2	2.13	8.67
	ρ [kg/m^3]	2211	1000	2243.7	15.69
	Cp [J/(kg K)]	800	600	779	30.18

6.2.3 Parameter Estimation, increased data

The four studies presented above all show an increased deviation between the measured and simulated results in the first parts of the tunnel. The quick temperature variations influence the first part of the tunnel the most, and even though the deviation was reduced through the Parameter Estimation, it is still present. Therefore, two additional Parameter Estimation studies are performed using the measured external temperature from the Gevingås Tunnel in 2016/2017, but in these studies, the temperature is not smoothed, meaning that the exact measured temperature is used, at a sampling rate of every other hour.

Study no.5 and 6

The set up in study no.5 is equal to that of study no.1, Table 6.4. Table 6.10 shows the results from Parameter Estimation study no.5, along with the average value for each parameter and the standard deviation.

Study no.6, used the same bounds as study no.1 and 5, but the scale factor was changed to one. The results from this study are not presented as it provides no extra information, because the results are close to equal the results from study no.5.

Table 6.10: Overview of the result from the Parameter Estimation study no.5, along with the average value and standard deviation (STD).

no.1	Rock			Concrete			
Location	k	rho	Cp	k	rho	Cp	htc
0.03m	3.88	2705.9	550	1.68	2209.8	797.1	8.3
0.08m	3.32	2669.3	550	1.96	2286.8	1000	8.98
0.1m	3.32	2706.6	682.8	1.96	2189.2	750	8.1
0.3m	3.56	2718	1175	1.96	2167	750	10
0.5m	4.31	2713.1	889.3	1.78	2167	750	10
0.75m	4.56	2708.1	698.6	1.67	2167.1	750	5.9
1m	4.1	2706.2	661.2	1.67	2208.1	792.1	5.97
2m	3.32	2632.2	555.7	1.96	2418	1000	9.9
Average	3.8	2694.9	720.3	1.8	2226.6	823.6	8.4
STD	0.5	42.8	215.7	0.1	87	110.6	1.7
STD [%]	14	1	30	8	4	13	20

Using the average values from study no.5 and the external temperature measured every other hour in the numerical one-dimensional model of the Gevingås Tunnel gave a nearly perfect match to the measured data, as shown in Figure 6.6. The largest deviation between the measured data and the simulated result is 1.02°C three centimeters from the surface, Figure 6.7.

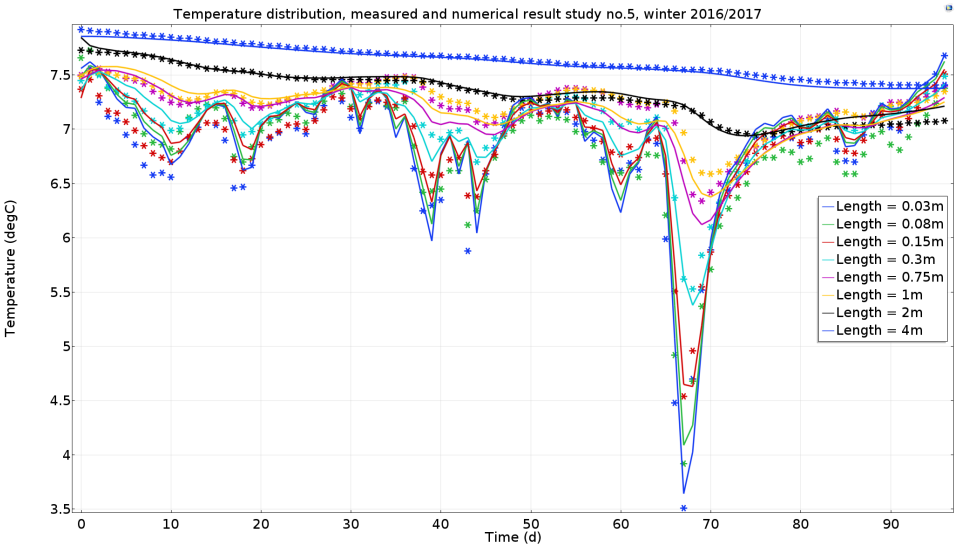

Figure 6.6: Numerical simulation based on the average values from study no.5, plotted as time (days) vs. temperature. Each solid line indicates the numerical simulation in one measuring point. The asterisks show the measured temperatures, the colors between the numerical and measured values corresponds.

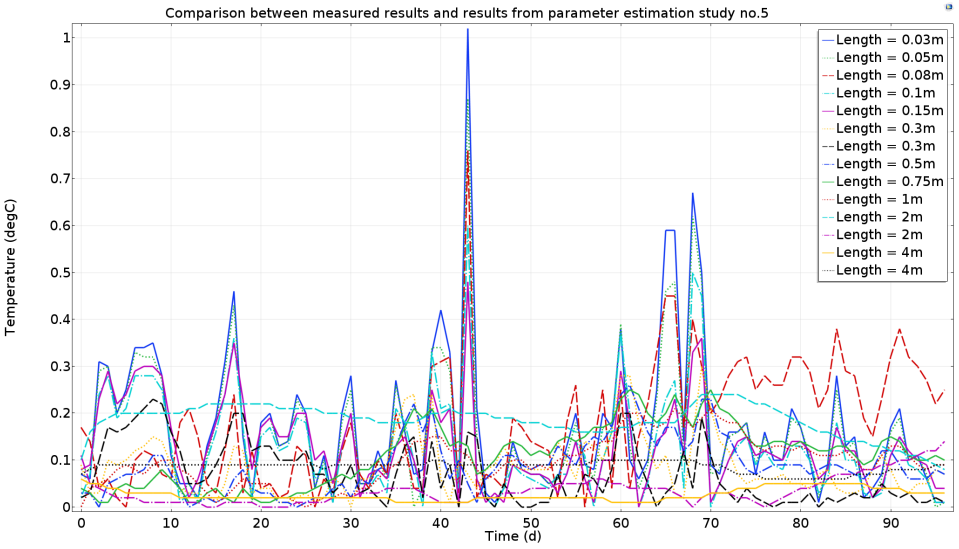

Figure 6.7: Showing the absolute difference between the measured temperature, and the numerical estimated values based on Parameter Estimation study no.5, in all measuring points. Simulated with external temperature presented as exact measured temperature, sampling every other hour.

Since the other numerical models use the smoothed temperature distribution, 4-day moving average, as the external temperature in the numerical model, when comparing the estimation parameters to the measured result, this is also done in this study, shown in Figure 6.8. This gave a more significant deviation in measuring point 0.03m, of 1.45°C.

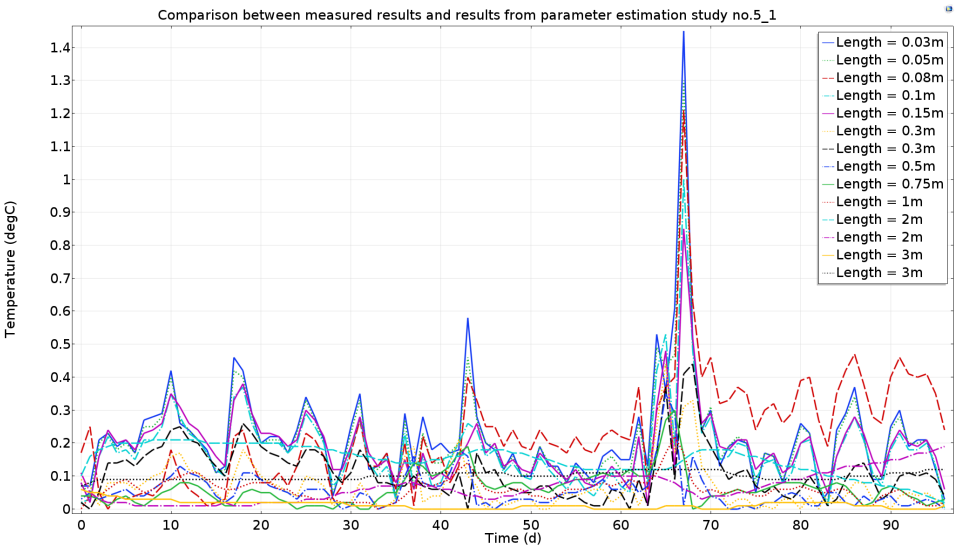

Figure 6.8: Showing the absolute difference between the measured temperature, and the numerical estimated values based on Parameter Estimation study no.5, in all measuring points. Simulated with external temperature presented as a four-day average.

6.3 Discussion

The benchmark analysis showed that one could obtain a near perfect curve fit, but there are several combinations of the parameters that provide these curves.

The model of the Gevingås Tunnel is a complex Parameter Estimation study, because the model consisting of two materials, a varying surface temperature, and an unknown heat transfer coefficient.

In all the Parameter Estimation studies, the parameters are held to be invariant. This is an inaccurate and a significant simplification of the problem. The heat transfer coefficient is not a constant value but varies with the temperature difference between the surface and air temperature. Constant heat transfer coefficient not plausible, but is the closest solution available, because the Parameter Estimation study does not allow for a varying parameter. From the studies, it seems that a

constant heat transfer coefficient is a good approximation. However, when evaluating the studies with an upper bound higher than 10 [W/(m^2 K)] the heat transfer coefficient lays between 13 and 17 [W/(m^2 K)], which is not a plausible value. Based on this, the heat transfer coefficient is the biggest source of uncertainty in the Parameter Estimation study.

The only parameters that are close to constant are the concrete properties because the concrete is a nearly homogeneous material. However, the way the concrete is applied, and other structural elements might impose differences in the material parameters.

The rock mass, is far from being a homogeneous material, as shown by the large span in measurements in Table 2.9. These measurements are taken on a relatively small sample, compared to the span of rock mass the Parameter Estimation is applied to, which means that one would expect the same or even more significant variations in the thermophysical properties of the rock mass in the measuring area.

The average value obtained from the Parameter Estimation studies does not provide the exact value of the rock mass or concrete, because the parameters are most likely not equal in all the measuring points, this is supported by the standard deviation seen in the estimated parameters. Regardless, the average value provides a reasonable estimation of the parameters at the north measuring station in the Gevingås Tunnel.

There is also uncertainty connected to the temperature measurements from tunnel, as discussed in earlier chapters. The possible flaws in the measurements are connected to the measuring location and accuracy in the measured value. If the measurement is not taken where one would expect, the Parameter Estimation in this point is based on the wrong reference data and provides inaccurate estimated values.

The main goal of the Parameter Estimation study was to approximate a model that presented the measurements better, and this was obtained. However, the Parameter Estimation did not provide one unambiguous set of parameters that accurately models the measured behavior. The hope was that the Parameter Estimation study would provide information about one sensitive parameter that would provide a better match because this information could then have been used in other models later.

Table 6.11 shows the standard deviation for all the parameters from all the six studies performed. A sensitive parameter would be one with a low standard deviation, meaning that any small change to this parameter would have a relatively larger effect on the temperature distribution. However, as Table 6.11 shows, the parameters have standard deviations which vary greatly, meaning that none of parameters have a large sensitivity.

Nonetheless, the Parameter Estimation study provided information on the model's sensitivity to input data and illustrated the importance of having control over the

boundary condition.

Table 6.11: Standard deviation or sensitivity for each parameter in all six studies. _r, is subscript for rock, and _c for concrete.

	Standard deviation [%]						
Study	htc	k_r	rho_r	Cp_r	k_c	rho_c	Cp_c
no.1	0	14	2	32	6	5	15
no.2	14	13	2	25	10	4	14
no.3	0	38	11	21	2	16	22
no.4	12	45	14	35	9	17	32
no.5	20	14	1	30	8	4	13
no.6	21	17	0	7	1	0	0
Range	0-21	13-45	0-14	7-35	1-10	0-17	0-32

Studies no.5 and 6 shows that using the external temperature with measures every other hour provides a match between the numerical and measured result to an accuracy of one degree Celsius. The study also showed that with the same parameter, the deviation could increase with half a degree Celsius by changing the way the external temperature is presented. Meaning that only a small part of the deviation between the measured result and the numerical simulation is related to the values of the parameters.

Using the hourly measured external temperature provided a much better curve fit in the first 30 centimeters of the lining, compared to the previous studies. However, in the rock mass, there is little difference between the studies, the deviation between the measured results and the numerical simulations is under 0.39°C in all the six studies. This means that in what way you choose to present the external temperature in a numerical model of this kind, either as an hourly measure or a four-day moving average, has close to no effect on the temperature distribution in the rock mass. The reason for this being that the rock mass is more affected by the low-frequency temperature variations, which are represented in a good way through the four-day average because the moving average only removes the noise represented by the high-frequency temperature variations.

Even though the Parameter Estimation study did not provide this one unambiguous sensitive parameter, the six Parameter Estimations studies provide a better fit to the measured temperatures in the Gevingås Tunnel, compared to the one-dimensional model presented in Chapter 5. Of the six studies, study no.3 gives the best fit to the measured results, when using the four-day moving average of the external temperature. Not only because the study provides the smallest difference between measured and numerical results, but also because the study has the lowest mean and STD when evaluating the difference between the numerical and measured results when considering all the measuring locations. Therefore, the average values obtained from this study are used in later evaluations of the Gevingås Tunnel.

Chapter 7

Scenario analysis

Through this thesis large amount of data has been handled. In the following section two ways of handling data noise is evaluated, along with which effect these methods have on a numerical simulation. Based on this knowledge data from the Værnes metrological station is collected and presented, for then to be used in a worst-case scenarios simulation of the temperature exposure of the Gevingås Tunnel.

7.1 Data presentation

Throughout this thesis, a four-day moving average has been used in the presentation of data. The four-day average of the tunnel temperature is said to be the temperature, that has the largest effect on the adjacent rock mass, based on earlier experience by Bane NOR. However, there is little knowledge about the difference between a four-day average, and a six-day average. A numerical simulation in COMSOL is performed, to increase the knowledge about these different ways of presenting data. The data used is collected from the Gevingås Tunnel, ten centimeters from the tunnel surface.

Up to this point in the thesis, the four-day average is found based on the daily average. In this section, another method for obtaining the four-day average is evaluated. This method calculates the average over four days based on a measured temperature every other hour. That means finding an average of 48 temperature measurements. The preceding average then has an overlap of 47 temperature measurements with the previous average. For the six-day average, the average temperature is based on 72 measurements. The difference between the four- and six-day average is shown in Figure 7.1 and 7.2, where Figure 7.1 is based on the daily average and Figure 7.2 on the hourly measurements.

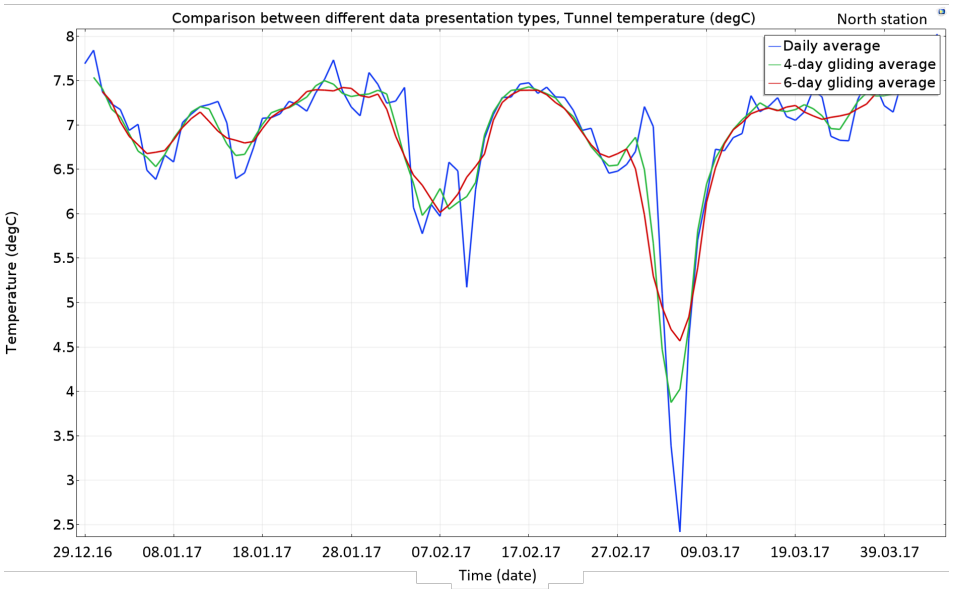

Figure 7.1: External temperature measured ten centimetres from the surface, presented as a daily, four- and six-day average, based on daily variations. Data collected from the North station, in the winter of 2016/2017.

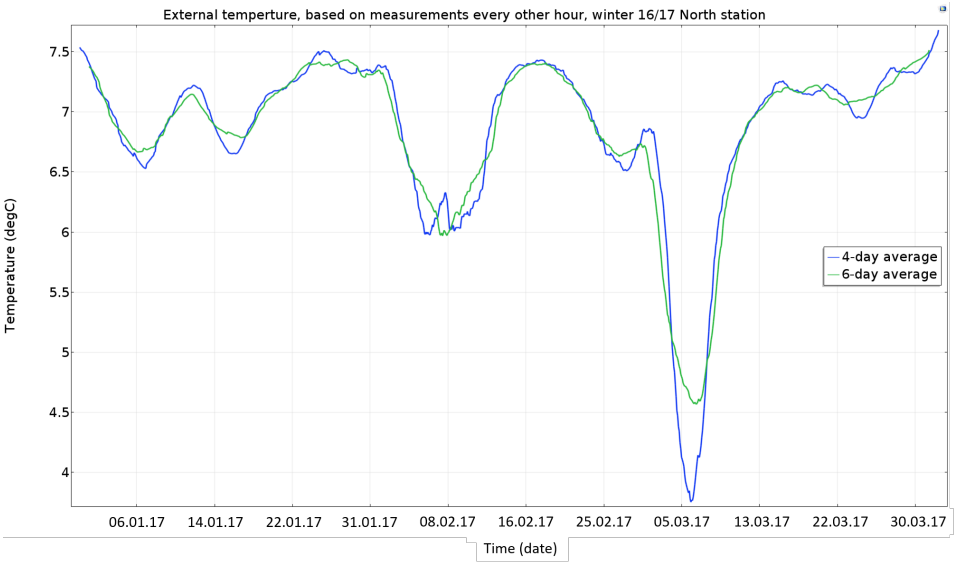

Figure 7.2: External temperature measured ten centimetres from the surface, presented as a four- and six-day average, based on measurements every other hour. Data collected from the North station, in the winter of 2016/2017.

Remarks

As one would expect, the four- and six-day average based on the daily average shows fewer small temperature variations. As seen, through the thesis, short-lived variations have less impact on the adjacent rock mass and larger effect on the concrete. However, the variations that show up in the average over the hourly variations are so small, that they will most likely not provide any difference in the temperature profile than the average based on daily variations.

Comparing a simulation using the four-day average based on the daily and hourly variations produce nearly the same temperature profile through both the concrete and rock mass. The largest difference between the two is 0.6°C, seen on the tunnel surface. In the outermost part of the concrete 0.03m from the surface, the average temperature based on the hourly variations gives a slightly lower temperature.

Therefore, which method one uses to calculate the moving average, is of little importance and depending on how the data is presented in the raw form. The four- and six-day average based on a daily average is detailed enough when the concern of the analysis is the rock mass. However, to show the effects in the concrete, the exact hourly measurements would most likely produce the best results, because these measurements include the temperature variations with high-frequency.

7.1.1 Numerical simulation

The next question is, then, does the four- and six-day average have a different impact on the numerical simulation? Figure 7.1 shows the tunnel temperature distribution through a season, as a one-, four- and six-day average. The four- and the six-day average is used in the numerical simulation. The numerical model is a one-dimensional model, similar to that used for the numerical presentation of the Gevingås Tunnel in Chapter 5.

Figure 7.3 and 7.4 shows the absolute difference between two numerical simulations, where one uses the four-day average as the external temperature and one the six-day average, for the winter of 16/17 and 17/18.

The numerical model shows that the difference between the four- and six-day average external temperature is minimal. The model is run both for the winter season of 2016/2017 and 2017/2018, and none of the models show a difference higher than 0.28°C. The small deviation is primarily present in the first six meters of the model. After this point, the two external temperatures show the same temperature distribution. The small deviation seen in the first six meters, shows that the four-day average gives lower temperatures, compared to the six-day average. Figure 7.1 shows that the six-day average has a subdued temperature variation, compared to the four-day average. This might explain the detected lower temperature in the simulation based on the four-day average.

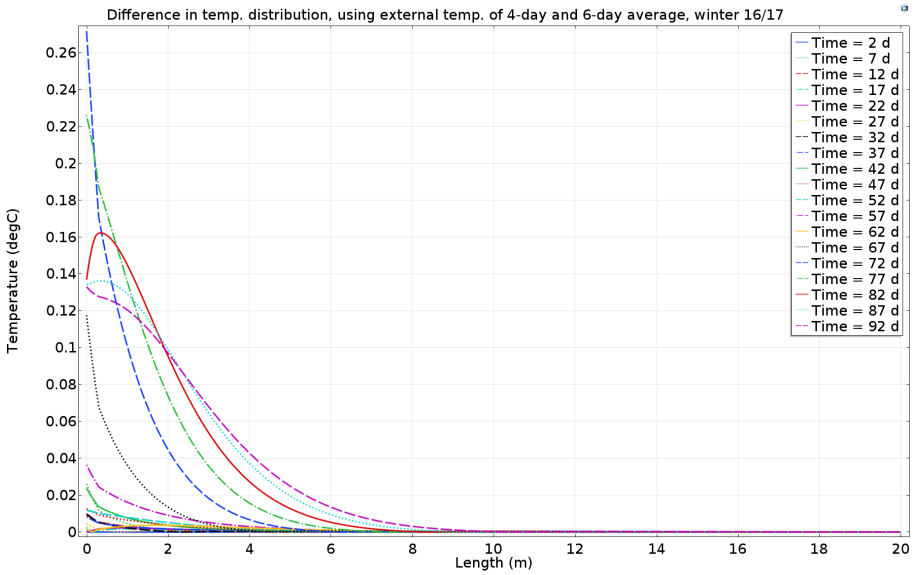

Figure 7.3: The absolute difference between a numerical simulation with external temperature presented as four-day and six-day average. Data from the Gevingås Tunnel measured 10cm from the tunnel surface, winter of 2016/2017.

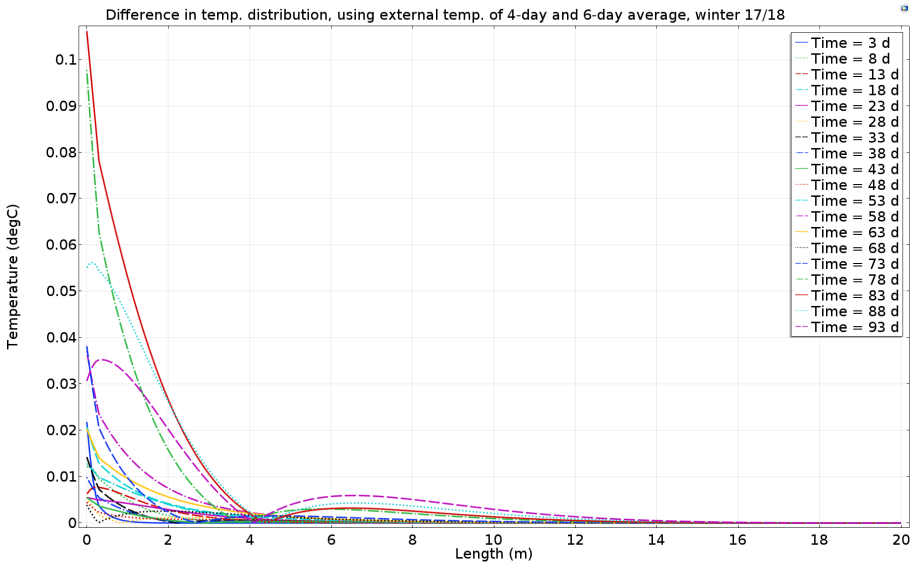

Figure 7.4: The absolute difference between a numerical simulation with external temperature presented as four-day and six-day average. Data from the Gevingås Tunnel measured 10cm from the tunnel surface, winter of 2017/2018.

Remarks

When interested in the bigger temperature variation, the method of which the average temperature is obtained is of little importance. The difference between the four- and the six-day average is small, and therefore, which average one chooses to use is not decisive. However, if presented with the choice, the four-day average would be preferable, because it represents the lower temperatures in the first six meters from the tunnel contour the best.

7.2 Historical data Værnes

There are three winter seasons with available measuring data from the Gevingås Tunnel, none of these can be said to be exceptionally cold over a more extended period. Nevertheless, two winters in Trondheim has stood out as unusually cold for a more extended period of time, namely the winters of 2010/2011 and 2011/2012. No data from the inside of the Gevingås Tunnel is available from this period, partly because the tunnel was opened for traffic November in 2011. Therefore, the nearest available data from this period is the weather station at Værnes airport, approximately 5.2km from the portal at Hell. There are few differences in elevation between the two locations, nor any significant change in terrain that would indicate temperature differences between Hell and Værnes. The data is collected from free access weather- and climate database, called eKlima, operated by the Norwegian Meteorological Institute.

The data from Værnes are presented as a daily average, available is also the minimum and maximum daily average, but to these, there are associated with some uncertainty. Therefore, the daily average is used to simulate in the Gevingås Tunnel. A four day-moving average is used to filter out some noise from the data set, and at the same time keeping the main variations distinct enough for the later simulation.

Figure 7.5 shows the four-day moving average for the winter of 2010/2011. Here the longest consecutive period, which shows temperature below zero, is 72 days. The coldest daily average measured is -18.1°C and the highest 11.7°C. Figure 7.6 shows the temperature as a four-day moving average for the winter of 2011/2012. The longest consecutive period is here much shorter than the previous season, with only 9 days. The coldest daily average measured is -11.6°C and the highest 11.3°C.

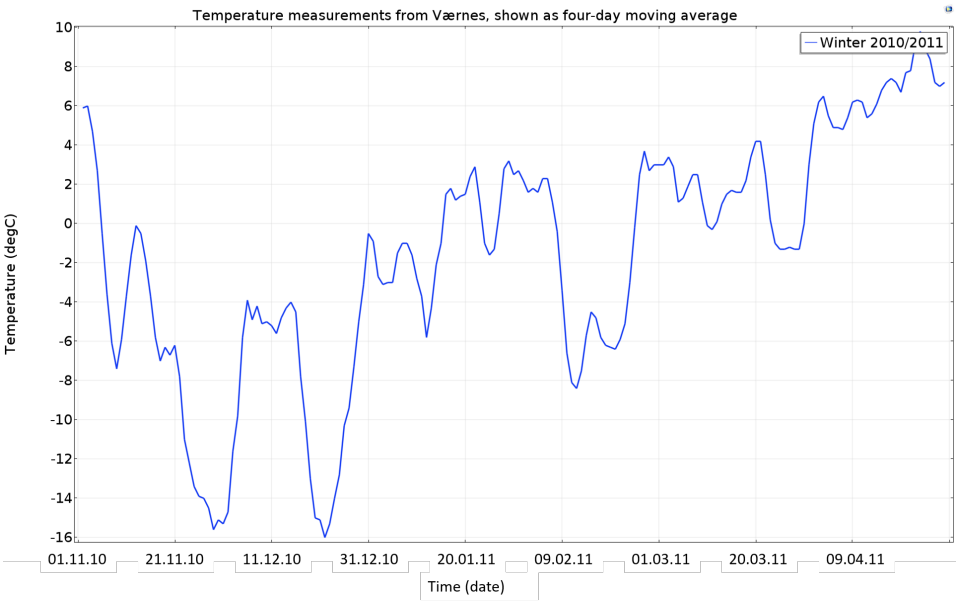

Figure 7.5: Air temperature measurements at Værnes, winter of 2010/2011, presented as a four-day moving average.

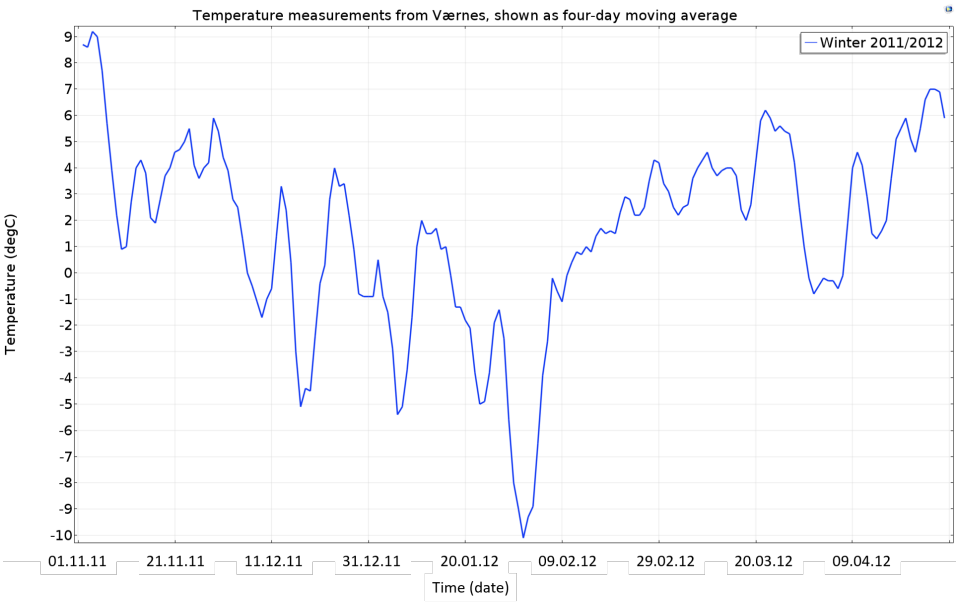

Figure 7.6: Air temperature measurements at Værnes, winter of 2011/2012, presented as a four-day moving average.

7.3 Worst case simulation of Gevingås Tunnel

Using the data from Værnes as the tunnel temperature is flawed. The reason being that, even though the temperature at the portal at Hell might be approximately equal to that of Værnes, the tunnel temperature is not equivalent, as discussed previously in this thesis. In spite of this, using the Værenes temperature could give an image of what to expect in a worst-case scenario, in the first meter of the tunnel near the portal at Hell.

Figure 3.14, shows how the tunnel temperature distributes through the tunnel. At Hell station, the temperature increases fast as one progresses inwards in the tunnel. Therefore the succeeding numerical analysis is only valid for the absolute first part of the tunnel.

The numerical simulation is presented as a worst-case not only because it uses outside temperature as tunnel temperature, but also because the model does not consider freezing water.

The model used for the numerical simulation is the improved Gevingås model from Chapter 6. Table 7.1 shows the parameters and study set up.

Table 7.1: Overview of the study set-up, from case no.3 of the Parameter Estimation study, for the numerical simulation using the measured temperature at Værnes as external temperature.

Study set-up	Parameter	
Rock	k [W/(m K)]	2.86
	ρ [kg/m^3]	2460
	Cp [J/(kg K)]	615
Concrete	k [W/(m K)]	1.19
	ρ [kg/m^3]	2396
	Cp [J/(kg K)]	899
	h [W/(m^2 K)]	10
External temperature 1	Winter 2010/2011	Figure 7.5
External temperature 2	Winter 2011/2012	Figure 7.6

7.3.1 Winter of 2010/2011

Figure 7.7 and 7.8 shows the temperature distribution in the concrete and rock mass, with the external temperature equal to the measured temperature in the winter of 2010/2011. This winter is the coldest of the two evaluated winters, Figure 7.7 indicates that there are temperatures below zero until approximately 2.5m from the surface. The temperature distribution in the first meter of concrete and rock mass follows the trend of the external temperature closely. This trend is also seen in the measured result from the Gevingås Tunnel.

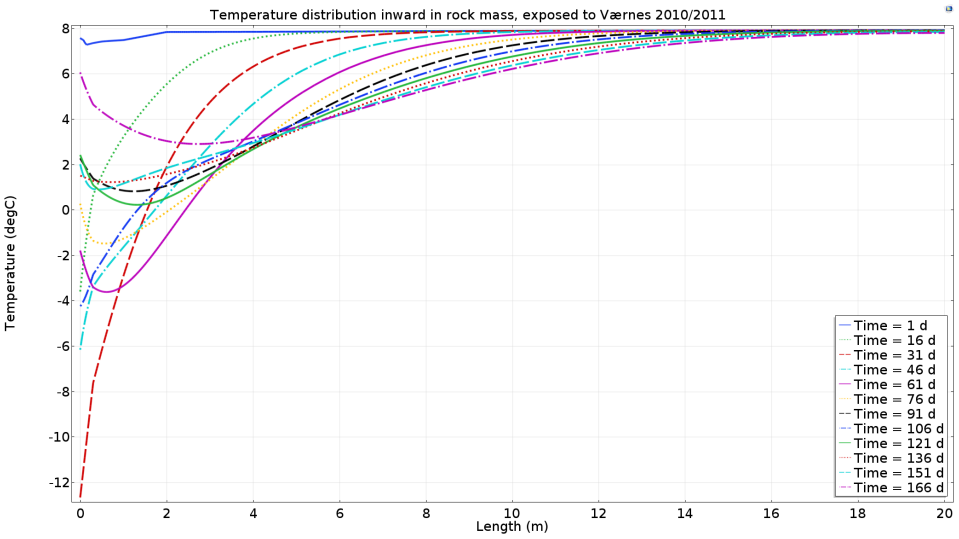

Figure 7.7: Temperature distribution through concrete and rock mass, at different dates though the winter season of 2010/2011.

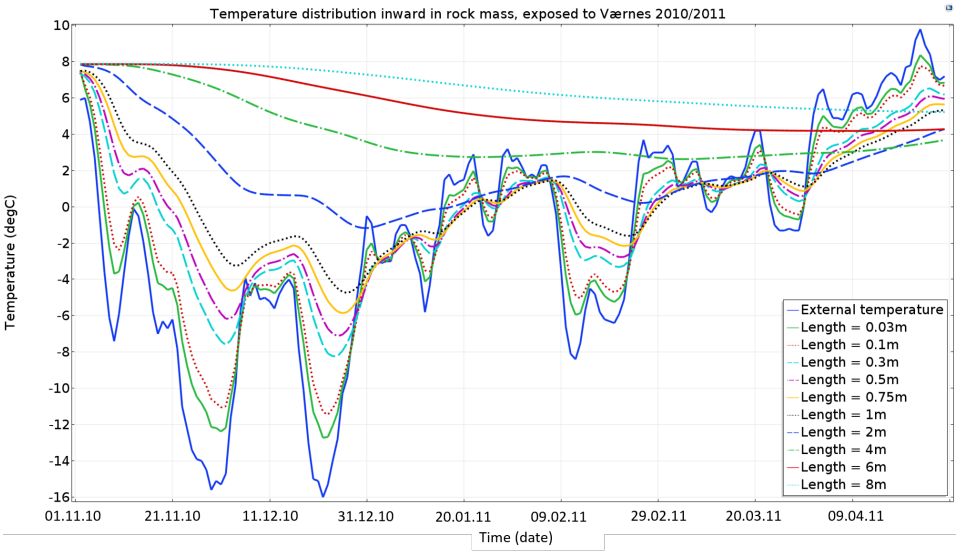

Figure 7.8: Temperature distribution through the winter season of 2010/2011, in different locations inwards in the concrete and rock mass. External temperature measured at Værnes.

7.3.2 Winter of 2011/2012

The temperature distribution in the concrete and rock through the winter season of 2011/2012, is shown in Figure 7.9 and 7.10. In this season temperatures below zero stretch no further than 1.5m from the exposed surface. The temperature from the surface to approximately one meter follows the external temperature variations, as seen in the previous season.

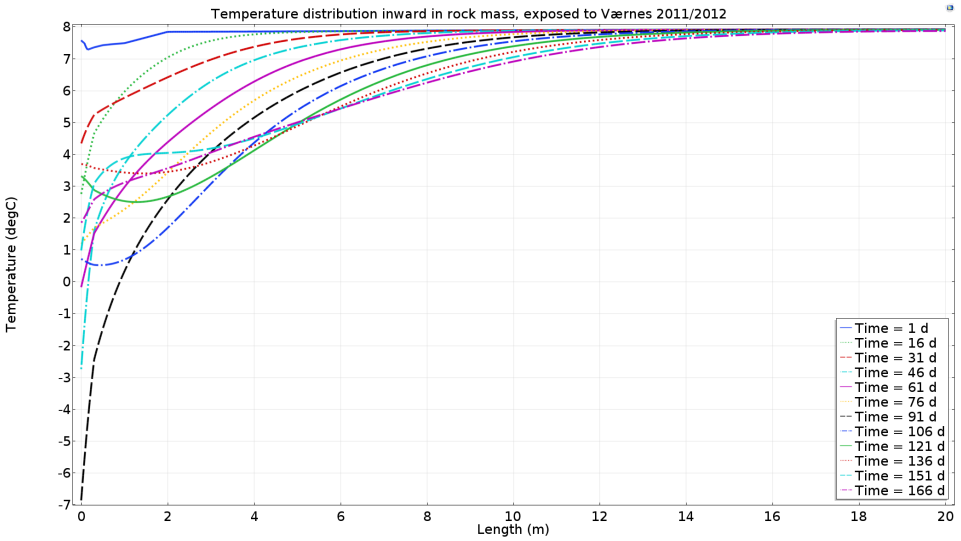

Figure 7.9: Temperature distribution through concrete and rock mass, at different dates though the winter season of 2011/2012.

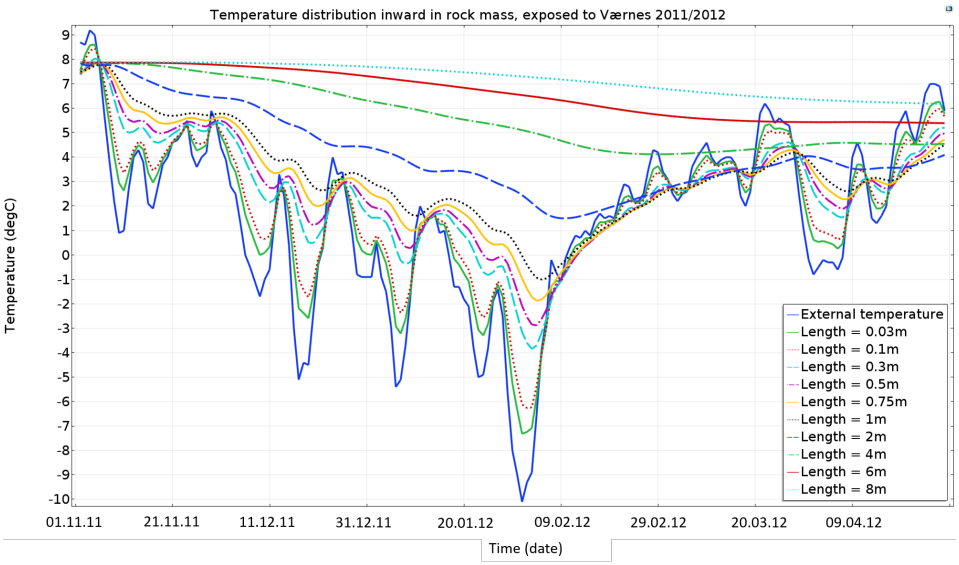

Figure 7.10: Temperature distribution through the winter season of 2011/2012, in different locations inwards in the concrete and rock mass. External temperature measured at Værnes.

7.3.3 Discussion

The in-situ validation of COMSOL showed that the numerically obtained results are close to what one can expect. One of the weaknesses of the numerical model was the prediction of the first 30cm, where the model did not handle the temperature variations as good as further into the rock mass when using the four-day moving average of the external temperature. In the model set up used for this analysis, study no.3, the model and measured result had a maximum deviation of 1.27°C. For the two numerical simulations performed using the Værnes data, one should expect a deviation of this magnitude, especially in the first 30cm.

One other aspect to consider in regards to the model is that it is improved to match one season, related to a specific external temperature, which is not equal to that used in these simulations. This might present a problem for the heat transfer coefficient. Using a constant heat transfer coefficient, fitted to other data, is as discussed earlier, not optimal and presents therefor a predominant source of error.

In the introduction to this numerical analysis, two other weaknesses related to this simulation is presented. The first of which is that the outside air is not equal to the tunnel air, meaning that this analysis presents a very extreme exposure case. The outside temperature is as mentioned present in the portal area, in the absolute first part of the tunnel. However, if it was the first part of the Gevingås Tunnel

that where to be simulated the model should be built with a PE-foam structure instead of using a bounded lining. The PE-foam structure is insulating, which would mean that the temperature exposure on the rock mass would be less than what is simulated in these cases. On the other hand, the model can give an image of how the temperature distribution would be if the tunnel were entirely constructed with a bounded system.

The second source of error is related to water. Water in motion affects the heat transfer, in which way depends on where the water is transported. Still, water that freezes or melts demands much energy and acts as a heat-drainage. If water freezes in the first part of the tunnel structure either in the concrete or rock mass, the heat transfer from the rock mass dissipate in the freezing zone. Ice also has a conductivity different from water, and the ice changes therefore the heat transport mechanisms. Since the model does not consider water, the effects of water are not considered in the presented numerical results.

Compared to these latter weaknesses the error related to the numerical model set-up is small, not entirely insignificant, but the very low external temperature and lack of water in the model makes the numerical results highly conservative, also in the first 30cm of the structure.

Chapter 8

Synthesis and summarizing discussion

This chapter sums up, discusses, and highlights the individual discussions that have been presented throughout the thesis.

8.1 Measurement of thermophysical properties

The tests performed, which gave the thermophysical properties, and the mineral composition of the Metasandstone shows how the mineral composition and lineament affects the thermophysical properties.

Since there is little to no difference in the mineral composition between the two test specimens, the reason for the difference in the thermophysical properties between the two is most likely connected to the foliation.

The test of the thermophysical properties shows that the conductivity is the highest parallel to the foliation. Mica is the second most abundant mineral in the test specimens, foliations are often composed of mica, and with the low conductivity mica has, this is most likely the case here as well. The low conductivity acts as a sort of a resistance zone, reducing the conductivity perpendicular to the structure.

High quartz content gives high thermal conductivity, and is the reason why the effective conductivity in this rock is relatively high for a Sandstone.

There is uncertainty connected to the considerable variation in the measured specific heat capacity. The mineral composition cannot explain the difference, and no other apparent reasons for the deviation is found. The density varies to little degree.

8.2 Field measurements

The temperature measurements from the Ulvin and Gevingås Tunnels show that the temperature in the concrete and rock mass remains above zero in all the three-seasons presented. Note that these winters are not very cold for a substantial amount of time. The longest consecutive period with outside temperatures below zero is 32 days, measured at Ulvin in the winter of 2017/2018. In the measuring station at Ulvin 1100m from the portal, the temperature ten centimeters into the concrete did not show any negative temperatures.

The measurements show that there is a quick increase/decrease in temperature in the first centimeters of the concrete. After the quick temperature change, the temperature has a slow and steady trend towards a rock mass temperature, around eight degrees Celsius.

Also noticeable from the measurements, is that the variations in rock mass temperature, as one progresses away from the exposed surface decreases, and that there is a phase shift in the temperature profile, meaning that the temperature change is delayed in time.

The quick temperature variations on the surface influence only the first parts of the concrete and rock mass, because the variations knock each other out. The seasonal variations, on the other hand, have a lower frequency, and influences the rock mass temperature deeper than seven meters.

There is some uncertainty connected to the measurements at Ulvin, especially toward the sensors operated by SINTEF. The sensors where installed before the concrete arch was constructed, and therefore, the largest concern in regards to these sensors is the positioning, and whether or not they were moved under construction. This concern is the reason why the inner and outer rod measurements are plotted separately, in some of the figures presented. In connection with the data handled by Cactus Geo, there is little information about the instrumentation process and related uncertainty. Sensors showing incorrect results are controlled and handled by the company.

The uncertainty connected to the measurements in the Gevingås Tunnel, is related to both the sensor location and the measured value. Therefore some sensors have been removed and considered unreliable. The source of the errors is not one-sided and depends on several aspects. One of these aspects is the placement of sensors. If the sensors are located at the wrong location, the measurements might seem strange even if it is not. The measured values might be affected by the installation of the sensors. Sensors installed so that water passes by or/and in the vicinity of large air gaps, might provide temperatures influenced by these occurrences, and by this providing incorrect results. Errors in the electrical coupling, or the sensors itself, may also affect the measured values. These latter aspects are also valid points for the measurements in the Ulvin Tunnel.

8.3 Validation of COMOSL

The laboratory validation of COMSOL highlights both the uncertainty of parameters and the strengths and weaknesses of a COMSOL simulation.

The uncertainty connected to a material parameter is dependent on the number of test specimens, the material composition, and the testing method. The Tonalite used in the laboratory is one of the most homogeneous bedrocks, which is confirmed in the sensitivity analysis. The concrete, on the other hand, had a more significant standard deviation. In general, concrete is seen as a reasonably homogeneous material but in this case, less homogeneous than the Tonalite. When measuring the thermophysical properties of concrete larger aggregates might influence the result. This means that in a small test specimen, or few tests, the material might seem quite inhomogeneous, compared to a larger test specimen, or many tests.

A simulation is only as good as the model and the input data. In the laboratory validation, one saw the effects of having a model built based on some assumptions, that turned out to be wrong. The error is most likely connected to leaking insulation, which made the numerical model not fit the real situation after some time. However, it might also be variations in the material properties, inaccuracy in the sensors and sensors locations, which made the comparison between the numerical result and measured result inaccurate.

The constant heat transfer coefficient might also contribute to the deviation. The heat transfer coefficient is dependent on the difference between the surface and air temperature, and as the concrete and rock mass in the laboratory is cooled down, the temperature difference between the surface and air decreases, resulting in a decreasing heat transfer coefficient.

Simultaneously the laboratory validation showed how good a numerical simulation could match a controlled environment, down to an error of only 0.35°C. These results from the validation are satisfactory, and COMSOL is thereby validated.

8.4 Numerical model of the Gevingås Tunnel and in-situ validation

The numerical simulation of the Gevingås Tunnel consisted initially of a two-dimensional and a one-dimensional model. The two-dimensional model showed, as the measurements from Ulvin, that the temperature in the roof is higher, and steadier compared to the temperature distribution in the vicinity of the wall.

The first one-dimensional model shows that COMSOL can give a good approximation of the temperature distribution, even in a more complex model. The average deviation between the numerical and measured results is 0.5 °C.

The benchmark Parameter Estimation study showed that COMSOL can obtain a near perfect curve fit, but that several combinations of parameters can obtain the desired fit.

The reason for the deviation between the measured and numerical model is complex, and connected to both the measurements and the numerical simulation. The reliability of the measurements is hard to change, but the numerical simulation can be improved by tweaking the parameters. The Parameter Estimation showed that the numerical simulation could be improved to obtain a better match between the measured result and the numerical results, reducing the deviation in the concrete with more than one degree Celsius. However, a perfect match between the numerical and simulated result was not obtained, which indicated that the deviation has several sources.

One of these other sources of deviation comes to light in the Parameter Estimation study, using the external temperature as exact measurements, a temperature every other hour. The study showed that with the same parameters obtained from a Parameter Estimation study, using the exact measured temperature in the simulation, provided a much better curve fit for the first 30cm compared to using the four-day average. This supports the assumption made in Chapter 5, that the deviation in the first 30cm is connected to the use of the four-day average. However, the study also showed that the rock mass temperature distribution is not affected by smoothening of the external temperature distribution. Meaning that for the rock mass temperature, there is little difference between using the four-day average and the exact measured result in the numerical simulation.

The one weakness of the numerical model is the invariant parameters, which might also be the source of the error and the reason why a perfect curve match is not obtained. A constant heat transfer coefficient in a numerical model is not plausible, and neither is constant thermophysical properties of a Metasandstone through a rock slab of four meters.

The Parameter Estimation study did not provide an unambiguous sensitive parameter. As discussed, the Gevingås model was improved, but the improvement cannot be quantified and used in other models. This corresponds to the sensitivity analysis performed for the Laboratory Validation, which showed that changing the input parameters could only to a small degree influence the temperature distribution. Since there is not one specific sensitive parameter, it is of even greater importance to have control over the boundary conditions. One example illustrating the importance of boundary condition is shown in study no.5 and 6. They showed the importance of knowing what the goal of the numerical simulation is when choosing the temperature boundary condition, i.e., the external temperature.

As an approximation, the numerical model with constant values, using external temperature presented as a four-day average, provides a simple tool to predict the temperature distribution, in the adjacent rock mass to a tunnel surface exposed to external temperature, with an accuracy of 1.27°C.

8.5 Data presentation

The impact on a simulation, using either the four- or six-day average to present the external temperature in a heat transfer problem, is minor. However, at the same time, the six-day average flattens out the peaks of the curves, resulting in a reduced reaction in the numerical model. This might present a problem because COMSOL has in previous parts shown a weakness in simulating temperature peaks, reducing the peak in the input data might enhance this weakness.

8.6 Case study Værnes

Both simulations of the Gevingås Tunnel, using the Værnes measurements, show that the temperature up to one meter from the surface, follows the variations of the external temperature. This is also seen in the measured results from the Gevingås tunnel, which means that the numerical simulation shows the same trends as reality. Other trends that are noticeable in both the simulated results and in the measurements, are the decrease in both temperature variations and reaction time as one progresses away from the exposed surface. The correlation with the measured results, gives the numerical result reliability.

The two measuring stations, in the Gevingås tunnel, that log the rock mass and concrete temperature, are positioned 1100m from the portals. In these two locations, the external temperature does not drop below zero degrees for a more extended period, in any of the three-winter seasons.

The external temperature measured at the portal at Hell in 2017/2018, has an extended period, 21 days, of temperatures below zero, and the same trend with several consecutive periods with temperatures below zero as the 2011/2012 Værnes data. The tunnel temperature in 2017/2018 200 meters into the tunnel, are still below zero in some parts, but the long consecutive period is reduced to only ten days. Further 800 meters into the tunnel, 1km from the portal, where the north measuring station is located, the temperature is several degrees above zero for the majority of the season. Only seven days out of 174 days are measured half a degree Celsius below zero. This shows that the numerical simulation case of 2011/2012, is very conservative for the middle part of the tunnel, but before the 200-meter mark, the results might give a plausible result.

However, keep in mind that the simulation is not simulated with a PE-foam, as is the case for the first kilometer of the tunnel. The PE-foam insulates, keeping the cold air away from the tunnel wall. The PE-foam also has the effect that cold air is transported further into the tunnel, because the insulation hinders heat transfer between rock and tunnel air.

There are no recorded temperatures in the concrete and rock mass, from the *cold* period seen in the winter of 2017/2018, and therefore no conclusion can be made on how the rock mass reacts to this *cold* period. However, as mentioned, one kilometer

from the portal the temperature barely drops below zero at the surface, so there is no reason why one would expect temperatures below zero in the rock mass.

A measuring station closer to a portal, would provide information about the rock mass and concrete reaction to tunnel air temperatures which are below zero for a more extensive period. In the data available, temperature loads of this kind is missing. These types of measurements could provide information to support an estimate of to which degree the results from the scenario analysis are conservative.

The cold period in 2010/2011 lasted for 72 days, where the temperature was below -14°C in two periods. The numerical simulation shows that the temperature drops below zero up to 2.5m from the tunnel surface. Given the above discussion, this could be the case in the first 200m of the tunnel, given an uninsulated tunnel.

Keep in mind that the numerical simulation is not only conservative in regards to the external temperature, but also because the effect of water is not taken into consideration.

Chapter 9

Conclusion

The following points highlights the main findings of the thesis:

- In the Metasandstone, which is a foliated rock, the thermal conductivity is the highest parallel to the structure.
- Mineral composition has a significant effect on the conductivity of the material.
- Quick temperature variations effect shallow, compared to temperature variations with low-frequency.
- The rock mass holds a steady state temperature around 8°C. And the rock mass is affected by the tunnel temperature further than seven meters, to approximately eight meters.
- The laboratory validation shows that a one-dimensional numerical simulation in COMSOL, can match a controlled environment down to an error of only 0.35°C. The results are satisfactory, and the model is thereby validated.
- A one-dimensional numerical model set-up with constant values, both for the thermophysical properties and the heat transfer coefficient, provides a simple tool to predict the temperature distribution, in the adjacent rock mass to a tunnel surface exposed to a known external temperature. The results from the numerical model of the Gevingås Tunnel are satisfactory, and COMSOL is also validated for in-situ cases.
- The boundary conditions have bigger impact on the numerical simulation result, than the thermophysical properties of the models materials.
- Uncertainty of measurements is connected to the sensors position, calibration, insufficient borehole filling, which can result in water- and/or air-filled vacancies in the vicinity of the sensor. The uncertainty in the measurements

influences the numerical simulation, both as the input data, but also as the reference data used to validate the model.

- When presenting data to be used in a numerical simulation, the moving four-day average is preferable over the six-day average. How one calculates the moving average, either over the daily or over the hourly measurements, is of little importance. However, keep in mind that this removes some of the high-frequency temperature variations, which might lead to errors in the first parts of the tunnel wall, namely the concrete. If the goal of the numerical model is to look at the first 30cm of the tunnel structure, then the external temperature should not be smoothed, and as much data as possible should be used.
- A tunnel wall, constructed with a bounded lining, exposed to temperatures below zero degrees Celsius for 72 days, can in the worst case have temperatures below zero degrees Celsius 2.5m into the rock mass.

Chapter 10

Further work

The continued work on this topic is extensive, and many questions remain unanswered. Some of the main points which should be considered are listed below.

- What effect does the tunnel air moisture have on the temperature exchange between the air and concrete? Will the moisture in the tunnel effect the concretes thermophysical properties?
- Which mechanisms govern the heat transfer coefficient? Does a passing train affect the air flow? Is the heat transfer truly turbulent, or is it governed by a passing train, still air until the air is set in motion by the train? Moreover, how can it best be implemented in a numerical model?
- The numerical model can be improved by implementing the heat transfer coefficient more realistically, and by including water.
- Which effect does water in the rock mass and concrete have on the heat transfer?
- How to predict the tunnel temperature based on external measurements? Before building a tunnel, one must have an estimate of the temperature load which the tunnel will be subjected to, to perform numerical analysis.
- When this thesis is written, spring of 2019, no measurements of the concrete and rock mass temperature have been made in a season where the tunnel temperature drops below zero degrees Celsius for a more extended period. Logging a season with tunnel temperatures below zero will make it possible to verify that the numerical model also works for those types of situations. Alternatively, a measuring station could be placed closer to the tunnel portal, within the first 200m of the tunnel, where the tunnel air temperatures to a larger degree drops below zero in a normal winter.

- The measurements presented in this thesis have as discussed, some uncertainty related to the results. How can this uncertainty be reduced; which measures need to be taken to get better control over the measurements?

Reference

Ausland, J. and Jonsson (2014), 'Ulvintunnelen - erfaringer fra beslutning til gjennomføring av membran og full utstpning'. (accessed: 2019-01-16).
URL: *http://www.nvfnorden.org/library/Files/Utskott-och-tema/Tunnlar/Seminarier-2012-2016/Effektivare-tunneldrivning-april-2014/3_Case_drift%20og%20vedlikeholdsfrie%20tunneler.pdf*

Bane NOR (2018*a*), 'Anbefalt konstruksjonsprinsipp for jernbanetunneler - prosjekteringsveileder'. (accessed: 13.02.19).
URL: *https://proing.opm.jbv.no/wiki/veiledere/konstruksjonsprinsipp*

Bane NOR (2018*b*), 'Tunneler dovrebanen'. (accessed: 2019-01-16).
URL: *http://orv.jbv.no/sjn/doku.php?id=tunneler:dovrebanen*

Bane NOR (2018*c*), 'Tunneler nordlandsbanen'. (accessed: 2019-01-16).
URL: *http://orv.jbv.no/sjn/doku.php?id=tunneler:nordlandsbanen*

Drevland, P., Buvik, H., Ausland, J., Georgsson, R. and Seljordslia, T. (2014), 'Erfaringer med støpt løsning, ulvin-tunnelen'. (accessed: 2019-01-16).
URL: *https://www.vegvesen.no/_attachment/704782/binary/989392?fast_title=Erfaringer+med+st%C3%B8pt+betonglining+ved+Fellesprosjektet.pdf*

Holter, K. G. (2015), Properties of waterproof sprayed concrete tunnel linings: a study of EVA-based sprayed membranes for waterproofing of rail and road tunnels in hard rock and cold climate, PhD thesis, NTNU, Trondheim.

Holter, K. G. (2016), 'Performance of eva-based membranes for scl in hard rock', *Rock Mechanics and Rock Engineering* **49**(4), 1329–1358.

Holter, K. G. and Geving, S. (2016), 'Moisture transport through sprayed concrete tunnel linings', *Rock Mechanics and Rock Engineering* **49**(1), 243–272.

Incropera, F. P., Dewitt, D. P., Bergman, T. L. and Lavine, A. S. (2017), *Incropera's principles of heat and mass transfer*, Wiley.

Johansen, Johnny M. and Holen, Åsmund (2012), Etatsprogrammet moderne vegunneler, 2008-2011 vegtunnelers oppetid, Technical report. Statens vegvesens rapport Nr. 143.

NGI (2015), *Using the Q-system. Rock mass classification and support design.*, NGI, Oslo.

NGU (2019), 'Berggrunn, nasjonal berggrunnsdatabase'. (accessed: 2019-01-16). **URL:** *http://geo.ngu.no/kart/berggrunn/*

Nilsen, B. (2016), *Ingenirgeologi-berg grunnkurskompendium*, NTNU, Institutt for geologi og bergteknikk, Trondheim.

Pedersen, K. B. (2002), Frostmengder i vegtunneler, Technical report, Statens vegvesen. Intern rapport nr. 2301.

Ramstad, R. K., Midttømme, K., Liebel, H. T., Frengstad, B. S. and Willemoes-Wissing, B. (2015), 'Thermal conductivity map of the oslo region based on thermal diffusivity measurements of rock core samples', *Bulletin of Engineering Geology and the Environment* **74**(4), 1275–1286.

Schlemminger, C. and Ness, E. (2013), Tunnel, isotropic thermal conductivity and specific heat capacity of various rock and concrete samples determined with the transient plane source technique, Technical report, Energilab, Trondheim.

Statens vegvesen (2016), *Vegtunneler, Håndbok V520*, Statens vegvesen, Vergdirektoratet, Oslo.

Tinderholt, S. M. (2018), 'Heat transfer - from rock mass to cold tunnel room'. Project thesis, NTNU.

Vassenden, S. (2010), Frostlaboratoriet - testing av varme/kuldeutveksling mellom tunnel og omkringliggende bergmasse, Master's thesis, NTNU.

Appendix A

Appendix

A.1 XRD

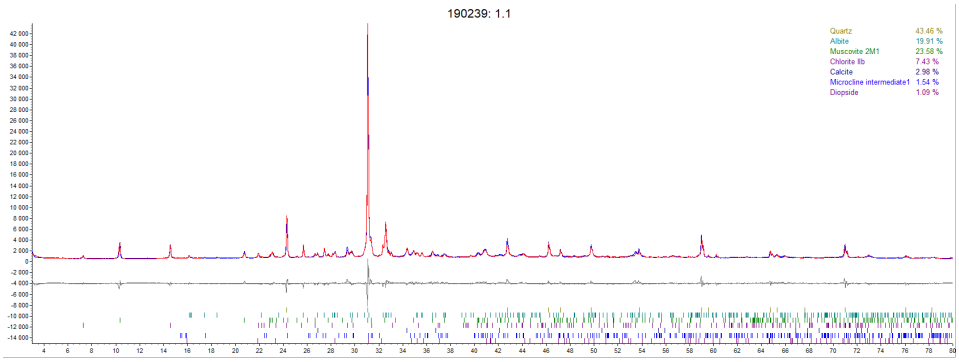

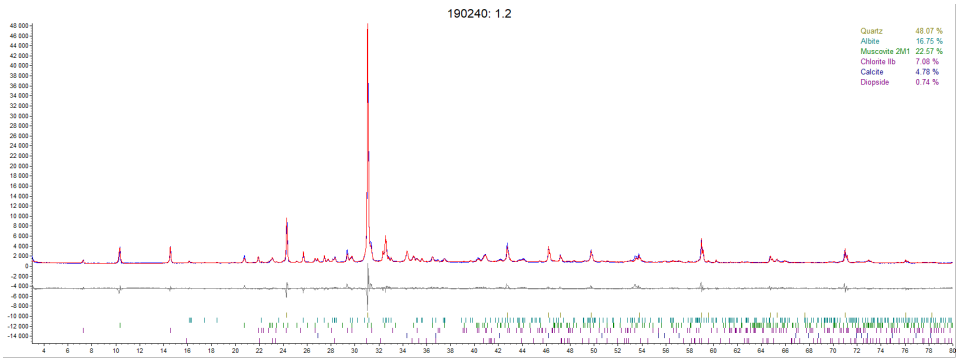

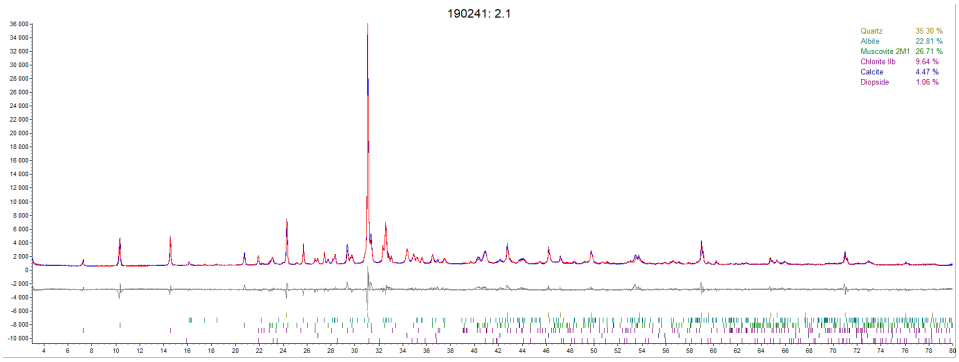
190241: 2.1
Quartz 35.30 %
Albite 22.81 %
Muscovite 2M1 26.71 %
Chlorite IIb 9.64 %
Calcite 4.47 %
Diopside 1.06 %

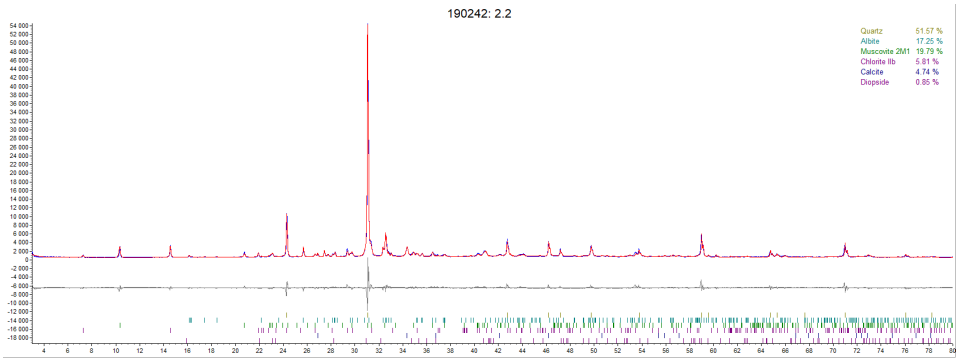
190242: 2.2
Quartz 51.57 %
Albite 17.25 %
Muscovite 2M1 19.79 %
Chlorite IIb 5.81 %
Calcite 4.74 %
Diopside 0.85 %

A.2 Plot Ulvin

A.2.1 Concrete measurements

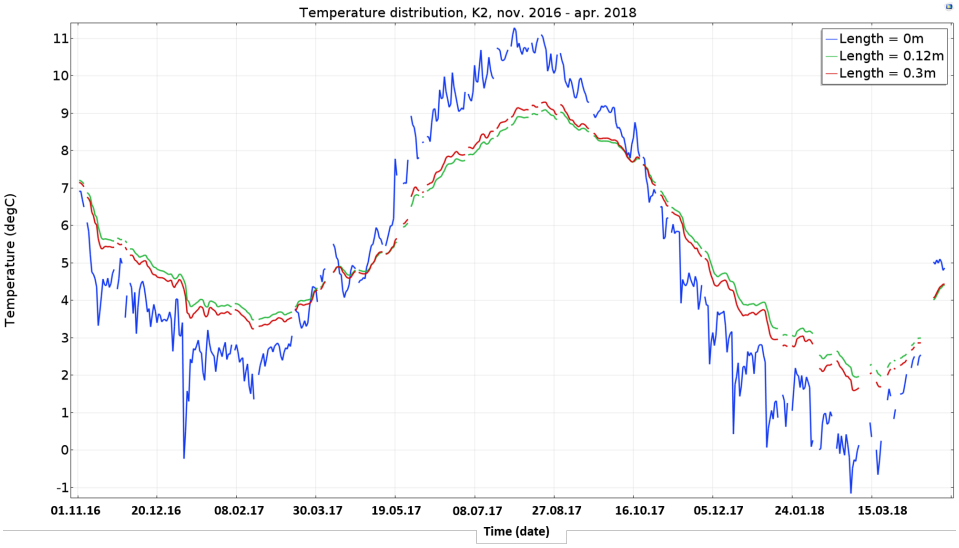

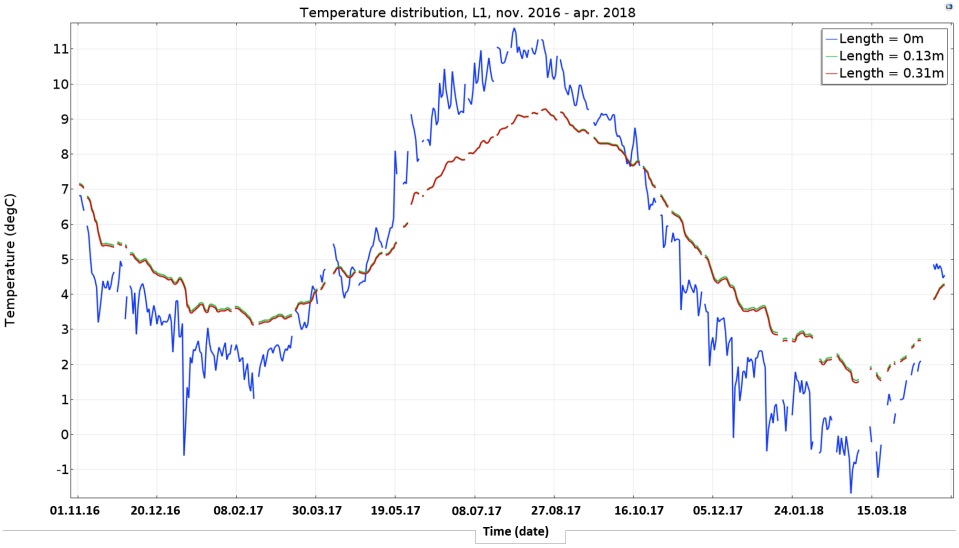

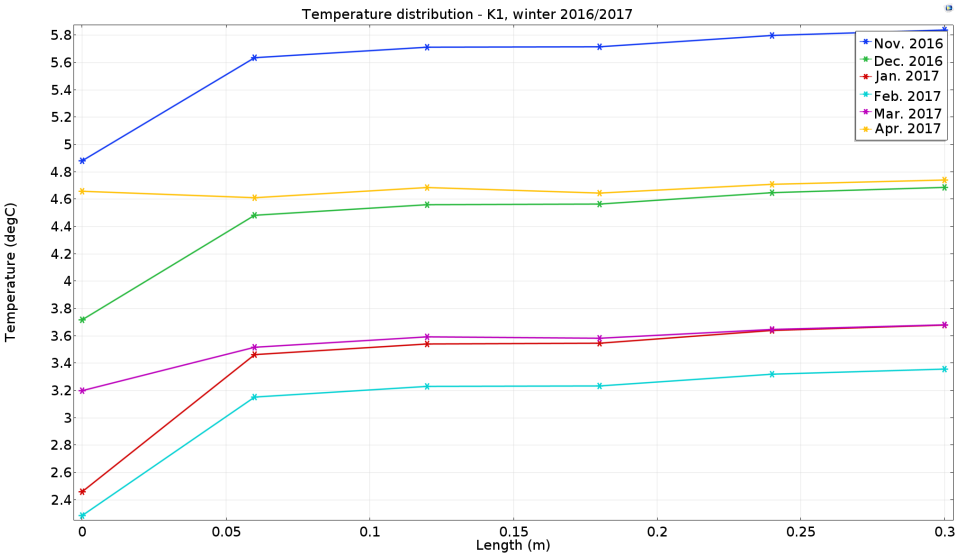
Temperature distribution - K1, winter 2016/2017
Temperature (degC)
Length (m)
Nov. 2016
Dec. 2016
Jan. 2017
Feb. 2017
Mar. 2017
Apr. 2017

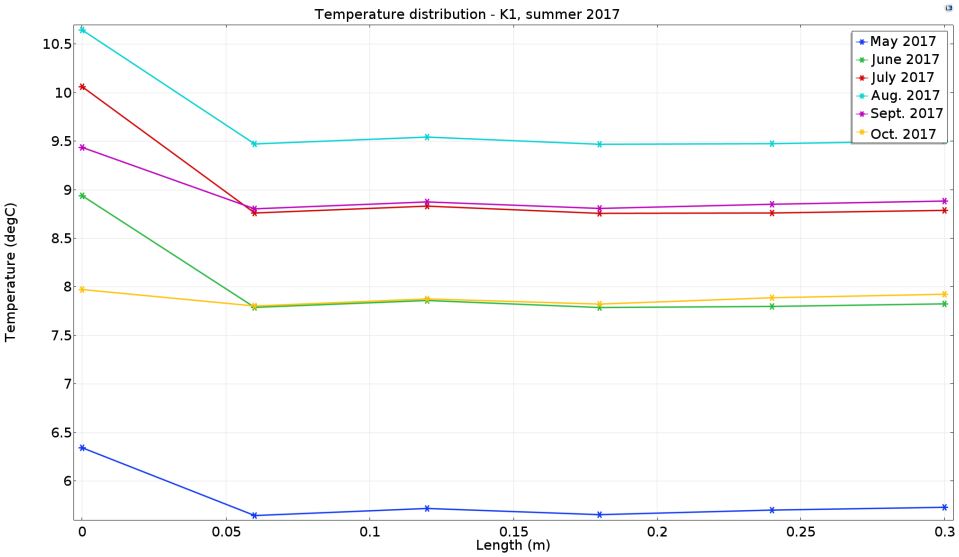
Temperature distribution - K1, summer 2017
Temperature (degC)
Length (m)
May 2017
June 2017
July 2017
Aug. 2017
Sept. 2017
Oct. 2017

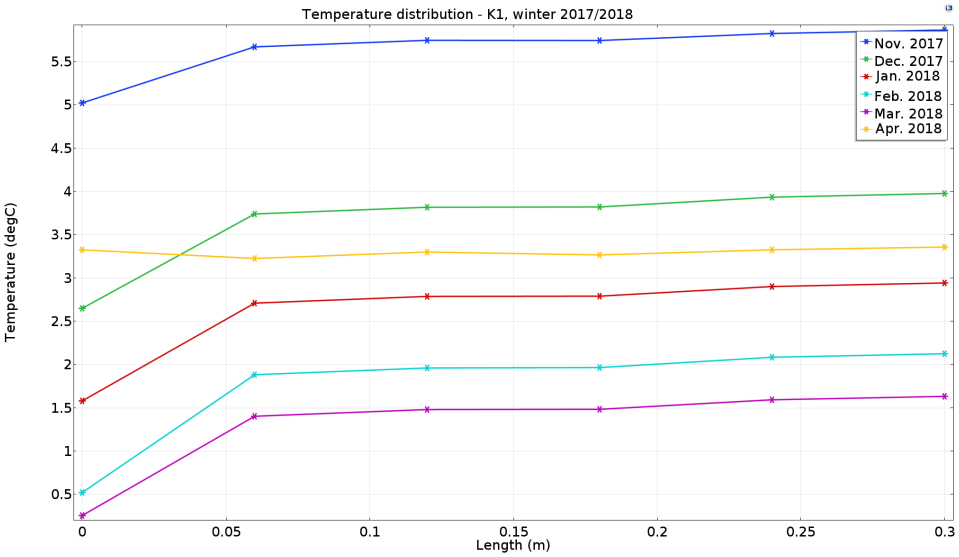
Temperature distribution - K1, winter 2017/2018
Temperature (degC)
Length (m)
Nov. 2017
Dec. 2017
Jan. 2018
Feb. 2018
Mar. 2018
Apr. 2018

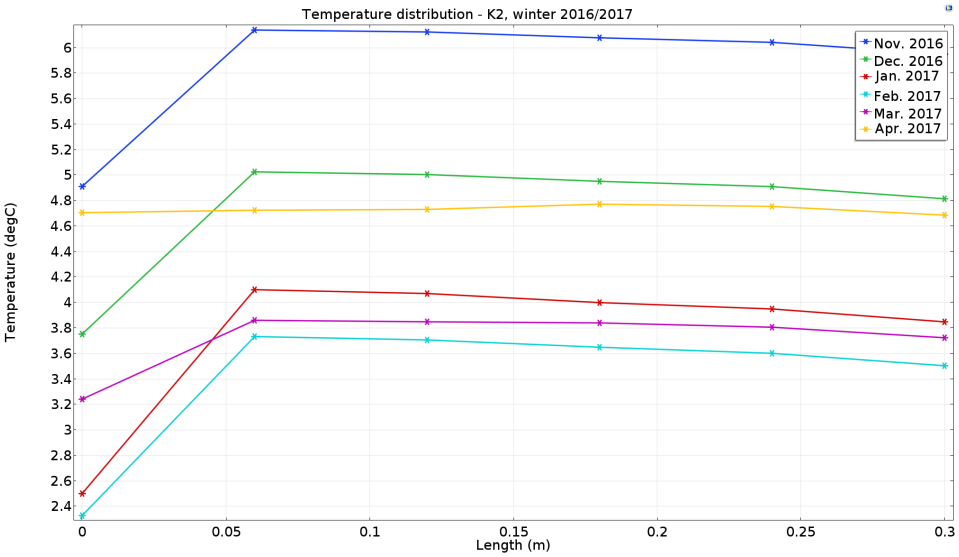
Temperature distribution - K2, winter 2016/2017
Temperature (degC)
Length (m)
Nov. 2016
Dec. 2016
Jan. 2017
Feb. 2017
Mar. 2017
Apr. 2017

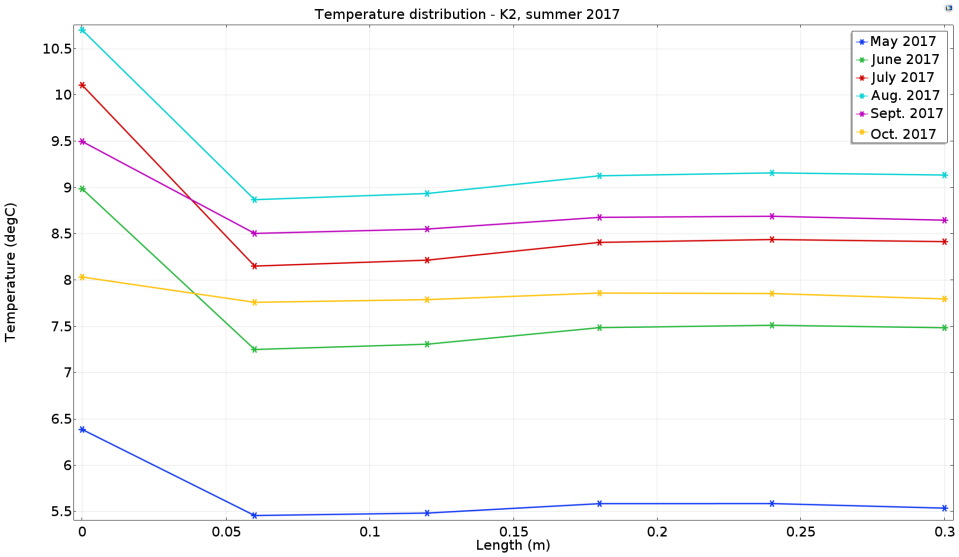
Temperature distribution - K2, summer 2017
May 2017
June 2017
July 2017
Aug. 2017
Sept. 2017
Oct. 2017
Temperature (degC)
Length (m)
10.5
10
9.5
9
8.5
8
7.5
7
6.5
6
5.5
0
0.05
0.1
0.15
0.2
0.25
0.3

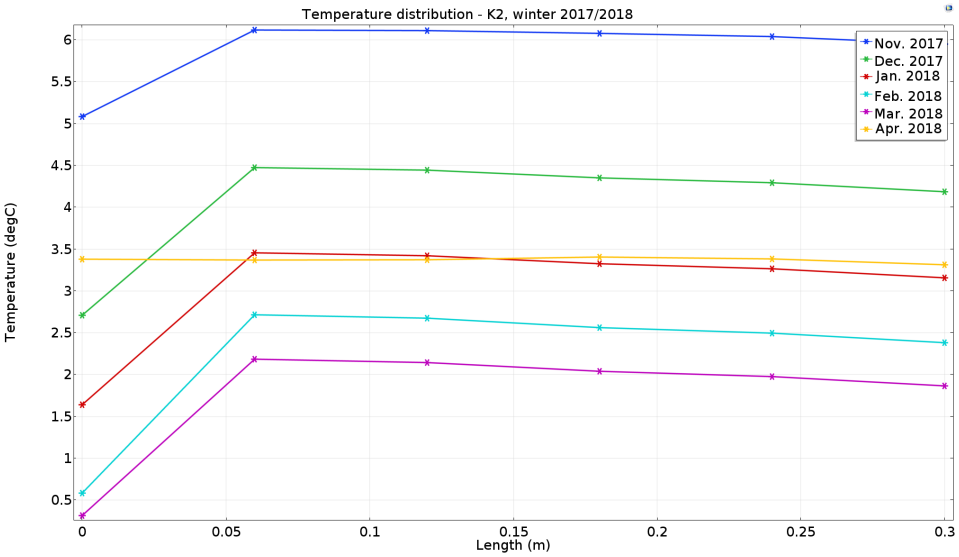
Temperature distribution - K2, winter 2017/2018
Nov. 2017
Dec. 2017
Jan. 2018
Feb. 2018
Mar. 2018
Apr. 2018
Temperature (degC)
Length (m)
6
5.5
5
4.5
4
3.5
3
2.5
2
1.5
1
0.5
0
0.05
0.1
0.15
0.2
0.25
0.3

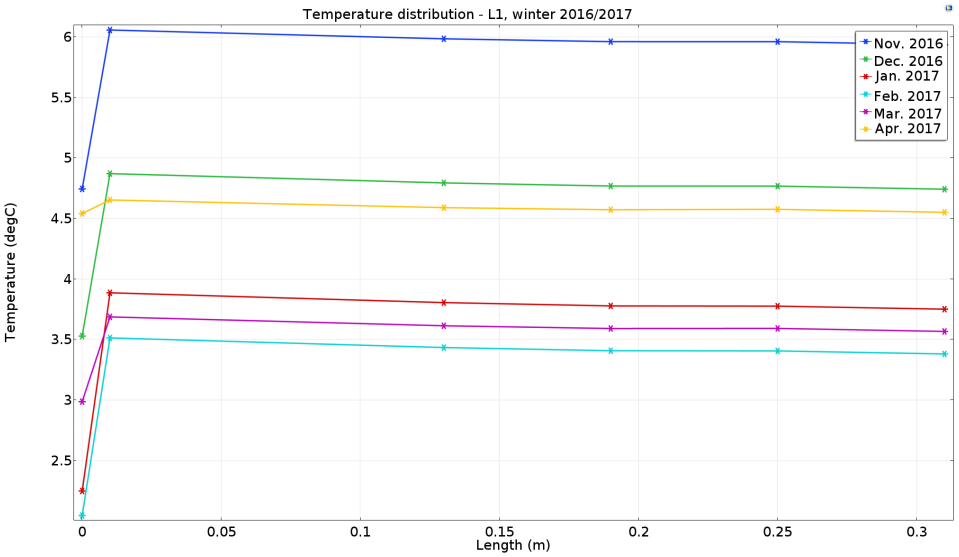
Temperature distribution - L1, winter 2016/2017
Temperature (degC)
Length (m)
Nov. 2016
Dec. 2016
Jan. 2017
Feb. 2017
Mar. 2017
Apr. 2017

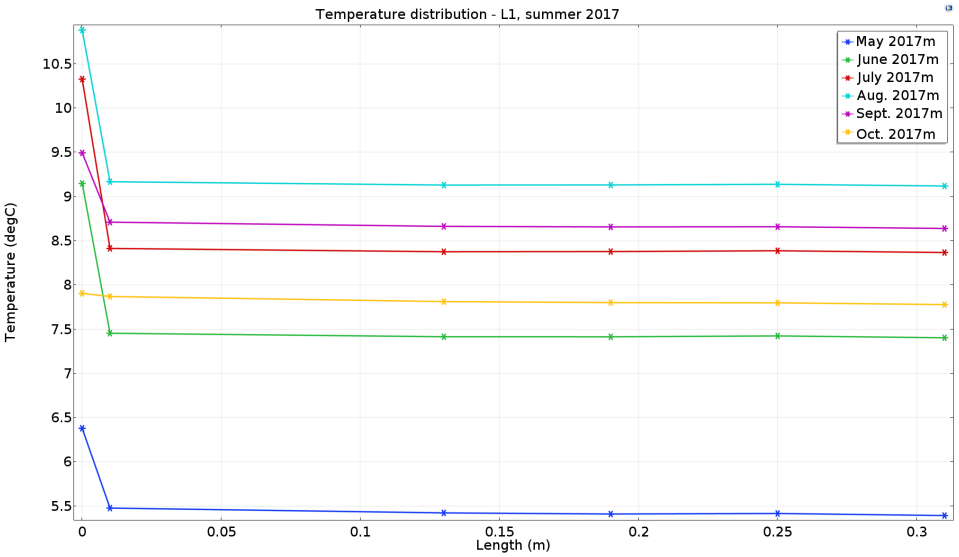
Temperature distribution - L1, summer 2017
Temperature (degC)
Length (m)
May 2017m
June 2017m
July 2017m
Aug. 2017m
Sept. 2017m
Oct. 2017m

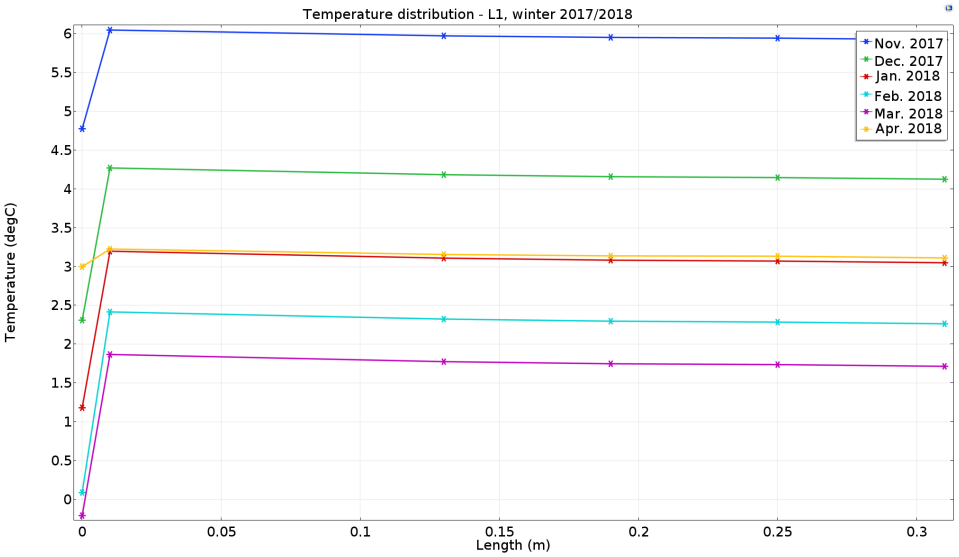

A.2.2 Rock mass measurements

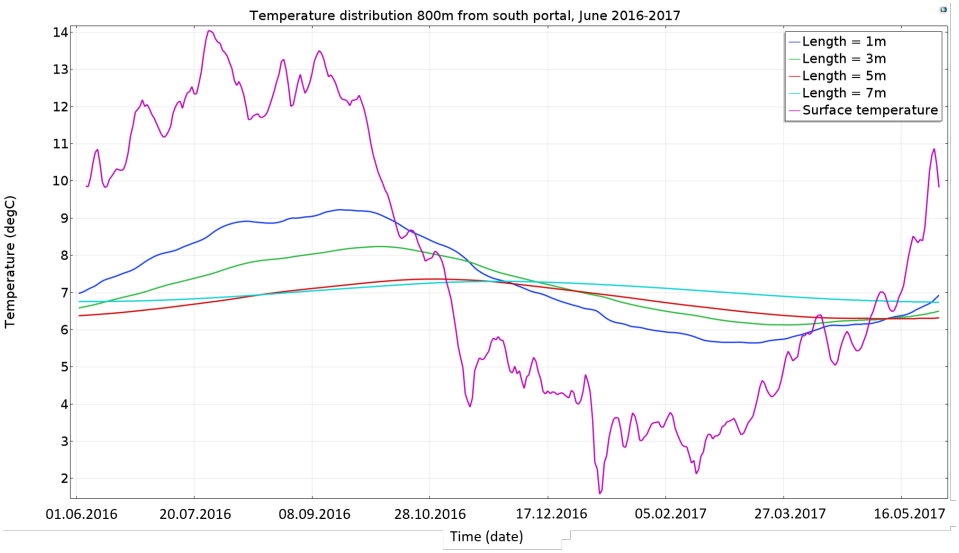

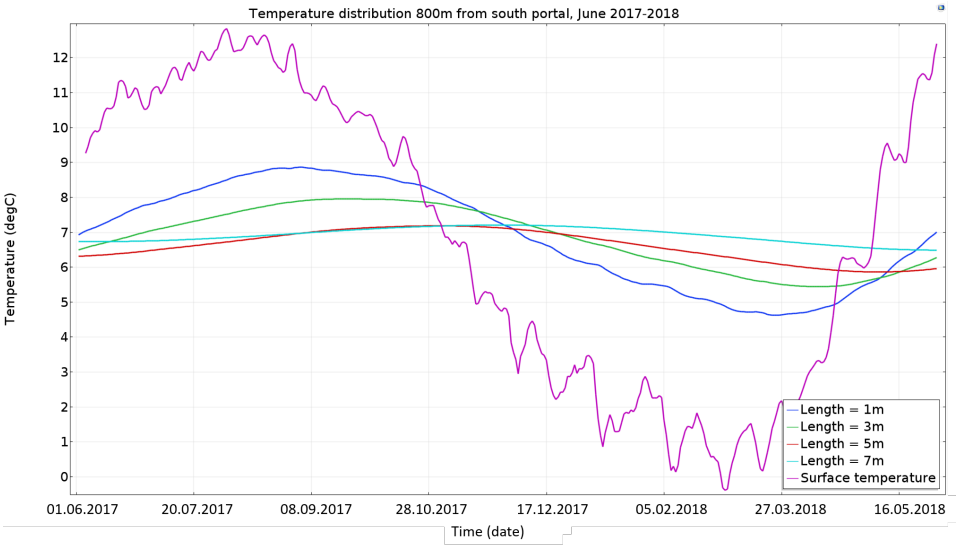
Temperature distribution 800m from south portal, June 2017-2018
Temperature (degC)
Time (date)
01.06.2017
20.07.2017
08.09.2017
28.10.2017
17.12.2017
05.02.2018
27.03.2018
16.05.2018
Length = 1m
Length = 3m
Length = 5m
Length = 7m
Surface temperature

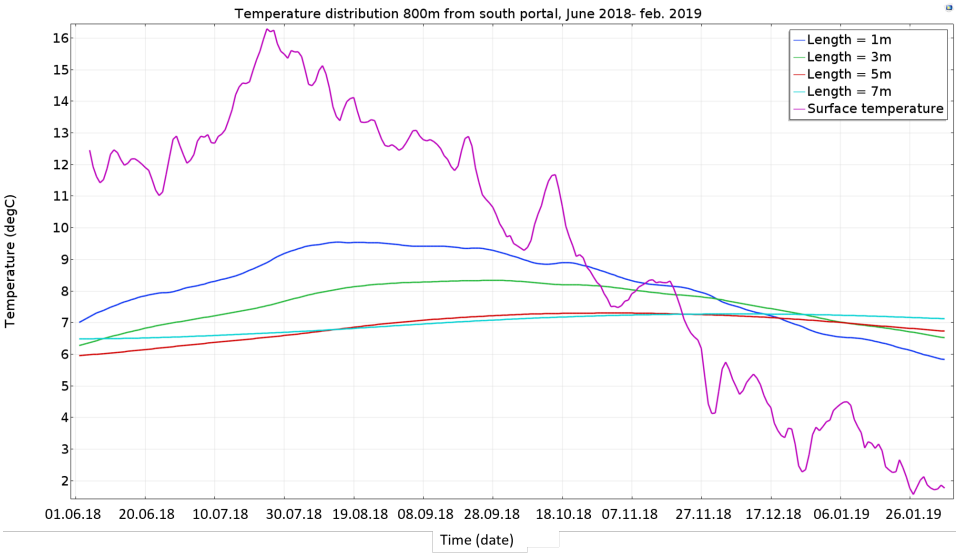
Temperature distribution 800m from south portal, June 2018- feb. 2019
Temperature (degC)
Time (date)
01.06.18
20.06.18
10.07.18
30.07.18
19.08.18
08.09.18
28.09.18
18.10.18
07.11.18
27.11.18
17.12.18
06.01.19
26.01.19
Length = 1m
Length = 3m
Length = 5m
Length = 7m
Surface temperature

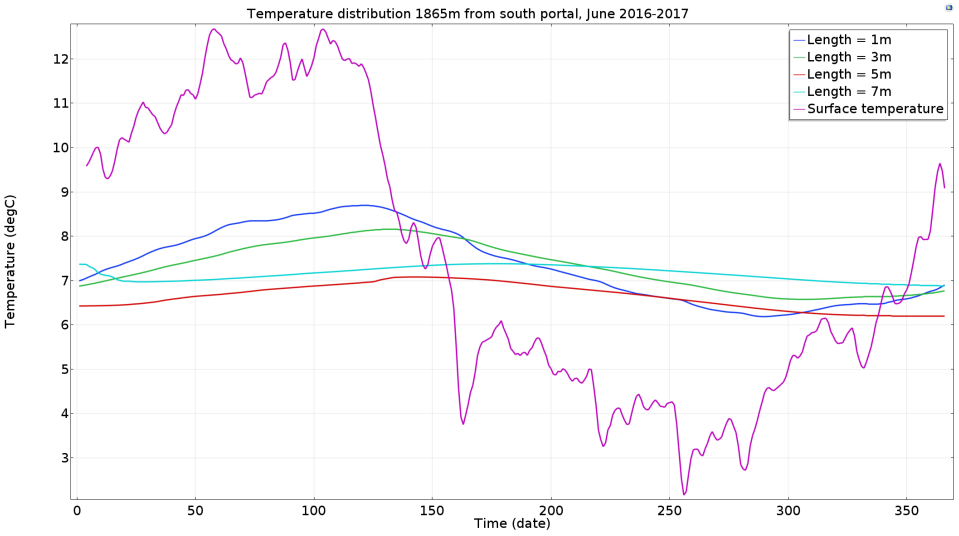
Temperature distribution 1865m from south portal, June 2016-2017
Length = 1m
Length = 3m
Length = 5m
Length = 7m
Surface temperature
Temperature (degC)
Time (date)

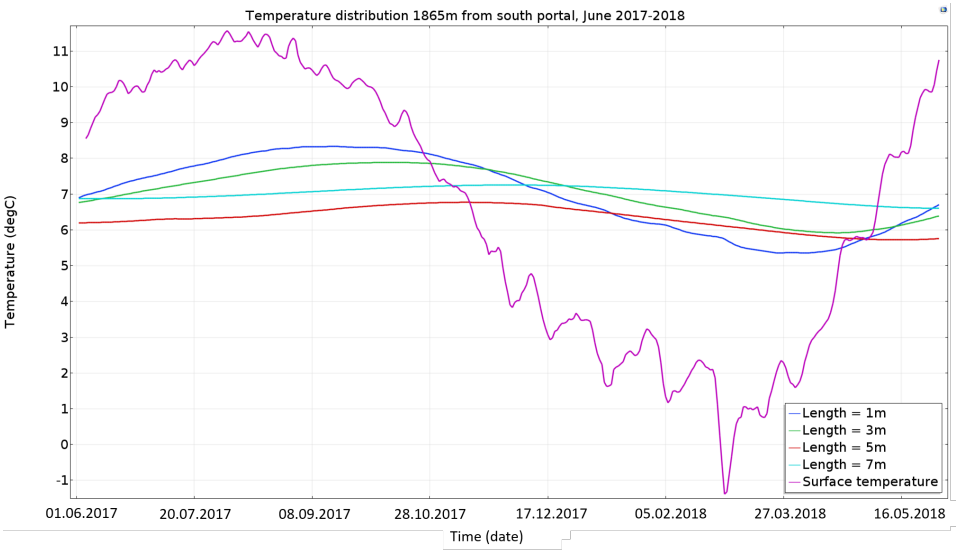
Temperature distribution 1865m from south portal, June 2017-2018
Length = 1m
Length = 3m
Length = 5m
Length = 7m
Surface temperature
Temperature (degC)
01.06.2017
20.07.2017
08.09.2017
28.10.2017
17.12.2017
05.02.2018
27.03.2018
16.05.2018
Time (date)

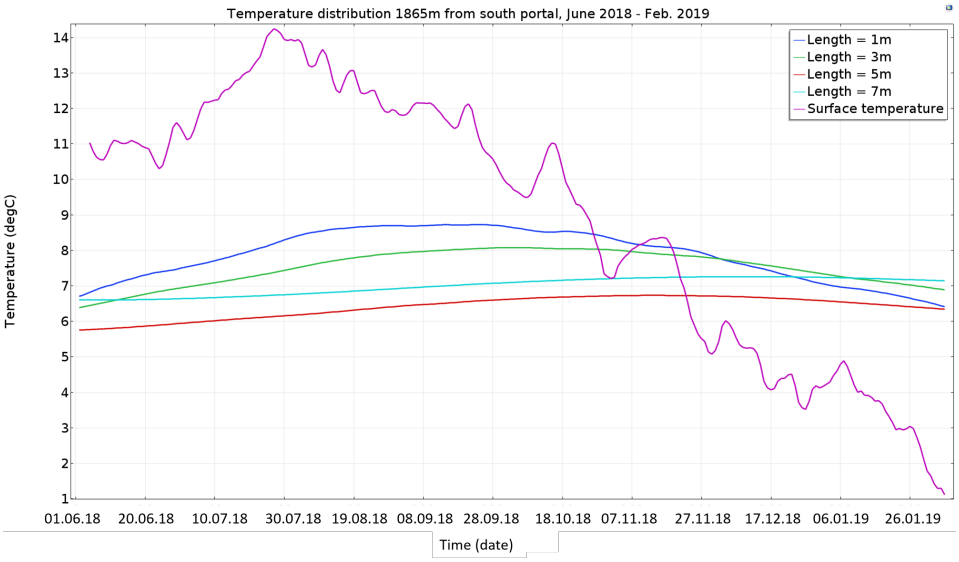
Temperature distribution 1865m from south portal, June 2018 - Feb. 2019
Length = 1m
Length = 3m
Length = 5m
Length = 7m
Surface temperature
Temperature (degC)
14
13
12
11
10
9
8
7
6
5
4
3
2
1
01.06.18
20.06.18
10.07.18
30.07.18
19.08.18
08.09.18
28.09.18
18.10.18
07.11.18
27.11.18
17.12.18
06.01.19
26.01.19
Time (date)

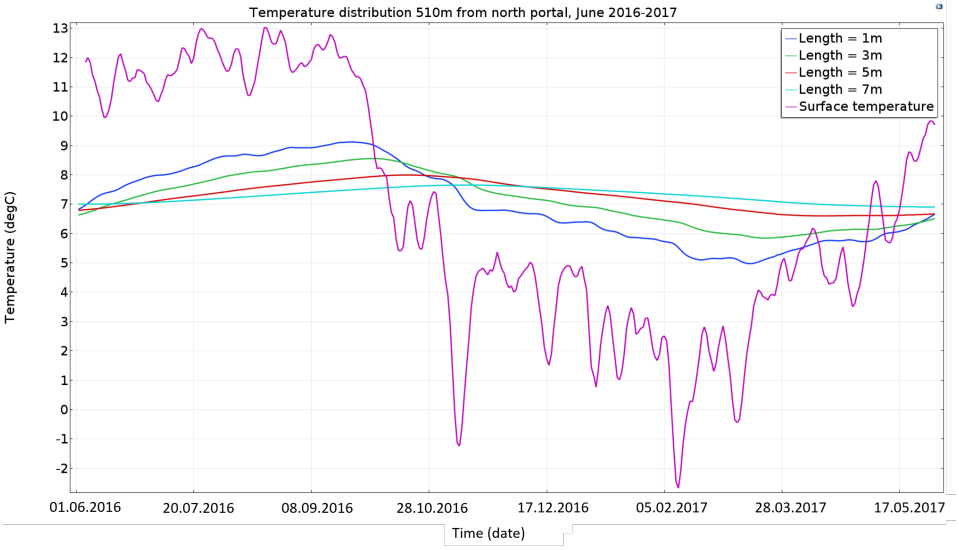
Temperature distribution 510m from north portal, June 2016-2017
Length = 1m
Length = 3m
Length = 5m
Length = 7m
Surface temperature
Temperature (degC)
13
12
11
10
9
8
7
6
5
4
3
2
1
0
-1
-2
01.06.2016
20.07.2016
08.09.2016
28.10.2016
17.12.2016
05.02.2017
28.03.2017
17.05.2017
Time (date)

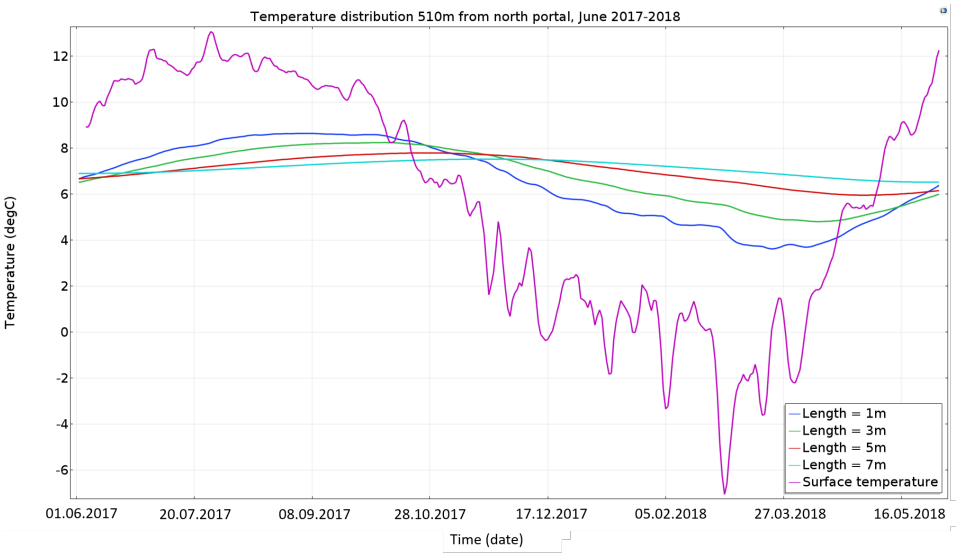
Temperature distribution 510m from north portal, June 2017-2018
Temperature (degC)
12
10
8
6
4
2
0
-2
-4
-6
01.06.2017
20.07.2017
08.09.2017
28.10.2017
17.12.2017
05.02.2018
27.03.2018
16.05.2018
Time (date)
Length = 1m
Length = 3m
Length = 5m
Length = 7m
Surface temperature

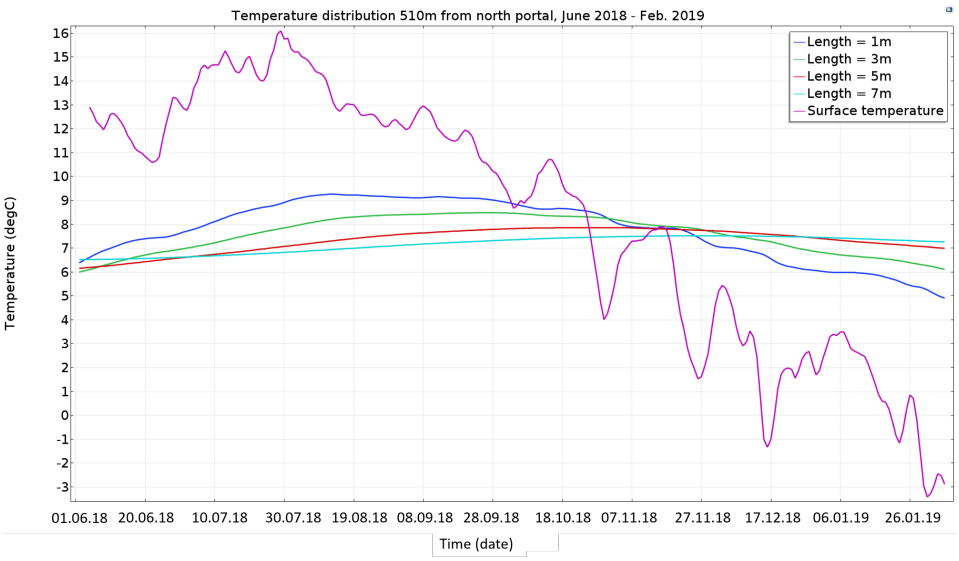
Temperature distribution 510m from north portal, June 2018 - Feb. 2019
Temperature (degC)
16
15
14
13
12
11
10
9
8
7
6
5
4
3
2
1
0
-1
-2
-3
01.06.18
20.06.18
10.07.18
30.07.18
19.08.18
08.09.18
28.09.18
18.10.18
07.11.18
27.11.18
17.12.18
06.01.19
26.01.19
Time (date)
Length = 1m
Length = 3m
Length = 5m
Length = 7m
Surface temperature

A.3 Plot Gevingås

A.3.1 Tunnel air measurements

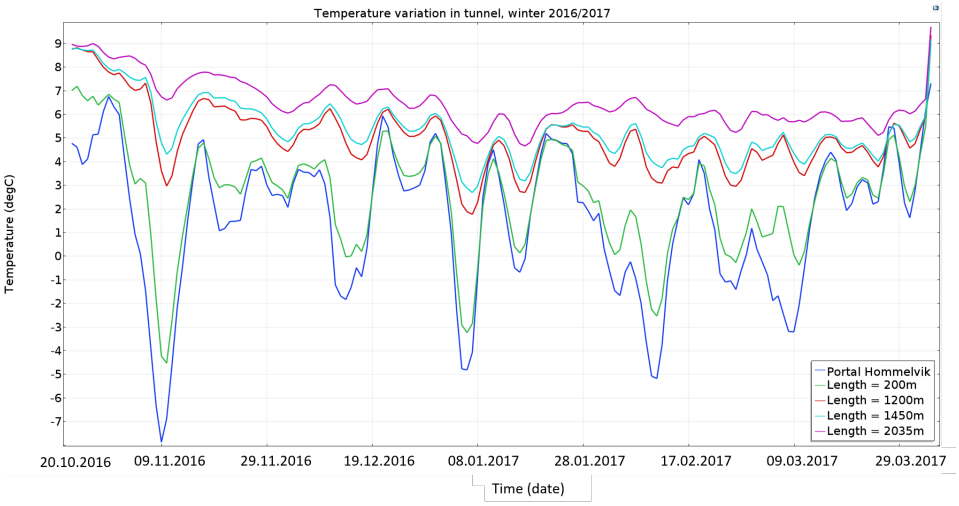

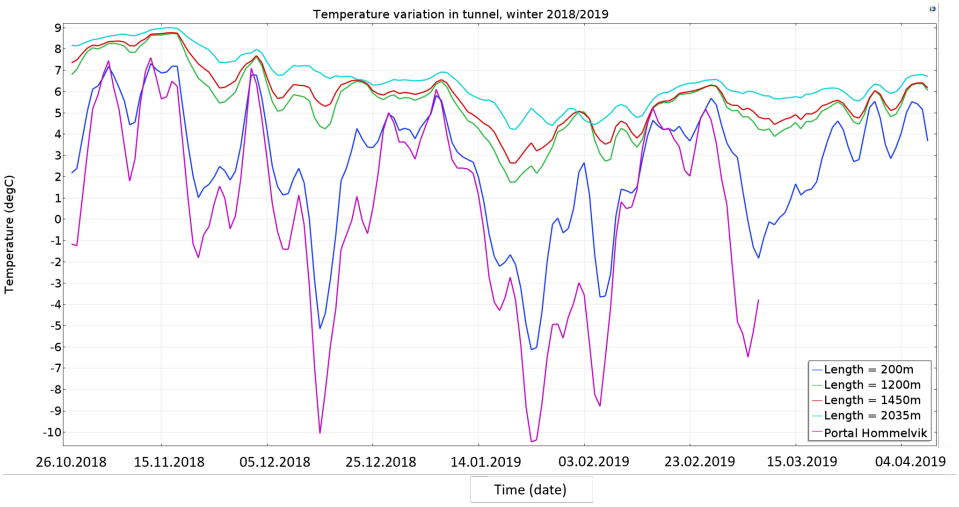

A.3.2 Concrete and rock mass measurements

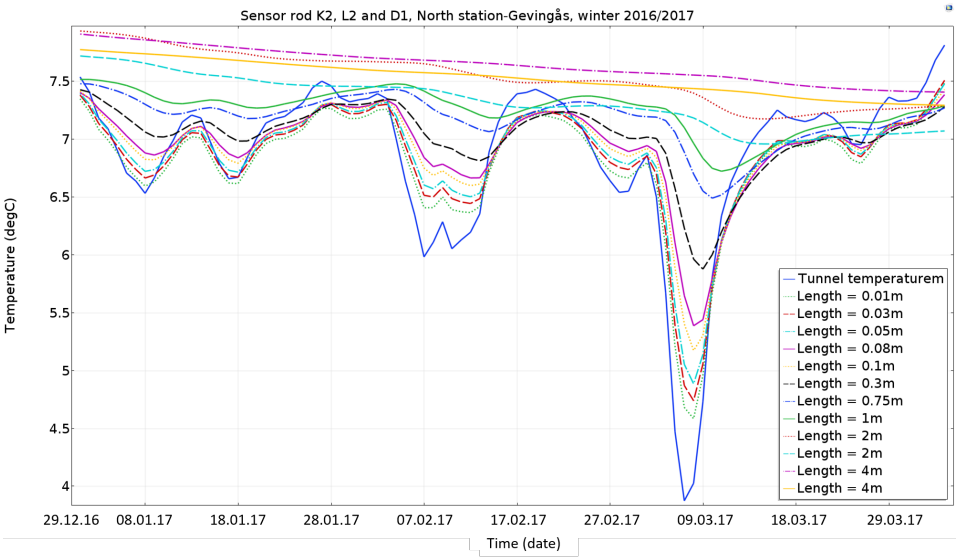

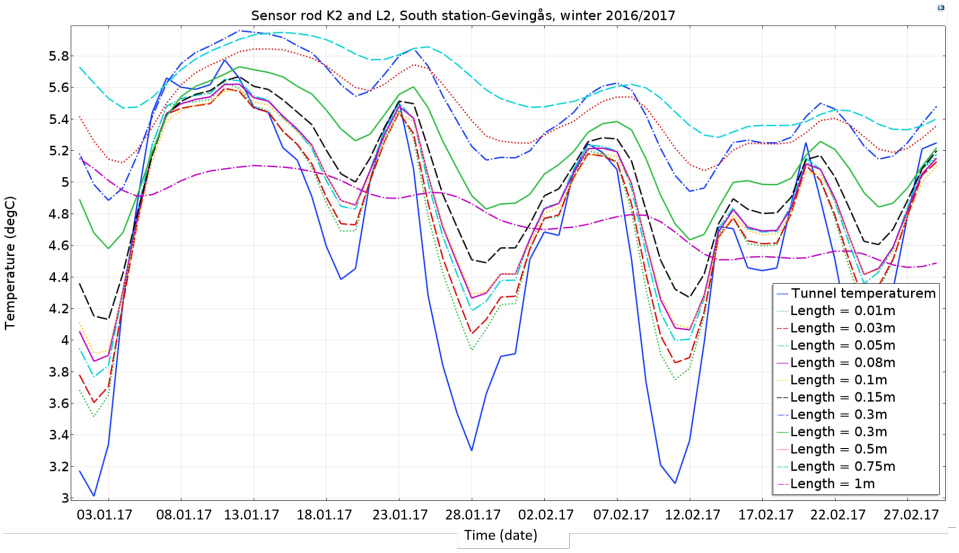

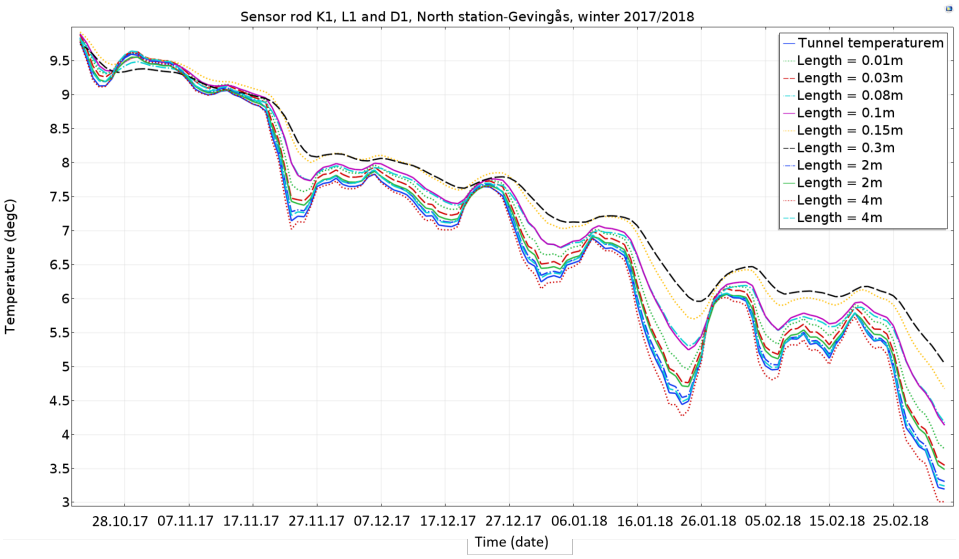
Sensor rod K1, L1 and D1, North station-Gevingås, winter 2017/2018
Tunnel temperaturem
Length = 0.01m
Length = 0.03m
Length = 0.08m
Length = 0.1m
Length = 0.15m
Length = 0.3m
Length = 2m
Length = 2m
Length = 4m
Length = 4m
Temperature (degC)
9.5
9
8.5
8
7.5
7
6.5
6
5.5
5
4.5
4
3.5
3
28.10.17 07.11.17 17.11.17 27.11.17 07.12.17 17.12.17 27.12.17 06.01.18 16.01.18 26.01.18 05.02.18 15.02.18 25.02.18
Time (date)

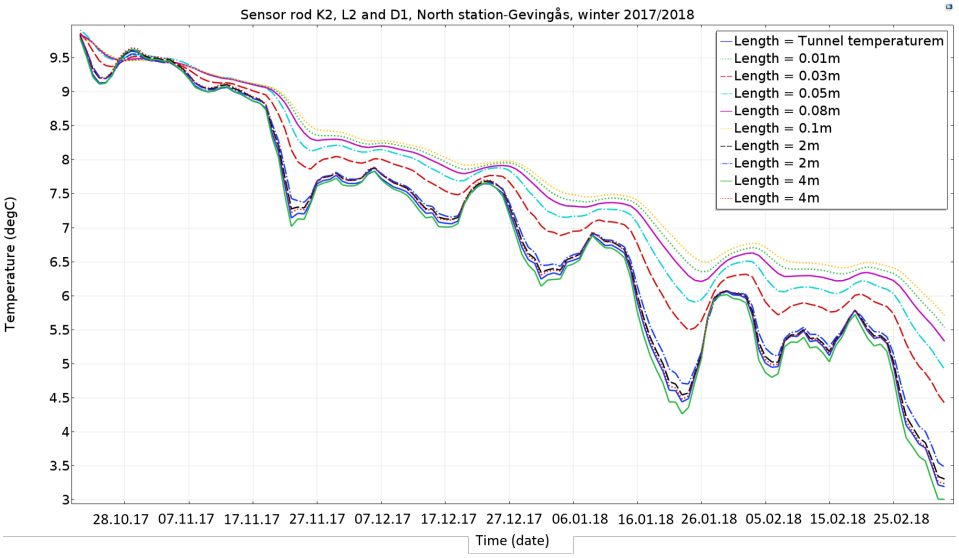
Sensor rod K2, L2 and D1, North station-Gevingås, winter 2017/2018
Length = Tunnel temperaturem
Length = 0.01m
Length = 0.03m
Length = 0.05m
Length = 0.08m
Length = 0.1m
Length = 2m
Length = 2m
Length = 4m
Length = 4m
Temperature (degC)
9.5
9
8.5
8
7.5
7
6.5
6
5.5
5
4.5
4
3.5
3
28.10.17 07.11.17 17.11.17 27.11.17 07.12.17 17.12.17 27.12.17 06.01.18 16.01.18 26.01.18 05.02.18 15.02.18 25.02.18
Time (date)

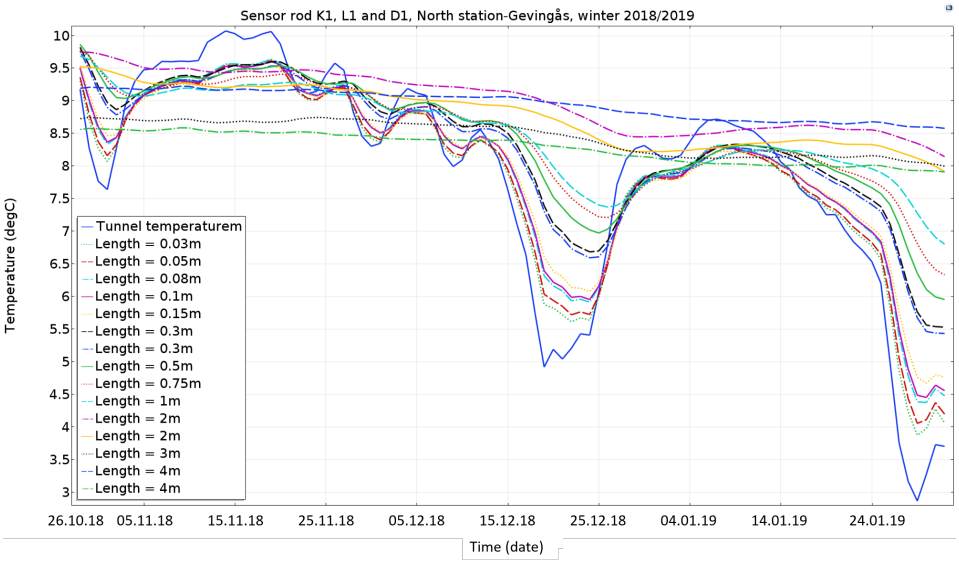
Sensor rod K1, L1 and D1, North station-Gevingås, winter 2018/2019
Temperature (degC)
Time (date)
Tunnel temperaturem
Length = 0.03m
Length = 0.05m
Length = 0.08m
Length = 0.1m
Length = 0.15m
Length = 0.3m
Length = 0.3m
Length = 0.5m
Length = 0.75m
Length = 1m
Length = 2m
Length = 2m
Length = 3m
Length = 4m
Length = 4m
26.10.18
05.11.18
15.11.18
25.11.18
05.12.18
15.12.18
25.12.18
04.01.19
14.01.19
24.01.19

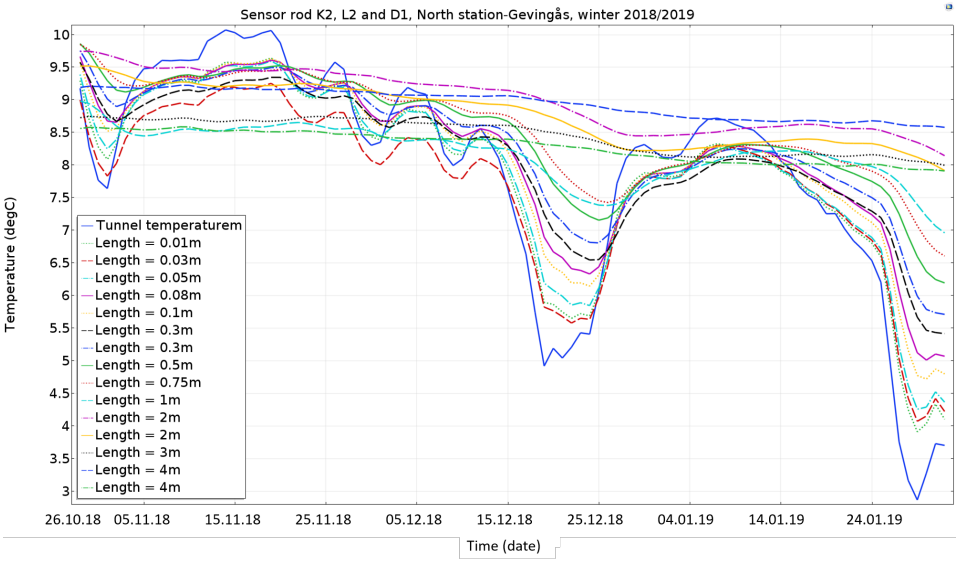
Sensor rod K2, L2 and D1, North station-Gevingås, winter 2018/2019
Temperature (degC)
Time (date)
Tunnel temperaturem
Length = 0.01m
Length = 0.03m
Length = 0.05m
Length = 0.08m
Length = 0.1m
Length = 0.3m
Length = 0.3m
Length = 0.5m
Length = 0.75m
Length = 1m
Length = 2m
Length = 2m
Length = 3m
Length = 4m
Length = 4m
26.10.18
05.11.18
15.11.18
25.11.18
05.12.18
15.12.18
25.12.18
04.01.19
14.01.19
24.01.19

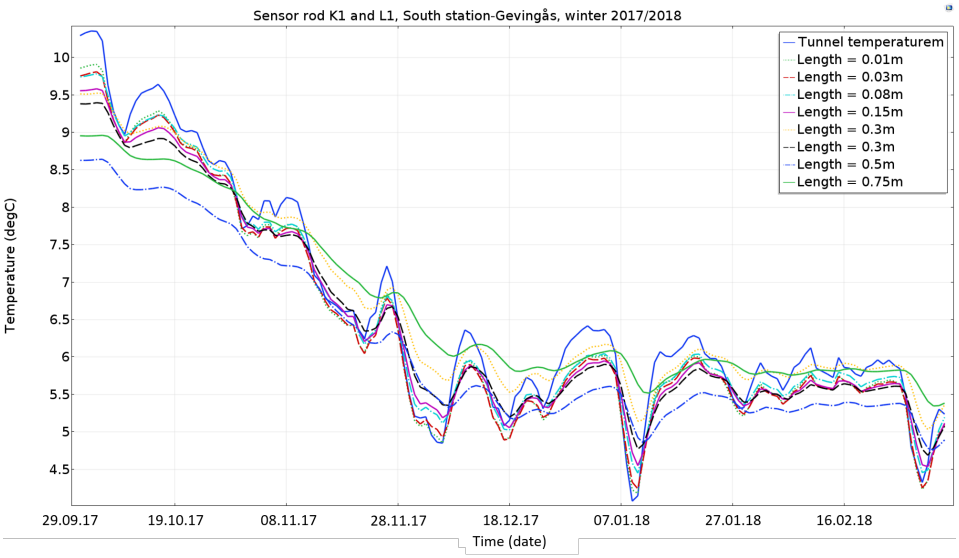
Sensor rod K1 and L1, South station-Gevingås, winter 2017/2018
Tunnel temperaturem
Length = 0.01m
Length = 0.03m
Length = 0.08m
Length = 0.15m
Length = 0.3m
Length = 0.3m
Length = 0.5m
Length = 0.75m
Temperature (degC)
10
9.5
9
8.5
8
7.5
7
6.5
6
5.5
5
4.5
29.09.17
19.10.17
08.11.17
28.11.17
18.12.17
07.01.18
27.01.18
16.02.18
Time (date)

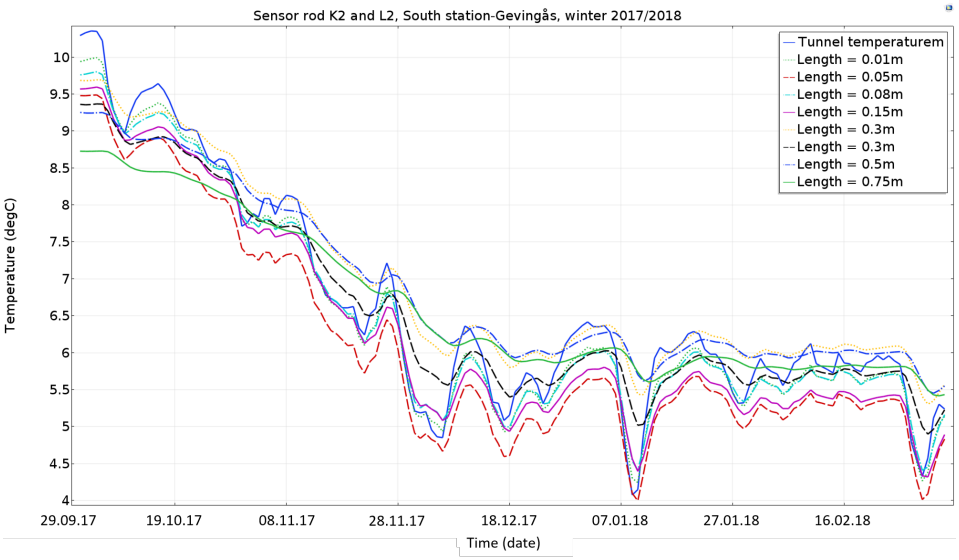
Sensor rod K2 and L2, South station-Gevingås, winter 2017/2018
Tunnel temperaturem
Length = 0.01m
Length = 0.05m
Length = 0.08m
Length = 0.15m
Length = 0.3m
Length = 0.3m
Length = 0.5m
Length = 0.75m
Temperature (degC)
10
9.5
9
8.5
8
7.5
7
6.5
6
5.5
5
4.5
4
29.09.17
19.10.17
08.11.17
28.11.17
18.12.17
07.01.18
27.01.18
16.02.18
Time (date)

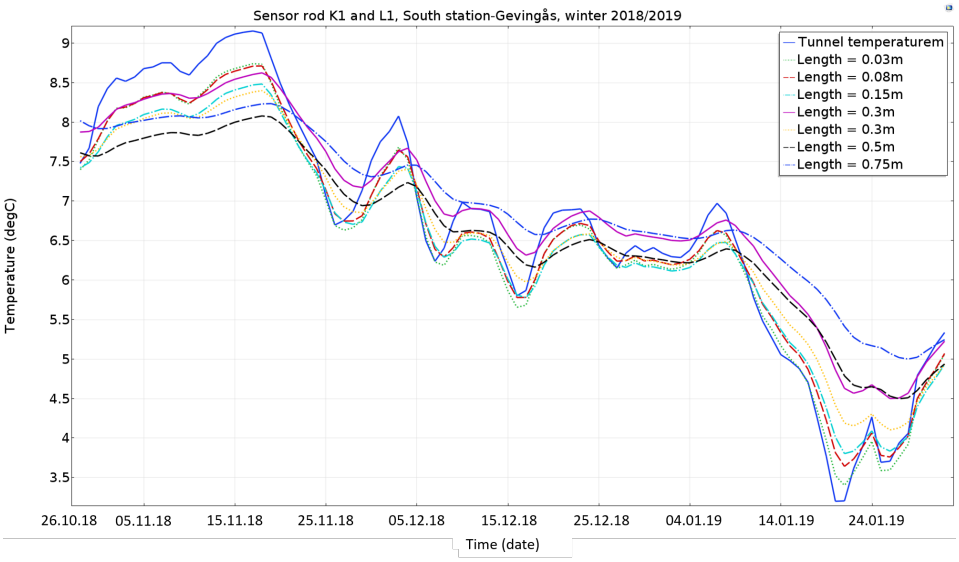
Sensor rod K1 and L1, South station-Gevingås, winter 2018/2019
Tunnel temperaturem
Length = 0.03m
Length = 0.08m
Length = 0.15m
Length = 0.3m
Length = 0.3m
Length = 0.5m
Length = 0.75m
Temperature (degC)
9
8.5
8
7.5
7
6.5
6
5.5
5
4.5
4
3.5
26.10.18
05.11.18
15.11.18
25.11.18
05.12.18
15.12.18
25.12.18
04.01.19
14.01.19
24.01.19
Time (date)

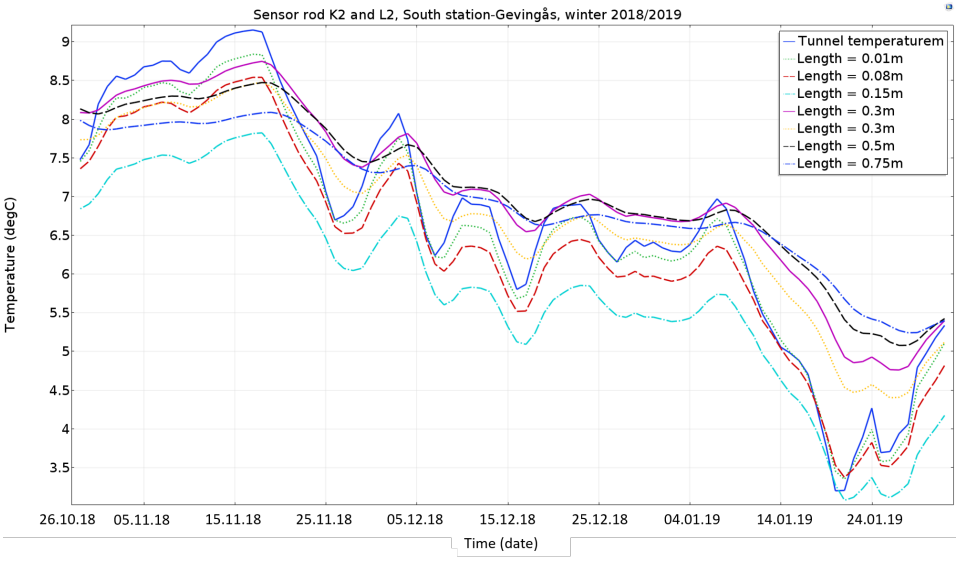
Sensor rod K2 and L2, South station-Gevingås, winter 2018/2019
Tunnel temperaturem
Length = 0.01m
Length = 0.08m
Length = 0.15m
Length = 0.3m
Length = 0.3m
Length = 0.5m
Length = 0.75m
Temperature (degC)
9
8.5
8
7.5
7
6.5
6
5.5
5
4.5
4
3.5
26.10.18
05.11.18
15.11.18
25.11.18
05.12.18
15.12.18
25.12.18
04.01.19
14.01.19
24.01.19
Time (date)

Silje Marie Tinderholt

Heat Transfer – Between Rock Mass and Tunnel Room

NTNU
Kunnskap for en bedre verden